Title	
Author(s)	Irawan, Ade
Citation	
Issue Date	2017-03
Type	Thesis or Dissertation
Text version	ETD
URL	http://hdl.handle.net/10119/14245
Rights	
Description	Supervisor: , ,

Feedback-Aided Source Correlation Exploitation in Error Control Techniques for Wireless Communication Systems

ADE IRAWAN

in partial fulfillment of the requrements
for the degree of
Doctor of Philosophy

School of Information Science

Japan Advanced Institute of Science and Technology

March, 2017

Supervised by

    Professor Tadashi Matsumoto

Reviewed by

    Professor Ping Li

    Professor Markku Juntti

    Professor Hidekazu Murata

    Associate Professor Kiyofumi Tanaka

    Associate Professor Brian Michael Kurkoski

Acknowledgments

This dissertation has been developed and written during my time as a doctoral student in Japan Advanced Institute of Science and Technology (JAIST). My special thanks to Prof. Tadashi Matsumoto, known as Tad, for his outstanding support as the supervisor of this work. To find the best teacher is one of the most important things in my life as a young scientist.

I appreciate my thank to Dr. Khoirul Anwar dan Dr. Brian Kurkoski for having nice and warm discussions during my study. Also, my thank to Dr. Szymon Scott for giving me chance to contribute to WP3 of RESCUE Project. I thank all my colleagues at JAIST who provided very nice environment and friendship. Finally, I appreciate my thanks to my family especially my father, Syahril Noekman, my mother, Cek Yun, and my wife, Laili Mutiara, who truly love me and always pray for me, as well as my daughter, Maryam Assyifa Irawan. Their cheeriness are my motivation to achieve the highest level of education.

Last but not least, hopefully this work will be a contribution for communication societies and for the life of human being in the future.

Abstract

The primary objectives of this dissertation are to improve the end-to-end throughput of parallel multihop relaying network and to fully mathematically analyze the performance of one-time retransmission in a single-hop system, with the utilization of the source correlation and the feedback. Hence, we arrange the analyses into two parts: multihop and single-hop transmissions.

In the first part, we consider a parallel multihop transmission where there is no direct link between the source and the destination. We introduce Lossy-Forwarding (LF) concept to Hybrid Automatic Repeat reQuest (HARQ) schemes, referred to as LF HARQ, and propose two techniques of LF HARQ: Fully-LF and Partially-LF HARQs. With Fully-LF HARQ, the relay nodes always forward the packet, regardless of whether or not the information part of the packet contains errors, to the next hop instead of discarding those containing errors as in the conventional lossless decode-and-forward schemes. With Partially-LF HARQ, the relay nodes select either forwarding the erroneous packets or requesting retransmission. The mode selection bases on the confidence indicator (CI) expressing the reliability of the received packets which is. Since the channels are assumed to suffer from block Rayleigh fading, the CI is calculated via online measurement of mutual information, block-by-block. The numerical results show that the average end-to-end throughput performances of the proposed techniques significantly outperforms the conventional techniques. Furthermore, Partially-LF HARQ outperforms Fully-LF HARQ for the packet loss ratio less than 60 percent.

As the number of retransmission in a link increase, the system throughput will be decreased. Therefore, in the second part, we focus on the single-hop transmission with only one retransmission in the form of a helper packet, referred to as M-in-1 helper transmission. The helper is constructed simply by taking binary exclusive-OR (XOR) of the M unrecovered information packets. We propose a way to analyze the achievable diversity order of M-in-1 helper transmissions taking into account the source correlation. To identify the trade-off between source correlation and performance gain due to coding and diversity relationship, we start in-depth analyses on rate regions and outage probabilities with $M = \{2, 3\}$. We also review the influence of unequal power or redundancy allocation between the helper and

information packets. Finally, we provide the analysis of achievable diversity order with arbitrary M. It is shown that the achievable diversity order depends on the correlation among the sources, the bit error probability of the helper packet, and the integer M being whether even or odd.

Table of Contents

List of Figures

Abbreviations

ACK	Acknowledgment
ARQ	Automatic Repeat reQuest
AWGN	Additive White Gaussian Noise
BER	Bit Error Rate
bps	bit per sample
BPSK	Binary Phase Shift Keying
CC	Chase Combining
CI	Confidence Indicator
CRC	Cyclic Redundancy Check
DN	Destination node
DSC	Distributed Source Coding
EXIT	Extrinsic Information Transfer
FEC	Forward Error Correction
FDM	Frequency Division Multiplexing
FLF-HARQ	Fully LF-HARQ
HARQ	Hybrid ARQ
HI	Horizontal Iteration
i.i.d.	independent and identically distributed
IR	Incremental Redundancy
LF	Lossy Forwarding

LF HARQ	Lossy Forwarding with HARQ
LLR	Log Likelihood Ratio
MAP	Maximum a Posteriori
MARC	Multiple-Access Relay Channel
MI	Mutual Information
NACK	Negative Acknowledgment
NSNRCC	Non-systematic Non-recursive Convolutional Code
OFDM	Orthogonal Frequency Division Multiplexing
PLF-HARQ	Partially LF-HARQ
PCC	Parallel Concatenated Code
PER	Packet Error Rate
pmf	probability mass function
QPSK	Quadrature Phase Shift Keying
RN	Relay node
RS	Reed-Solomon
RSCC	Recursive Systematic Convolutional Codes
SCC	Serially Concatenated Code
SISO	Single Input Single Output
SN	Source node
SNR	Signal-to-Noise Ratio
VI	Vertical Iteration
XOR	exclusive-OR

Notations

$\bullet^C$	complementary set of $\bullet$
$\bar{\alpha}$	average of α
$\alpha * \beta$	binary convolution, i.e., $\alpha(1-\beta) + (1-\alpha)\beta$
DA	doped-accumulator
D_{DA}	decoder of doped-accumulator
$H(X)$	entropy of random variable X
$H_b(p)$	binary entropy with probability p
$H(X|Y)$	conditional entropy of random variable X given random variable Y
$H(X,Y)$	joint entropy of random variable X given random variable Y
$I(X;Y)$	mutual information between random variable X and random variable Y
k	packet length (bits)
Π	interleaver
P_b	bit error rate
$\mathbb{P}(\cdot)$	probability function
Π^{-1}	deinterleaver
$\oplus$	modulo-2 summation
R	information rate
Q	spectrum efficiency
γ	instantaneous SNR
Γ	average SNR

M number of NACK-ed packets

$\mathcal{M}$ Mapper

$\mathcal{M}^{-1}$ Demapper

N length of a packet

T   the total number of transmission of the same packet (including the retransmissions)

ξ doping rate

Chapter 1

Introduction

Billions of devices are predicted to be connected to wireless networks in the future [1, 2]. Consequently, an enormous amount of data transfer is anticipated to impose excessive transmission problems in wireless communication networks. Such trend of the increasing demands is projected to grow continuously at an exponential speed [3]. The network components in such communications systems commonly
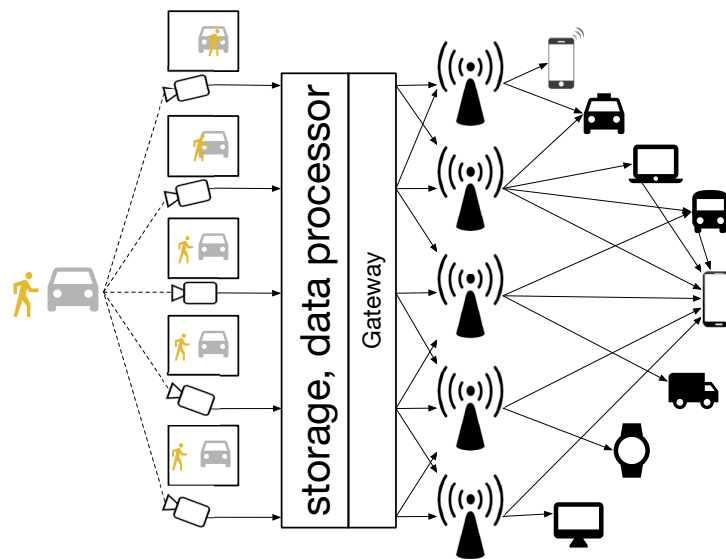
Figure 1.1: The data storage of a server in the wireless network system stores correlated packet.

have data storage to save a significant amount of data, from which multiple streams are formed based on, for example, the multiple observations of the same object [4, 5] as illustrated in Figure 1.1. As a consequence, the server stores correlated packets
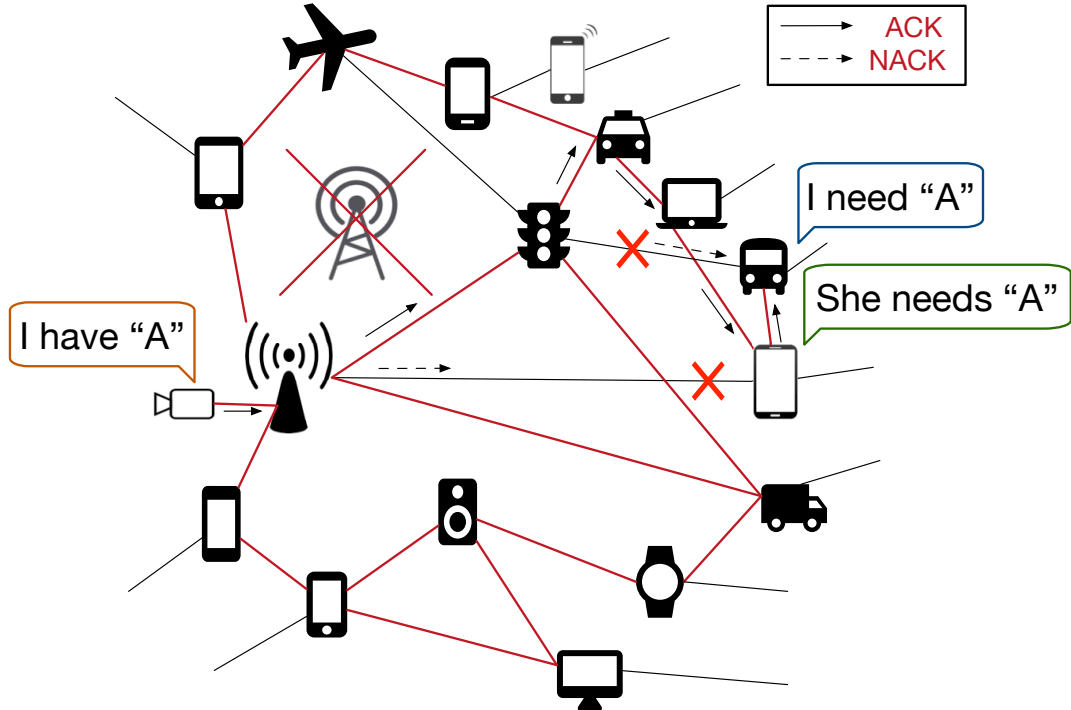
Figure 1.2: Interaction among multiple nodes supported by a joint operation with feedback channels.

due to the collaborative nature of the monitoring or sensing devices, in brief, sensors. The correlation among the information packets at the server exists, not only in the form of *spatial* data correlation [6] between the information streams obtained from the *spatially* nearby sensor observations but also the *temporal* data correlation between packets acquired consecutively in time by the same sensor [4, 7].

Besides, designing very highly reliable data transfer mechanism for massively connected devices in wireless communication networks is of crucial importance in many cases [8]. Hence, the interaction among multiple nodes is commonly supported by a joint operation with feedback channels to satisfy the reliability requirement. The most classical method of the feedback information utilization is Automatic Repeat reQuest (ARQ) where the receiver feedbacks acknowledgement (ACK) or negative ACK (NACK), depending on whether or not the received packet contains no errors, respectively, as illustrated in Figure 1.2. The transmitter then decides whether to transmit new packets or to retransmit the packets found to be received in error, respectively, depending on the feedback information ACK or NACK. Hence, ARQ is preferable for high-reliability requirement systems with the

transmission over noisy channels.

Furthermore, the connected enormous devices for some applications demand not only reliability but also robustness in data transfer [9, 10]. In this case, the communication between devices barely has the need for common infrastructure or centralized control. Instead, they cooperate with each other by relaying or forwarding each others' packets. The relaying or forwarding packets enables devices that cannot directly interact each other to communicate via relays, known as multihop transmission.

Multihop transmission is a relay-assisted transmission scheme which has long been considered very beneficial for enhancing the signal coverage of limited-power transmitters [11]. It commonly employs relay nodes in a serial configuration. However, such schemes do not increase the diversity order to overcome the effects of fading variation in wireless environments. On the other hand, due to the nature of wireless communications, multiple nodes (in addition to the intended next-hop recipient) can overhear transmissions and serve to assist forwarding. It enables the multihop transmission with a parallel configuration, which can gain diversity order [12].

This dissertation deals with the design of reliable and robust parallel multihop transmission exploiting the source correlations and feedback, and focus the theoretical analysis of the achievable diversity in one link. This chapter begins with the motivation and the related work, followed by the author's contributions. Finally, the outline of this dissertation is provided.

1.1   Motivation and Related Work

We consider exploiting the source correlation and the feedback so that the reliable and robust wireless multihop transmission can be efficiently designed. One of the challenges in the multihop transmission is that the end-to-end delay may be larger compared to that of single-hop due to processing needed in each hop. Moreover, there is still no guarantee that shorter hop is always reliable due to the time-varying nature of wireless channels. Therefore, the reliability of a single-hop transmission is worth being analyzed at a deep level. This dissertation details the methodology to deal with the challenges of both multihop and single-hop transmissions as summarized as follows.

1.1.1 Parallel Multihop Transmission
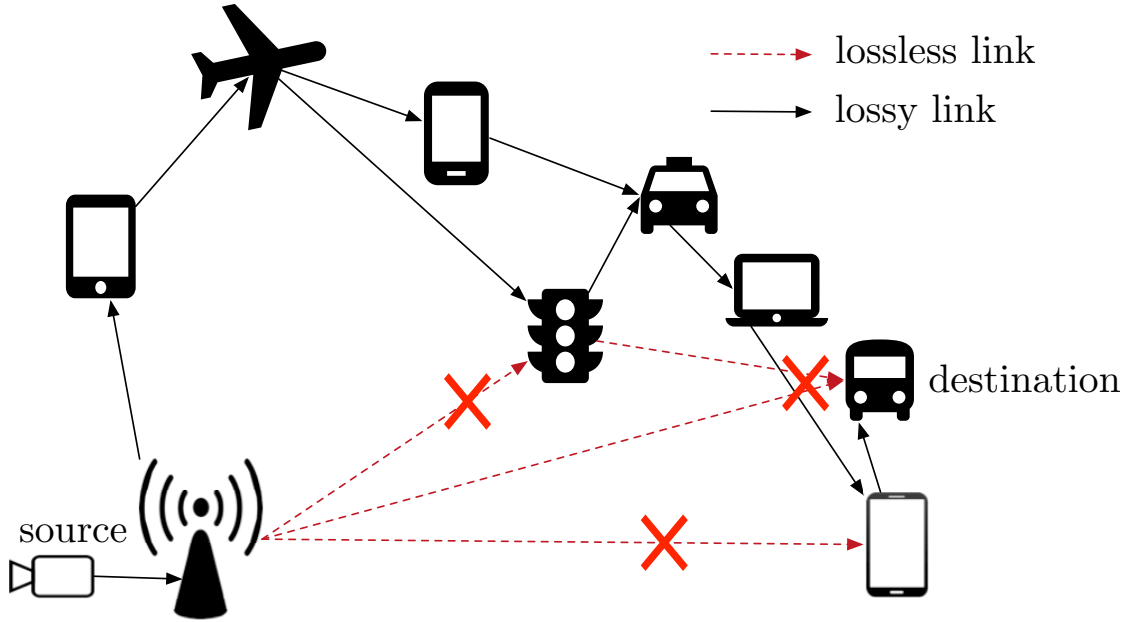
Figure 1.3: Overhearing relay cooperatively forward the packet until it reaches the destination node.

In general, the performance of multihop transmission relies on the forwarding strategy and technique. Regarding the relaying strategy, the overhearing relay nodes can be either selected opportunistically or cooperatively forward the packet until it reaches the destination node [13], as illustrated in Figure 1.3. The numerical results in [13] show that due to the greater number of connected transmitters in cooperative forwarding, the throughput is lower than the opportunistic forwarding. As for the forwarding technique, it can be classified into three categories: amplify-and-forward (AF), compress-and-forward (CF), and decode-and-forward (DF).

AF is the simplest relaying technique concerning signal processing complexity. Basically, a relay node with AF only scales the received packets and then forward the amplified version to the destination node [14]. However, the noise component is also amplified with the received packets, which degrades the performance of the system. Another drawback of the AF technique is the necessity of transmitting the channel state information in the previous hop, which requires additional bandwidth.

With CF, the received packets at the relay node are quantized and compressed before being forwarded to the destination node [15, 16]. This technique is also

known as estimate-and-forward [17]. The packet with CF technique can be seen as the noisy version of the original packet. Therefore, CF is suitable for parallel multihop relaying instead of the serial configuration since the destination node can recover a packet by combining the correlated copies of the same packet from the several parallel links. However, compressing the received packet at the relay node may be computationally expensive.

With DF, the relay node decodes the received packet and detects whether the packet contains errors or not by utilizing, for example, cyclic redundancy check (CRC) [18]. Based on the detection, the relay node either re-encodes and forwards the error-free packet or discards the erroneous packet. In the case of cooperative communications where a relay node assists the direct source-destination nodes transmission, the conventional DF gives no diversity gain when the source-relay nodes link is lossy. In this case, Adaptive DF in [19] utilizes feedback information to achieve the diversity by letting the source node retransmits the packet to the destination node via using, again, the direct link. As for the parallel multihop transmission, utilizing DF and the feedback may increase the end-to-end latency, and decrease the end-to-end throughput.

In contrast to DF, Lossy forwarding (LF) technique–a technique allowing erroneously decoded packets to be forwarded– is effective in reducing the end-to-end latency and increasing the throughput of parallel multihop transmission. One way to utilizing the LF concept is the soft relaying technique [20]. It is a derivative technique of CF where the relay node uses a soft encoder to acquire the *a posteriori* probabilities of the coded bits, and then forwards the soft values, which are exploited as *a priori* information by the soft decoders of the destination to improve decoding performance. However, a significant disadvantage of the technique is that it requires additional bandwidth and power consumption, due mainly to the requirement for transmitting the soft values or their quantized versions. The other way is by re-interleaving and re-encoding the erroneously decoded packets at the relay node, in such a way that the destination can exploit the correlation of the information parts of the packets received via multiple links, as presented in [20]. In fact, the correlation exists because the packets are generated from the same source. This fact is utilized in Chapter 3, where an efficient algorithm for utilizing the correlation in the ARQ protocols for parallel multihop transmission is presented.

With the existence of the feedback, the multiple copies of correlated packets are

received not only from parallel links but also from retransmitted packets following an ARQ protocol. In general multihop transmission, conventional ARQ protocol always requests the source node to retransmit whenever the destination node failed in recovering the packet. This end-to-end ARQ is a very simple mechanism to ensure the successful recovery of the packets at the destination node. However, larger transmission delay is a detrimental drawback. Hence, additional techniques initiated by the relay nodes are needed, for instance, the hop-by-hop ARQ proposed in [21], and the relay ARQ in [22]. Reference [23] shows that the delay increases exponentially as the packet-error-rate (PER) per link in two-hop transmission increases, and the hop-by-hop ARQ, as well as the relay ARQ mechanism, perform similar even though they outperform the end-to-end ARQ in term of throughput. The superior performance of the hop-by-hop ARQ and the relay ARQ over the end-to-end ARQ is shown in [23], also in terms of throughput.

Every time a packet is retransmitted, the receiving node will increase the amount of information. Hence, by accumulating sufficient information, the node will be able to decode the message. In this case, ARQ based on packet combining techniques with forward error correction (FEC) in a hybrid ARQ (HARQ) scheme can achieve not only coding gain but also the time diversity through retransmissions, as well as the spatial diversity through the relays which retransmit the source information, as described in [24]. Therefore, employing HARQ in multihop relay networks can further improve the reliability.

Many different schemes of HARQ for multihop relaying systems have been proposed in the literature, for example, the HARQ for one-relay-per-hop systems in [25–27]. Those protocols may not be optimal for a system with more than one relay per hop since the spatial diversity is not taken into consideration. The system becomes more complex as the number of relay per hop increases as shown in [28–30]. However, the relay nodes of all those schemes do not forward erroneous packets, but instead request for retransmissions, and hence the end-to-end latency increases. Furthermore, they do not consider the correlation between multiple information sequences[1] so that further potential improvement using correlation property between the received sequences is not exploited.

---

[1]The correlation among packets from parallel links exists since they were originally sent from the same source.

1.1.2 Single-hop Transmission

It is noticeable that a drawback of the conventional retransmission systems is that all the NACK-ed packets invoke retransmission requests in several rounds of attempt until they are recovered, which reduce the system throughput. Many techniques have been proposed to eliminate the shortcoming of ARQ by HARQ [31–33].

With HARQ, incremental redundancy is known as an effective scheme to achieve high throughput in static additive white Gaussian noise (AWGN) channels [34]. With incremental redundancy, the information bits are firstly encoded using a low rate code, referred to as the mother code, and then the encoded bits are punctured, according to the puncturing table [35, 36], to produce a series of high rate codes. The aim of this scheme is to inherently make an adaptive adjustment between the unknown received signal-to-noise power ratio (SNR) and FEC code rate through accumulative redundancy retransmissions [37]. However, its performance is very sensitive to the design of the mother code and the puncturing table. Moreover, it still requires packet-wise ACK/NACK feedback.

Those technique described above consider effectiveness in achieving high throughput and reliability in static AWGN channels where the transmitter does not know the received SNR.[2] With the block fading assumption [38], the transmitted packet is always correctly received if a capacity-achieving code is used and the instantaneous received SNR is larger than the threshold SNR supported by the code; otherwise, it is always received in error. However, the received instantaneous SNR varies in fading channels, and hence the fading variation dominates the *average performance* such as the diversity order. Therefore, considering the enormous dynamic range of the fading variation, say, $30 - 40$ dB dynamic range, packet-wise feedback may still be useful compared to the block-wise feedback.

Nevertheless, various retransmission-protocol-based techniques with block-wise feedback using rateless codes have been proposed to overcome the shortcomings of incremental redundancy HARQ [39–41]. Rateless codes, such as Luby Transform (LT) codes [42], fountain codes [43], and raptor codes [44] can achieve reliable communication without channel knowledge at the transmitter. With rateless coding, the transmitter generates a potentially limitless number of independent packets, and the receiver attempts to decode the information block from the received packets. The corrected received packets are stored for future decoding; otherwise,

---

[2]Channel State Information (CSI) feedback is out of the scope of this dissertation.

the corresponding packet is discarded. The receiver sends an ACK once it has collected enough packets to recover the information, otherwise send no feedback. In the very fast fading channel, it is shown in [45] and [46] that rateless codes are reliable for delay-constrained transmission. However, the performance evaluation used in [45] and [46] is only by simulations. Overall, the decoding latency of rateless codes is still large since the decoder needs to acquire sufficient, typically large, number of packets to recover the information. On the contrary, with the packet-wise feedback ARQ, the recovered packets can immediately be released to the higher layer, and hence reduces the latency, in the average.

Instead of block-wise feedback, the packet-wise feedback based techniques have been revisited recently, where its effectiveness has been investigated by utilizing the network coding techniques [47–49]. The broadcast transmission in [47] and the multiple unicast schemes in [48] use the binary exclusive-OR (XOR) network coding to reduce the number of transmissions compared with conventional ARQ schemes. Authors of [49] apply random network coding for point-to-point communication to further reduce unnecessary redundancy transmission. However, those techniques described above do not take into account the impact of the source correlation.

The theoretical works on packet-wise feedback-assisted correlated source transmission with a helper, are somehow related to the systems over broadcast or multiple access channels. For instance, it is shown in [50] that the proposed XOR operations among packets of several users with 1-bit feedback can achieve the capacity of packet transmission over an erasure broadcast channel. In [51], the authors characterize the rate region of the broadcast channel where every receiver has a partial message as side-information of others. For multiple access channels with feedback, [52] presents the achievable rates for correlated sources, and provides the coding strategies to achieve the rates where the receiver can exploit the information of one out of the two transmitters as a helper.

With the use of a capacity-achieving code,[3] packet-wise feedback invokes another fundamental interest that how the ARQ process can well utilize the source correlation knowledge and how the redundancy should be constructed. There arises a lot of interesting questions which are all related to *the theorem of multiple sources coding with a helper* [53]. This interest motivates us to investigate the achievable

---

[3]The capacity achieving assumption is only for analysis. In practice, the code should not necessarily be exactly capacity achieving.

diversity, outage probability, and impact of source correlation, all in block Rayleigh fading channels with packet-wise feedback, of which starting point is the analysis of the inadmissible rate region in static AWGN channels.

1.2   Contributions

To improve the performance of multihop multi relaying systems, we introduce LF with HARQ (LF HARQ), where erroneous packets are forwarded to preserve as many parallel links as possible to exploit the correlation among the erroneous messages, resulting in larger diversity gain. Furthermore, the end-to-end throughput can be enhanced because LF HARQ improves the reliability retransmission-by-retransmission. In particular, LF HARQ utilizes the knowledge of the correlation between the information sequences received in the previous transmissions. Therefore, the correlation knowledge or the redundancy among packets coming from different links is significantly beneficial. However, the more hops in transmission, the larger the distortion in the forwarded packet, which results in decreased redundancy hop-by-hop. To solve this problem, we introduce a confidence indicator (CI) as a threshold by which each relay node selects either forwarding the erroneous packets or requesting retransmission. Therefore, LF-HARQ is initiated by the relay nodes, depending on the CI value, to reduce the number of end-to-end retransmissions, and hence it increases the end-to-end throughput.

For the single-hop transmission problem, we start in-depth analyses on rate regions and outage probabilities of M correlated information sources transmission with $M = \{2, 3\}$, to identify the trade-off between source correlation and performance gain due to coding and diversity. Eventually, we generalize the analyses of achievable diversity order into any integer M.

Accordingly, we first investigate M correlated information sources transmission over a static AWGN channel with $M = \{2, 3\}$. Each packet is encoded by a capacity-achieving code at a certain *specified* instantaneous SNR. By utilizing Shannon's source-channel separation theorem, we focus on the case where the channel capacity[4] is smaller than entropy per-information packet of the source; it corresponds to the case where the packet contains errors after decoding at the receiver. The receiver

---

[4]The terminology "channel capacity" is the channel capacity corresponding to the *specified* SNR, divided by the signaling spectrum efficiency which is including channel coding rate and modulation multiplicity. Unless otherwise stated, however, we use the terminology "capacity" for the simplicity.

notifies the decoding failure to the transmitter via the feedback channel. Thus, a helper packet, formed by utilizing the XOR operation to the M packets which are failed to be recovered at the receiver,[5] is then transmitted.

Therefore, the system considered as a single-hop transmission is regarded as two-dimensional channel coded packet-wise transmission, horizontal and vertical codes. The horizontal code is the packet-wise capacity-achieving code, and the vertical code is binary single parity check code over M information packets. This system is referred to as M-in-1 helper transmission in this dissertation.

Under this assumption, we derive the inadmissible rate region of the system, where the correlation among the source information and the bit error rate of the helper packet are fully theoretically analyzed. We use *the theorem for multiple sources coding with a helper* [53, Theorem 10.4], for analyzing the inadmissible rate region. Given the derived inadmissible rate region, we then derive the upper bound of the outage probability of M-in-1 helper transmission over block Rayleigh fading channels.[6] Each packet, including helper, suffers from statistically independent block Rayleigh fading, where the channel varies packet-by-packet but is static within each packet.

The scenario described above may arise in ARQ systems, where the transmitter stores the NACK-ed packets in a buffer with a size of M; a helper is transmitted whenever the buffer is full. In the analysis, we only focus on the buffer-full state and derive the outage probability of the M-in-1 helper transmission system utilizing the obtained rate region. In fact, the process of how the full buffer state is reached has to be taken into account for the exact calculation of the *system outage*. In this dissertation, however, we make use of the statistically independent occurrence of the two events, per-packet decoding success and failure at the receiver. Hence, we define the outage event such that decoding of the M NACK-ed packets after transmitting the helper packet is failed *for the first time*, and thereby the outage probability derived in this dissertation is an upper bound. With this outage definition, the upper bound of the outage curve apparently exhibits at least M-th order diversity with any integer M.

In the rate region analysis for the single-hop transmission, the rate region

---

[5]Afterward, we use terminology NACK-ed packet to refer the packets that are unable to be recovered at the receiver by independent (packet-by-packet) decoding.

[6]The outage probability of the systems with $M > 3$ may be possible to be derived if we can solve the difficulty of managing M dimensions rate region.

supported by the channel being larger than the source information entropy does not have to be taken into account. This is because the packet is always received correctly in this case due to the use of a capacity-achieving code. Hence, such packet does not have to be included when forming the helper packet.

On the top of the diversity gain, the source information correlation further reduces the required average SNR, but it is in the form of a parallel shift of the outage curve. An interesting observation is that with $M = 2$, the diversity order being two is not affected by the information correlation, but with $M = 3$, the diversity order asymptotically approaches to four, if the information correlation is very close to one. The achievable diversity order assessment can further be extended to any integer M, where the achievable diversity order is not affected by the information correlation with M being an even value, while with M being odd, the achievable diversity order approaches $M + 1$ if the information correlation is close to one. The achievable diversity order with arbitrary M value is investigated in Section 4.6.

We summarize the main contributions of this dissertation as follows.

- Applying lossy forwarding technique with HARQ for parallel multihop transmissions for both fully and partial HARQ.

- Introducing CI as a threshold by which a relay node selects either forwarding the erroneous packets or requesting retransmission to reduce the number of end-to-end retransmissions, and hence it increases the end-to-end throughput.

- Providing verification of performance improvement by a semi-analytical method, including EXtrinsic Information Transfer (EXIT)-chart analysis.

- Presenting theoretical derivation of inadmissible rate region and upper bound of outage probability of feedback-assisted system with a helper transmission by considering the case that the per-packet entropy is larger than the channel capacity at a certain specified instantaneous SNR.

- Analyzing the effects of the source information correlation and the bit error rate of the helper packet on the inadmissible rate region and the upper bound of the outage probability of the M-in-1 helper transmission, theoretically.

- Providing proof for the achievability of Mth and $(M + 1)$th order diversities with M being even and odd, respectively, of M-in-1 helper transmission in

block fading channels.

1.3 Dissertation Outline

The common theme of this dissertation is the design and analysis of wireless communication systems with feedback over Rayleigh fading channel by exploiting the source correlation. The major goal is to create a reliable-and-robust cooperative wireless communication, which is indicated by high throughput performance. The key to achieving this goal is to exploit the beneficial nature of the correlated packets in the network. The reliability can be maintained high by utilizing HARQ via the joint design of network and channel coding scheme. On the other hand, significant increases in the network throughput can be achieved by decreasing the number of retransmissions in the network. Therefore, the trade-off between reliability and robustness is of the major scope of this research. In this case, the robustness is shown by the achievable diversity order.

For better understanding the main part of this dissertation, some basic concepts and background knowledge about information theory and wireless communication theory are provided in Chapter 2. The main part is divided into two, multihop transmission in Chapter 3 and single-hop transmission in Chapter 4. Eventually, we present the conclusions and future work in Chapter 5.

Part I: Chapter 3. This part deals with LF HARQ techniques for parallel multihop transmission, which utilizes the knowledge of the correlation between the information sequences in the decoding process. Two LF HARQ techniques are considered in this chapter: Fully-LF HARQ and Partially-LF HARQ. With Fully-LF HARQ, the relay nodes always forward erroneous packets and the transmission involve end-to-end ARQ protocol. With Partially-LF HARQ, a relay node decides either forwarding the erroneous packet or requesting retransmission based on CI. Therefore, Partially-LF HARQ has a control to guarantee at least one connection, where errors are not introduced in the relay before re-encoding, is established. The brief mathematical expression for the CI calculation is provided in this chapter. The system performances are evaluated through simulations, and the performances are compared with existing techniques.

Part II: Chapter 4. This part deals with the analysis of achievable diversity order in a single link, where the number of retransmission is limited to one. Moreover,

the retransmission of M unrecovered packets is combined into one transmission in the form of a helper packet. The information theoretical limit of the system is given in this chapter. Furthermore, the inadmissible rate region with $M = 2$ and $M = 3$ are provided at first. Then, the outage probabilities and upper bound approximation are theoretically derived. Afterward, this chapter presents the numerical analyses and reviews the influence of unequal power or redundancy allocation between the helper and information packets. Eventually, the achievable diversity order analysis for any integer M is given in this chapter.

Chapter 2

Preliminaries

This chapter provides the preliminary definitions and necessary basic knowledge for the forthcoming chapters. First of all, an overview of entropy and mutual information, and their properties are given in Section 2.1. Then, basic communication systems and Shannon's source-channel separation theorem are briefly discussed in Section 2.2.

The fading channel and the diversity technique for mitigating the fading effects are discussed in Section 2.3. Then, the overview of the error control techniques to improve the performance of a communication system is given in Section 2.4. Section 2.4 also provides the turbo encoding-decoding techniques which are utilized in Chapter 3. This chapter briefly introduces the LF techniques employing turbo encoding as well as the M-in-1 helper transmission in Section 2.4, of which the details are discussed in Chapter 3 and Chapter 4, respectively. In addition, a tool for the analyses of convergence property of iterative decoding such as turbo decoding, EXIT chart, is given in Section 2.4.5.

Finally, to support the theoretical derivation of M-in-1 helper transmission in Chapter 4, the fundamental of *the theorem for multiple sources coding with a helper* including the achievable-rate-region analyses, and the relationship between the entropy rate and packet-wise transmission are given in Section 2.5 and Section 2.6, respectively.

The following notations are used throughout the dissertation. Vectors are expressed with bold lowercase and scalars with standard text notation. The probability function is expressed by $\mathbb{P}(\cdot)$. Operators $\oplus$ and $*$ indicate binary XOR and convolution operations, respectively, e.g., $\alpha * \beta = \alpha(1 - \beta) + (1 - \alpha)\beta$.

Function $H_b(\cdot)$ denotes the binary entropy function where $H_b(\alpha) = -\alpha \log_2 \alpha - (1-\alpha) \log_2(1-\alpha)$. For M-in-1 helper transmission, we use $M2$ and $M3$ to denote the schemes with $M = 2$ and the $M = 3$, respectively.

2.1 Entropy and Mutual Information

Entropy measures the average uncertainty inherent in the distribution of a random variable. If a random variable has an entropy of α, we gain information α when we get a signal that tells us the value of that random variable, i.e. the value eliminates the uncertainty. Let X be a random variable taking identical and independently distributed (i.i.d.) values from a finite alphabet $\mathscr{X}$ with a probability mass function (pmf) $p_X(x) = \mathbb{P}(X = x)$, in short $X \sim p_X(x)$, the entropy of X is defined by

$$H(X) = -\sum_{x \in \mathscr{X}} p_X(x) \log p_X(x). \tag{2.1}$$

Note that entropy is always positive, i.e. $H(X) \geq 0$, since $0 \leq p_X(x) \leq 1$ for all $p_X(x)$.

Let $Y \sim p_Y(y)$ be another i.i.d. random variable taking values from a finite alphabet $\mathscr{Y}$, the joint entropy $H(X,Y)$ measures the uncertainty in the joint distribution of a the pair random variables $(X,Y) \sim p_{XY}(x,y) = \mathbb{P}(X = x, Y = y)$. It is defined by

$$H(X,Y) = -\sum_{x \in \mathscr{X}} \sum_{y \in \mathscr{Y}} p_{XY}(x,y) \log p_{XY}(x,y). \tag{2.2}$$

The conditional entropy $H(Y|X)$ refers to the average entropy of Y conditional on the value of X, averaged over all possible values of X, as

$$H(Y|X) = -\sum_{x \in \mathscr{X}} p_X(x) H(Y|X = x), \tag{2.3}$$

where $H(Y|X = x) = \sum_{y \in \mathscr{Y}} p_{Y|X}(y|x) \log p_{Y|X}(y|x)$. We can further derive (2.3) into

$$H(Y|X) = -\sum_{x \in \mathscr{X}} p_X(x) \sum_{y \in \mathscr{Y}} p_{Y|X}(y|x) \log p_{Y|X}(y|x)$$

$$= -\sum_{x \in \mathcal{X}} \sum_{y \in \mathcal{Y}} p_{XY}(x,y) \log p_{Y|X}(y|x). \tag{2.4}$$

The chain rule for joint entropy states that the total uncertainty about the value of X and Y is equal to the uncertainty about X plus the uncertainty about Y once we know X, or the uncertainty about Y plus the uncertainty about X once we know Y. Thus, it is expressed by

$$\begin{aligned} H(X,Y) &= H(X) + H(Y|X) \\ &= H(Y) + H(X|Y). \end{aligned} \tag{2.5}$$

In general, if we have random variables $X_1, X_2, \cdots, X_n$, then

$$H(X_1, X_2, \cdots, X_n) = \sum_{i=1}^{n} H(X_i | X_{i-1}, \cdots, X_1). \tag{2.6}$$

Mutual Information

The mutual information $I(X;Y)$ measures how much the realization of random variable Y tells us about the realization of X or vice versa. In other words, it also measures how much the entropy of X is reduced if we know the realization of Y or vice versa. Thus,

$$I(X;Y) = H(X) - H(X|Y) = H(Y) - H(Y|X) = I(Y;X). \tag{2.7}$$

Note that the mutual information between a random variable and itself is its entropy, e.g. $I(X;X) = H(X)$.

2.2 Communication Systems and Separation Theorem

General system model of point-to-point (p2p) communication is shown in Figure 2.1. The mission of the system is to deliver information from a source to a destination over a channel. We assume a discrete memoryless source $\mathcal{S}$ emitting binary sequence $\boldsymbol{u}$ with a finite length k per-transmission in the form of a packet, referred to as the information packet. The information packet $\boldsymbol{u}$ is first encoded by the channel encoder to add redundancy for the error correcting at the destination. Then, the output of the channel encoder, $\boldsymbol{w}$, is mapped into a sequence of signal waveforms

$$H(\mathcal{S})=R \longmapsto Q \longmapsto C$$

| Source $\mathcal{S}$ | $\boldsymbol{u}$ | Channel Encoder | $\boldsymbol{w}$ | Mapper | $\boldsymbol{x}$ | Channel | $\boldsymbol{y}$ | Demapper | $\hat{\boldsymbol{w}}$ | Channel Decoder | $\hat{\boldsymbol{u}}$ | Destination |

$$|\boldsymbol{u}| = \mathtt{k} \qquad\qquad |\boldsymbol{x}| = \mathtt{n}$$

$$\longmapsto\!\!\!\!-\!\!\!\!-\!\!\!\!-R_{T_x}\!\!\!\!-\!\!\!\!-\!\!\!\!-\!\longmapsto$$
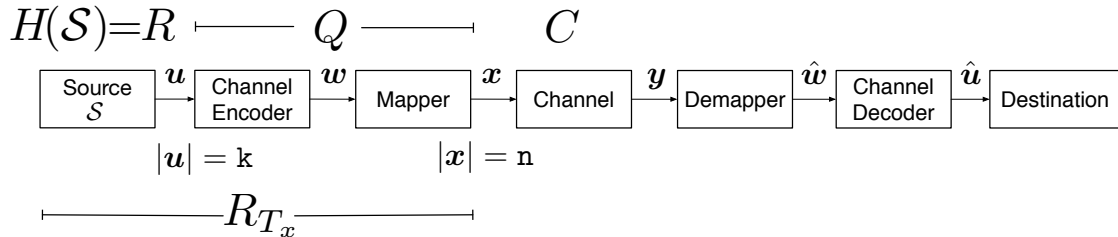
Figure 2.1: System model of a general communication system.

$\boldsymbol{x}$ to be transmitted through the channel, according to the modulation scheme of the system. At the destination, the received coded packet, $\boldsymbol{y}$, is first demapped into $\hat{\boldsymbol{w}}$ and then channel-decoded into $\hat{\boldsymbol{u}}$.

It is obvious that we can identify $\hat{\boldsymbol{u}}$ for the communication systems with noiseless channels. However, information distortion can be produced when noise is introduced to the channel. Let P_b denotes the probability of bit error; the noise creates a non-zero P_b in transmission. Introducing a simple channel coding like a repetition code or a linear error correcting code will reduce P_b, but simultaneously reduce the transmission rate R_{T_x}. Let R and Q denote the source rate and the normalized spectrum efficiency including channel coding rate and modulation multiplicity, respectively, then R_{T_x} is equal to Q when the entropy coding is used for source coding. Moreover, since we assume finite length packet, as described in the previous section, the packet-wise entropy is $H(\mathcal{S}) = R = 1$.

Shannon showed that a source could be channel encoded in a way that makes P_b arbitrarily small [54]. There is a non-negative number C with the following property. For any $\epsilon > 0$ and $R_{T_x} < C$, for large enough N, there exists a block code of length N and rate larger than or equal R_{T_x} and a decoding algorithm such that the maximal P_b is less than ϵ [55]. In a simple word, the maximum transmission rate with vanishing P_b is C, known as the channel capacity.

Applying source encoding or compression to the information before channel encoding brings up the question: is a two-stage encoding method as good as any method to transmit the information over a noisy channel? Shannon's source-channel separation theorem shows that we can design the source and channel code separately and combine the results to achieve optimal performance [54].

Let us consider the source emitting the binary sequence $\boldsymbol{u}$ with period T_s. The information rate of such source is $\frac{H(\mathcal{S})}{T_s}$ $^{\text{bits}}/_{\text{second}}$. Suppose that $\mathtt{k}$ information bits is channel encoded and mapped to modulation constellation points such that the

output length is **n** bits, then transmitted via a discrete memoryless channel with period T_c seconds, the maximum possible data transfer rate would be $\frac{C}{T_c}$ $^{\text{bits}}/_{\text{second}}$. The noisy-channel coding theorem states the following [54]. If $\frac{R}{T_s} \leq \frac{C}{T_c}$, then there exists a coding scheme that guarantees arbitrarily small P_b transmission. Conversely, if $\frac{R}{T_s} > \frac{C}{T_c}$, the communication cannot be made reliable, i.e. P_b cannot be made as small as desired.

Note that $\frac{T_c}{T_s} = \frac{\text{k}}{\text{n}} = Q$, and therefore the reliability of the communication system in noisy-channel with lossless source coding is constrained by

$$RQ \leq C. \tag{2.8}$$

Since the output of channel decoder may still contain errors, if (2.8) is satisfied, a distorted information may be received. Now, let $d(s, \hat{s})$ be an average distortion measure with rate-distortion function $R(\mathcal{D})$, the lossy Shannon's source-channel separation theorem states that if

$$R(\mathcal{D})Q \leq C, \tag{2.9}$$

then there exists a sequence of codes such that $\lim_{\text{n} \to \infty} E[d(X_i, \hat{X}_i)] \leq \mathcal{D}$, where $i = 1, 2, 3, \cdots$. When a binary source is concerned, $\mathcal{D}$ is equivalent to P_b.

2.3 Fading Channels

Typically, all the transmitted packets are corrupted by the addition of white Gaussian noise at the receiver. However, the most distinctive features of a wireless channel come from the time-varying nature of the physical media rather than the effect of the noise. In a wireless environment, the path between the source and destination is subject to various obstacles and reflections. The received composite packet's signal is composed of many component signals such as reflected, diffracted, scattered, and the direct signal from the source. In this case, the path lengths of the direct, reflected, diffracted, and scattering signals are different, resulting in different arrival timing at the destination, and each experiencing different attenuations and phase rotations. Consequently, the destination receives a superposition consisting of several component signals having different phases, amplitudes, and times of arrival. The fluctuation of received signal strength due to multipath is known as *fading*.
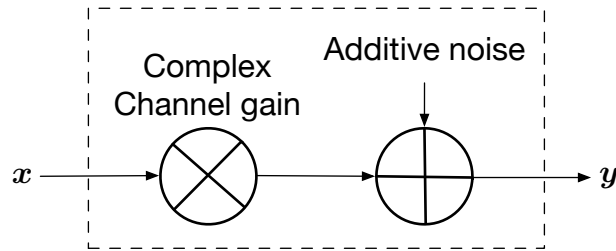
Figure 2.2: An additive-noise flat fading channel.

The time-varying characteristic of wireless channels is dominated by two factors: large-scale and small-scale propagation effects. The large-scale propagation effect is caused by path loss and shadowing as the transmit packets travel over distance and get blocked by large obstacles. In this work, we are more interested in smaller-scale effects, which is due to the multipath propagation and is called *fading*.

Because of the dispersion due to multipath propagation, the transmitted packet experiences either flat or frequency selective fading. If the symbol period is much larger than the multipath time delay spread of the channel, or equivalently if the coherence bandwidth of the channel is much larger than the bandwidth of the signal, the received packet experiences *flat fading*. In this case, the impact of the arrival time dispersion of the component signals can be eventually ignored. Hence, all frequency components of the signal experience the same fading variation, i.e. the same attenuation and phase shift. Conversely, if the symbol period is smaller than the multipath time delay spread of the channel, or equivalently if the coherence bandwidth of the channel is less than the bandwidth of the signal, the received signal experiences *selective fading*.

The selective fading channel is usually modeled as a time-varying tapped delay line with complex-valued coefficients. Transmission over this channel results in inter-symbol interference (ISI), and hence additional signal processing for equalization is required. Moreover, since the goal of this dissertation is to analyze the performances of error control techniques, the utilization of equalizer is out of the scope.

The flat fading channel is modeled as an equivalent time-varying one-tap filter with a complex-valued coefficient or channel gain, as illustrated in Figure 2.2. When the channel gain is modeled as a zero-mean complex Gaussian random variable, and the amplitude is Rayleigh distributed, such a channel is called a Rayleigh fading.

Accordingly, the received packets can be expressed as

$$\boldsymbol{y} = h \cdot \boldsymbol{x} + \boldsymbol{v}, \tag{2.10}$$

where h and $\boldsymbol{v}$ represent the complex channel gain and the complex zero mean AWGN vector with variance σ^2, respectively.

For the applications requiring strict delay constraints such as real-time voice and video transmission, a packet can only span a finite number of fading blocks. In this dissertation, we focus on the extreme case where a packet duration is equal to only one fading block, i.e., the so-called quasi-static fading channel or block fading channel. With the block Rayleigh fading assumption, h is constant within a packet, and varies independently packet-by-packet; it has Rayleigh-distributed amplitude $|h|$ with $E[|h|^2] = 1$. The instantaneous received SNR for the transmission of the packet $\boldsymbol{x}$ is then given by $\gamma = \frac{|h|^2}{\sigma^2}$. The probability density function (*pdf*) of γ is

$$p(\gamma) = \frac{1}{\Gamma} \exp(-\frac{\gamma}{\Gamma}), \tag{2.11}$$

with $\Gamma = \frac{E[|h|^2]}{\sigma^2}$, where Γ is the average SNR.

The performance of a packet transmission over fading channels can be characterized into two categories: the average packet error probability and the outage probability. The average packet error probability is the packet error ratio (PER) averaged over the distribution of γ for a specific practical code, while the outage probability, P_{out}, is the average probability that the received instantaneous SNR is below a threshold value [56]. For example, the outage probability of p2p communications over Rayleigh fading channels, relative to a threshold γ_0, is given by

$$P_{\text{out}} = \mathbb{P}(\gamma < \gamma_0) = \int_0^{\gamma_0} p(\gamma) d_{\gamma} = 1 - \exp(-\frac{\gamma_0}{\Gamma}). \tag{2.12}$$

It should be emphasized that the block fading assumption not practical if we use a very long sequence for error protection, even though the assumption is used for the ease of analyses. However, it is quite straightforward to replace the signal detector by an equalizer which allows us to still assume block fading in the frequency-selectivity [57].

2.3.1 Diversity

Diversity is utilized in wireless communication systems to combat fading. It is based on the fact that independent signal paths have a low probability of simultaneously encountering deep fades. These independent paths are combined at the receiver in such a way so that the fading of the resultant signal is reduced. The number of independently fading paths characterizes the diversity in a system, which is known as the diversity order.

The diversity achieving of a system can be evaluated by their average PER or outage probability performance. The average PER performance, $\overline{\text{PER}}$, can be expressed by [56]

$$\overline{\text{PER}} = \mathsf{c}\Gamma^{-\Theta}, \tag{2.13}$$

where c is a constant that depends on the specific modulation and coding, and Θ is the *diversity order* of the system. The diversity order shows how the slope of the $\overline{\text{PER}}$ as a function of Γ changes with diversity. Likewise, the diversity order also indicates how the slope of an outage probability performance as a function of Γ changes with diversity.

There are many ways to obtain diversity. Common diversity techniques include time and frequency. With frequency diversity, the signals carrying the same information are transmitted on several carrier frequencies. If the separation between any two carrier frequencies exceeds the coherence bandwidth, then each received version can be considered to undergo independent fades. The frequency diversity is typically exploited in the systems with frequency division multiplexing (FDM), including Orthogonal FDM (OFDM).

Diversity over time can be achieved by transmitting the same information at different times, where the time difference coding is greater than the channel coherence time. The diversity can also be achieved by (repetition) coding the information and dispersing the coded symbols over time by an interleaver so that different parts of the codewords experience independent fades. Hence, the time diversity is typically exploited in the system utilizing ARQ like, for example, M-in-1 helper transmission in Chapter 4.

Additionally, diversity can also be obtained over space in a channel with multiple transmit and/or receive antennas. The space can also refer to the virtual transmit antennas constructed from multiple relays as in parallel multihop network topology

as discussed in Chapter 3.

2.4   Error Control

In wireless communication systems over fading channels, transmissions experience difference channel realizations, transmission-by-transmission. Each transmission introduces errors to the transmitted signals. Therefore, error control techniques are important to establish robust data transmission of wireless communication systems. In general, two techniques are widely used for the error control: (1)ARQ, to detect errors by using feedback channel, and (2)FEC, to correct errors even without a feedback channel. Additionally, both techniques can be combined to be a technique known as HARQ.

2.4.1   Forward Error Correction (FEC)

FEC or channel coding appends redundancy when encoding an information packet so that the receiver can correct the errors occurring during the process of transmission. Another purpose of adding the redundancy is to detect errors when the number of errors in a packet exceeds the FEC's error correction capability. Based on the presence or absence of memory, FEC can be classified into two types: convolutional codes and block codes.

Block codes have no memory since it collects `k` information bits before the processing and has no retention within the encoding system of information related to the previous sample bits. Block codes can be utilized for: (1)error correction, for example: Hamming Codes, Low Density Parity Check (LDPC) Codes, Bose-Chaudhuri-Hocquenghem (BCH) Codes, Reed-Solomon Codes, and (2)error detection, for example, CRC and Parity Check Codes.

Convolutional codes have memory, where each bit in the output stream is not only dependent on the current bit, but also on those processed previously. Convolutional codes are utilized only for error correction and are widely exploited by serial concatenated codes (SCC) [58] and parallel concatenated codes (PCC) [59], as illustrated in Figure 2.3 and Figure 2.4, respectively.

With SCC, the outer encoder is concatenated with the inner encoder via an interleaver. The inner encoder protects the data by correcting random errors. However, some errors may remain so that the outer encoder provides protection
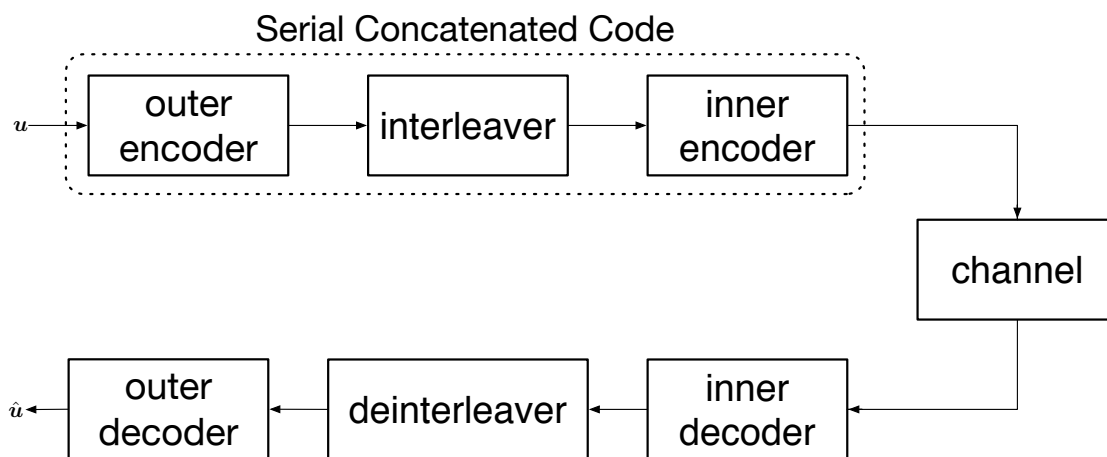
Serial Concatenated Code

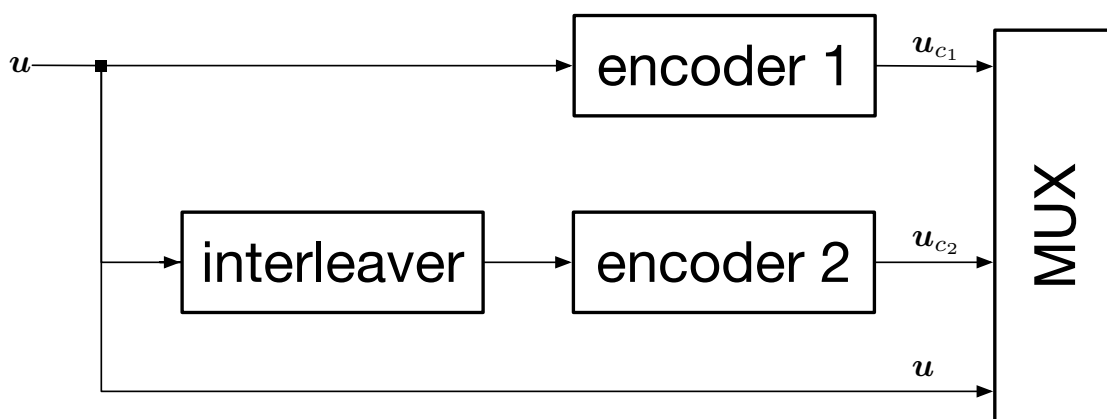Figure 2.3: FEC with serial concatenated code.

Figure 2.4: FEC with parallel concatenated code.

against these errors. With PCC, the parallel codeword is obtained from the first code by interleaving the information part and then encoded by the second encoder. The interleaver enables an iterative decoding at the receiver. We utilize both SCC and PCC for the proposed LF HARQs, where their performance can be evaluated by examining the convergence behavior of the iterative decoding, as given in Section 2.4.5.

2.4.2 Automatic Repeat reQuest (ARQ)

FEC works on the assumption that the information flow only towards one direction, i.e. simplex channel. However, if the channel is duplex, the acknowledged information can be sent back to the transmitter via a feedback channel. In this case, before transmitting the packet, the information packet is encoded by CRC for the error detection at the receiver. The receiver sends either ACK or NACK signal via the feedback channel to indicate respectively whether or not the transmitted data packet has been correctly recovered. In ARQ system design, it is commonly assumed that feedback channel is error-free because the information to be transmitted via the feedback channel is only one bit, i.e. ACK and NACK.

Based on the retransmission strategies, there are three basic protocols of ARQ schemes: stop-and-wait, go-back-N, and selective-repeat [18]. Stop-and-wait is the simplest protocol. After transmission, the transmitter waits for a feedback from the receiver. If an ACK is received, the next message is transmitted; if a NACK is received, the message is retransmitted. Packet retransmission continue until an ACK is received. With the go-back-N protocol, groups of N packets are transmitted, and each group requires only one feedback, i.e. ACK or NACK. If one or more packets in a group is/are received incorrectly, the last N packets are retransmitted. This scheme eliminates the idle time between transmissions for every message, which is a negative point of the stop-and-wait scheme. Selective-repeat protocol further improve the efficiency of go-back-N protocol by retransmitting only packets that have not been received correctly. However, the go-back-N protocol requires large buffer at the transmitter and the receiver, and the selective-repeat protocol requires, in theory, infinite size of buffer.

Also, there are several derivative techniques that eliminate the throughput loss due to the round trip delay happening to the stop-and-wait and go-back-N ARQ. However, this dissertation does not focus on the ARQ protocol itself, but it does

focus on the forwarding techniques for parallel multihop transmission in Chapter 3 and techniques for encoding packet in Chapter 4. Therefore, for the ease of analysis, we assumed the simplest ARQ protocol, i.e. stop-and-wait ARQ.

2.4.3   Hybrid ARQ (HARQ)

The term HARQ is used to represent the joint used of FEC and ARQ. With HARQ, FEC is first utilized to correct the errors in the information part of the received packet, however, if the number of errors exceeds its correction capability, which is found by error detection code such as CRC after the FEC decoding, then a retransmission is requested. This causes the decoder structure simple while improving the reliability and enhancing the throughput. Therefore, HARQ can eliminate the drawbacks of both/either FEC and/or ARQ schemes/alone.

The HARQ can be classified into two types: type-I HARQ and type-II HARQ [60]. For type-I HARQ, retransmitted packet is FEC-decoded, and the packet is discarded if errors are detected after the FEC-decoding. Hence, the receiver combines the current packet with none of the previously received packets in decoding. This is inefficient because even if there are some bits in error, the data still contains valuable information. For type-II HARQ, all transmitted packets associated with the same information data block are jointly decoded instead of discarding the packet of which decoding is failed, thus reducing the probability of decoding error.

The type-II HARQ can be further classified into two categories: the first category is often called *Chase combining* (CC), where all retransmitted packets, including the parity part, are identical. The other is often called incremental redundancy (IR), where all retransmitted packets have different redundancy information. One kind of IR employs the rate compatible punctured code (RCPC), as proposed, for example, in [35]. Another kind of IR uses iterative soft-decision-based FEC decoders [61], such as Turbo codes, where soft information represented by the log likelihood ratios (LLRs) is exchanged between the constituent BCJR decoders [62]. Furthermore, the employment of IR has found applications in cooperative networks, for examples, the techniques proposed in [63] and [64], as well as our proposed technique in Chapter 3.
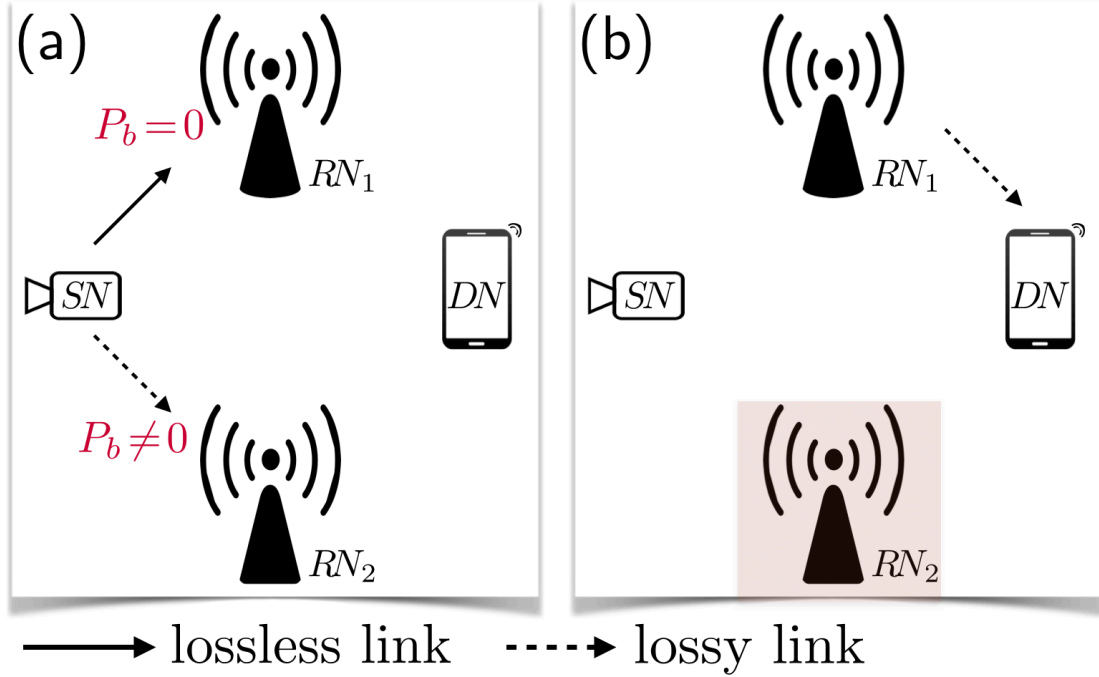
Figure 2.5: With conventional forwarding techniques, RN_2 keep silent by discarding erroneous packets instead of forwarding those to DN.
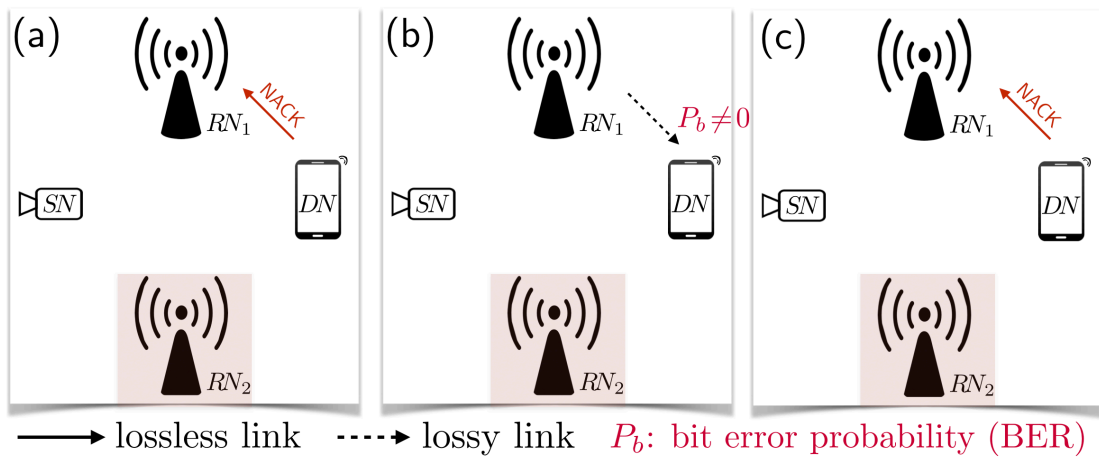
Figure 2.6: SHARQ I utilizing Partial ARQ.
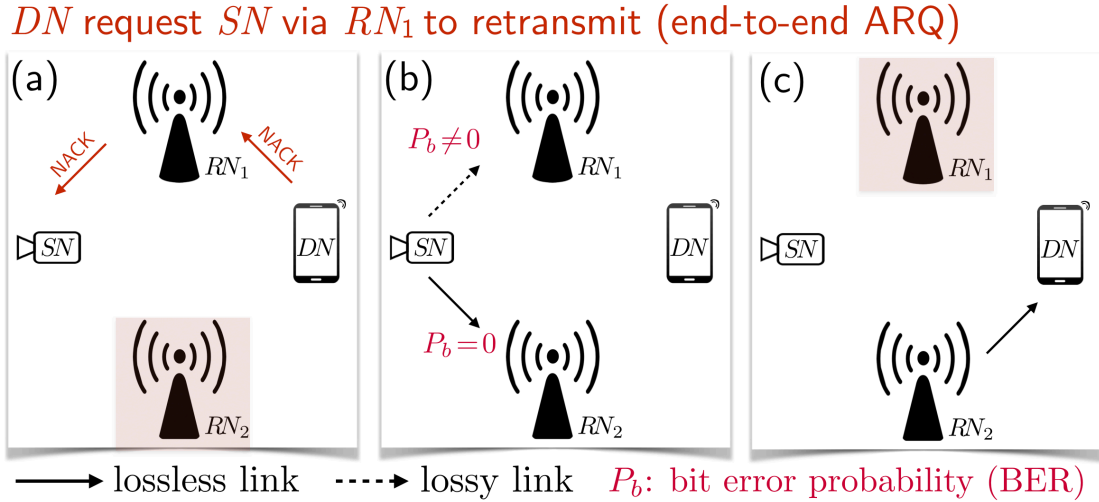
Figure 2.7: SHARQ II utilizing end-to-end ARQ.

2.4.4 HARQ-Aided Forwarding Techniques

In this subsection, we briefly summarize the forwarding technique protocols utilized in parallel multihop transmission. The differences between the conventional and the proposed techniques are shown in Appendix A. Let SN, RN, DN denote the source node, relay node, and destination node, respectively. In conventional forwarding techniques, RN always discards erroneous packets instead of forwarding those to the node of the next hop, as illustrated in Figure 2.5. When DN receives a packet in error after decoding, it can decide to (1) ask RN to retransmit, referred to as Partial ARQ, or (2) ask SN via RN to retransmit, referred to as end-to-end ARQ.

Smart HARQ (SHARQ), proposed in [30], follows the conventional forwarding technique. The author proposed two types of SHARQ, SHARQ I and SHARQ II. With both types, the DN requests for retransmission only to the RNs from which the packets were sent whereas other RNs keep silent, as illustrated in Figure 2.6.a and Figure 2.7.a. SHARQ I applies Partial ARQ in the network, and accordingly, the DN will always request the RNs to retransmit until the packet successfully recovered, as shown in series of Figure 2.6.b and Figure 2.6.c. On the other hand, SHARQ II applies end-to-end ARQ in the network, and accordingly, the DN will always request the SN, via the RNs, to retransmit. Then, again all RNs forward the non-erroneous packets, and so on, as illustrated in series of Figure 2.7b and Figure 2.7c.
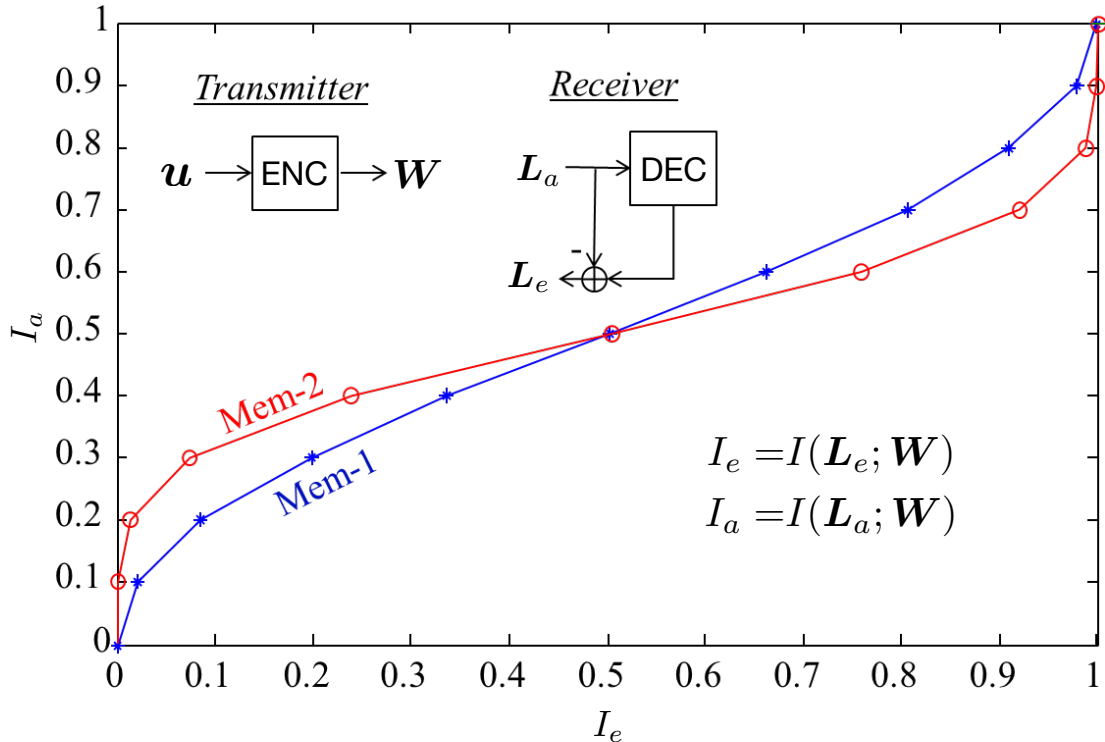
Figure 2.8: EXIT Chart of Convolutional codes decoder.

In contrast with the conventional, Fully-LF HARQ always forwards the erroneous packets, whereas Partially-LF HARQ relies on the CI whether or not to forward the erroneous packets. Furthermore, Fully-LF HARQ applies end-to-end ARQ, whereas Partially-LF HARQ applies Partial ARQ. Both techniques are discussed in detail in Chapter 3.

2.4.5 EXIT Chart

In this subsection, we provide the EXIT chart analyses of our proposed encoding scheme used in the proposed LF HARQs, to show the advantage of using QPSK mapper with non-Gray compared to that with Gray, as well as to verify the numerical results presented in Section 3.3.

EXIT Chart is first introduced by Stephan ten Brink in [65]. It can be used for visualizing the flow of extrinsic information exchange between the inner and outer decoders of SCC, or between the upper and lower decoders of PCC. It also visualizes the convergence behavior of iterative decoding algorithms; thereby we

can predict the convergence property, the algorithms based on which we can design good codes as well. Specifically, we can achieve infinitesimally low BER if the EXIT curves reach the [1.0,1.0] mutual information (MI) point, while keeping the convergence tunnel open.

Generate the EXIT Curve of the Outer Code

Figure 2.8 illustrates an example of EXIT chart, showing the EXIT curves of memory-1 and memory-2 convolutional codes decoders that are utilized in Chapter 3. The sequence of information bits **u** is encoded by ENC with generator polynomials of $G = [3, 2]_8$ and $G = [7, 5]_8$ for the memory-1 or the memory-2 codes, respectively, into $\boldsymbol{W}$. At the decoder, DEC, of the receiver side, we generate *a priori* LLR $\boldsymbol{L}_a$ as

$$\boldsymbol{L}_a = \sigma^2/2 \cdot \boldsymbol{W} + \boldsymbol{V}, \tag{2.14}$$

where $\boldsymbol{W} \in \{+1, -1\}$ denotes the binary phase shift keyed (BPSK) sequence of $\boldsymbol{W}$ and $\boldsymbol{V}$ denotes zero mean AWGN. It is necessary to assume that a large enough interleaver is employed to assure statistical independence and Gaussian distribution of $\boldsymbol{L}_a$.

The information transfer function $\mathcal{T}_f$ is measured as

$$I(\boldsymbol{L}_e; \boldsymbol{W}) = \mathcal{T}_f(I(\boldsymbol{L}_a; \boldsymbol{W})), \tag{2.15}$$

where the input, $I(\boldsymbol{L}_a; \boldsymbol{W})$, denotes the MI between the transmitted encoded bit sequence $\boldsymbol{W}$ and the *a priori* LLR, and the output, $I(\boldsymbol{L}_e; \boldsymbol{W})$, denotes the MI between $\boldsymbol{W}$ and the extrinsic LLR. We use I_a to denote *a priori* MI $I(\boldsymbol{L}_a; \boldsymbol{W})$ and I_e to denote extrinsic MI $I(\boldsymbol{L}_e; \boldsymbol{W})$. It is found that MI is a function of the variation of LLR. Given $0 \leq I_a \leq 1$, we can convert the MI value to its corresponding LLR variation σ by an approximation given by [66]

$$\sigma(I) \approx \left[-\frac{1}{H_1} \log_2(1 - I^{\frac{1}{H_3}}) \right]^{\frac{1}{2H_2}}, \tag{2.16}$$

where $H_1 = 0.3073$, $H_2 = 0.8935$, and $H_3 = 1.1064$, and $I = I_a$ or I_e, depending on LLR $= \boldsymbol{L}_a$ or LLR $= \boldsymbol{L}_e$, respectively. It should be noted that for inner decoder, the channel SNR is also an input parameter.
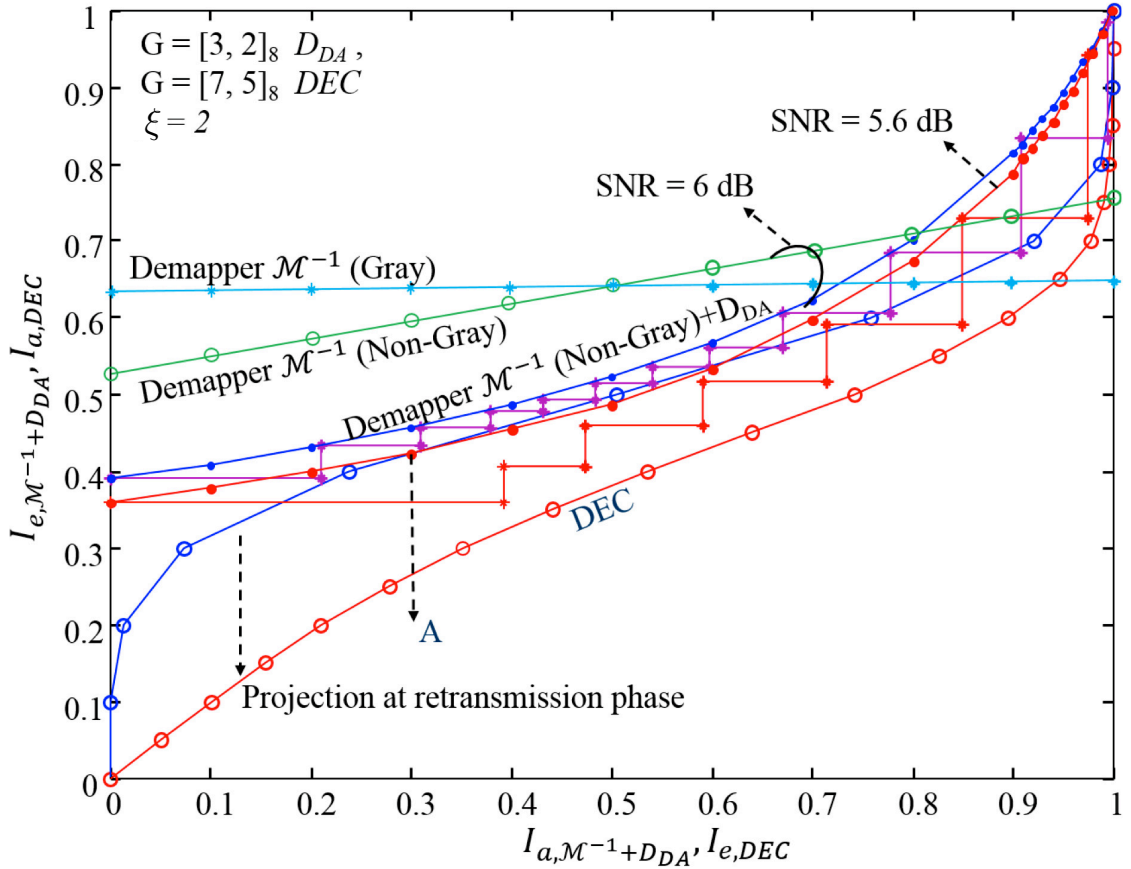
Figure 2.9: EXIT Chart of Demapper+D_{DA} for single snapshot of channel realization and DEC.

The EXIT Chart Analyses

Even though we use the block-Rayleigh fading channel assumption in the parallel multihop transmission system, link-by-link as well as transmission-by-transmission, evaluating the convergence property of the proposed signal detection and decoding technique in static AWGN channel provides us with an in-depth understanding of the behavior of the decoder.

Fig. 2.9 shows the EXIT curves of $\mathcal{M}^{-1}$ using QPSK with Gray and non-Gray mapping, assuming the receive SNR being 6 dB, for comparison. It is found that with Gray mapping, the EXIT curve is entirely flat regardless of the *a priori* information. It means that the feedback from DEC does not help $\mathcal{M}^{-1}$ to improve performance through the iterative process. On the other hand, by using non-Gray mapping, the EXIT curve rises up as the given *a priori* information increases, but

still, it can not reach a point close enough to (1.0,1.0) MI point. The extrinsic MI exchange between the $\mathcal{M}^{-1}+D_{DA_t}$ and DEC_t is evaluated. The structure of Turbo HARQ technique enables the use of different doping rate, ξ, of the DA transmission-by-transmission to achieve better matching of the EXIT curves. The ξ_t value is determined by evaluating the EXIT curves of inner and outer codes so that they are best matched with the all possible values of the ξ while keeping the convergence tunnel open. With a proper setting of code parameters, no retransmission is required if its received SNR is larger than the threshold at which the convergence tunnel opens.

Suppose that the destination node combines the two received packets, the original transmission, and its subsequent first retransmission. Fig. 2.9 shows the EXIT curve where D_{DA} uses a generator $[3,2]_8$ non-systematic non-recursive convolutional code (NSNRCC), and DEC uses a generator $[7,5]_8$ NSNRCC. The figure also shows the trajectory of the MI exchange with the maximum iteration of 350. We set the interleaver length to $10,000$. The DEC's EXIT curve is obtained after the one round of HI-VI from the two different decoders for (re)transmitted packets until no relevant improvement in MI between $\boldsymbol{u}$ and $\boldsymbol{L}_{a,DEC}^u$ is achieved.[1]

We set the doping rate $\xi = 2$ for the two transmissions, and the instantaneous SNR is kept at 6 dB. It is found that the $\mathcal{M}^{-1}+D_{DA_m}$ makes the convergence tunnel open until a point very close to the (1.0, 1.0) MI point. This means that no retransmission is needed. When SNR is 5.6 dB, the $\mathcal{M}^{-1}+D_{DA_m}$ curve intersects at the point "A". However, this problem can be solved with the help of VI that pushes down the decoder curve, resulting in better matching between Demapper$+D_{DA}$ and DEC curves. Moreover, the gap between the two curves can further be reduced by adjusting the doping rate [67].

2.5   Distributed Source Coding

Distributed source coding (DSC) refers to the problem of separate compression of correlated sources. Even though this dissertation does not touch upon the source coding or compression, the concept of DSC, especially with lossless source coding, is necessary for the theoretical limit analyses of the correlated sources. The origin of the concept is Slepian-Wolf Theorem, which characterizes the admissible rate

---

[1]In this sense, the EXIT Chart analysis provided in this section is based on [57] projection technique.

region of two correlated and independently compressed sources [68].

Slepian-Wolf Theorem. *The optimal rate region for distributed lossless source coding of two i.i.d. discrete memoryless sources $(X_1, X_2) \sim p_{X_1 X_2}(x_1, x_2)$ is the set of rate pairs (R_1, R_2) such that*

$$R_1 \geq H(X_1|X_2),$$
$$R_2 \geq H(X_2|X_1), \qquad (2.17)$$
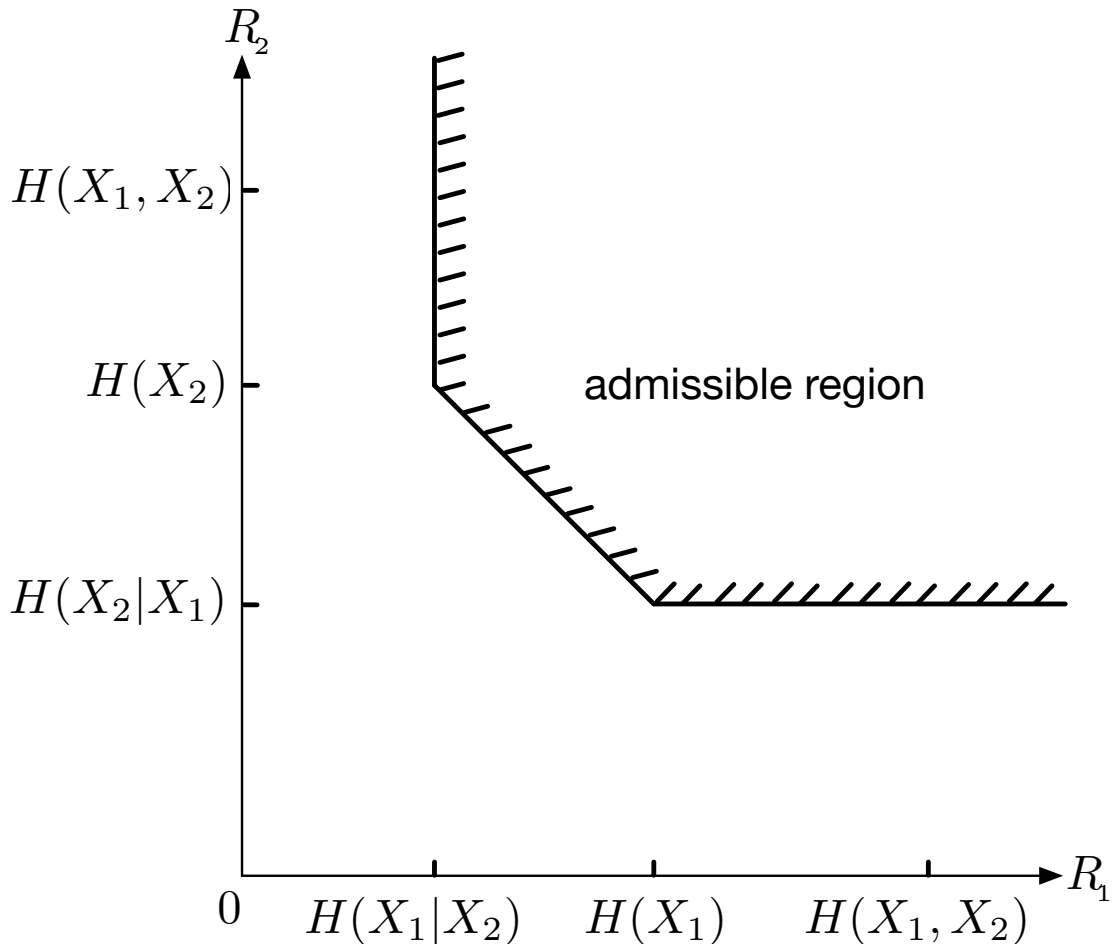$$R_1 + R_2 \geq H(X_1, X_2).$$

Figure 2.10: Slepian-Wolf rate region.

Figure 2.10 illustrates the Slepian-Wolf rate region. The theorem can be interpreted as the following. Suppose that we want to encode the two sources (X_1, X_2), if the encoder has access to both X_1 and X_2, it is sufficient to use rate

$H(X_1, X_2)$. For example, we can first encode X_1 with rate $H(X_1)$ bits per sample (*bps*), and based on the complete knowledge of X_1, we then encode X_2 with rate $H(X_2|X_1)$ *bps*. If we want to encode both X_1 and X_2 separately for a destination who want to reconstruct those, then rate $H(X_1) + H(X_2)$ is sufficient, i.e. we encode X_1 with rate $H(X_1)$ *bps* and X_2 with rate $H(X_2)$ *bps*. However, Slepian and Wolf have shown that it is still sufficient to use a total rate $H(X_1, X_2)$ for separate encoding, even for correlated sources.

The Slepian-Wolf theorem can be extended to DSC for an arbitrary number of sources. Let $(X_1, X_2, \cdots, X_n) \sim p_{X_1 X_2 \cdots X_n}(x_1, x_2, \cdots, x_n)$ be i.i.d., then the set of rate vectors $(R_1, R_2, \cdots, R_k)$ achievable for DSC with separate encoders and a common decoder is defined by [53]

$$\sum_{j \in \mathtt{S}} R_j \geq H(X(\mathtt{S})|X(\mathtt{S}^C)) \text{ for all } \mathtt{S} \subseteq [1:n]. \tag{2.18}$$

2.5.1 Distributed Source Coding with A Helper
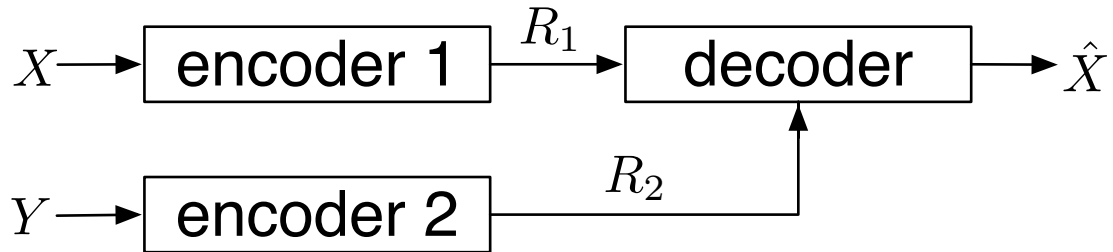
Figure 2.11: Distributed source coding with a helper.

Let us consider the one-helper DSC problem, where only one of the two sources $(X, Y) \sim p_{XY}(x, y)$ is to be recovered, and the encoder of the other source provides coded side information, known as the helper, as illustrated in Figure 2.11. The optimal source coding for source X with a helper Y is the set of rate pairs (R_1, R_2) such that [53, 69]

$$\begin{aligned} R_1 &\geq H(X|U), \\ R_2 &\geq I(Y;U) \end{aligned} \tag{2.19}$$

for some $p_{U|Y}(u|y)$, where U is a random variable taking i.i.d. values from a finite alphabet $\mathcal{U}$ and $|\mathcal{U}| \leq |\mathcal{Y}| + 1$. For example, if we encode Y with rate $R_2 = I(Y; \hat{Y})$,

then we need at least $R_1 = H(X|\hat{Y})$ to encode X.

Multiple Source Coding with A Helper. Similar to the Slepian-Wolf Theorem, we can generalize the one-helper DSC problem to the multiple number of sources. The optimal rate region for the source coding of $(X_1, X_2, \cdots, X_n)$ with a helper Y is the set of rate $(R_{X_1}, R_{X_2}, \cdots, R_{X_n}, R_Y)$ such that [53]

$$\sum_{j \in \mathtt{S}} R_{X_j} \geq H(X(\mathtt{S})|U, X(\mathtt{S}^C)) \text{ for all } \mathtt{S} \in [1:n],$$

$$R_Y \geq I(Y;U) \tag{2.20}$$

for some $p_{U|Y}(u|y)$ with $|\mathcal{U}| \leq |\mathcal{Y}| + 2^n - 1$.

For having a comprehensive survey and concepts on DSC, we refer the interested reader to [70, 71].

2.6 Relationship Between Entropy Rate and Packet-Wise ARQ

For a stationary stochastic process X_i, the entropy rate can be defined with the conditional entropy of the last random variable given the past, as [72]

$$H(\mathcal{X}) = \lim_{n \to \infty} H(X_n|X_{n-1}, X_{n-2}, \cdots, X_1). \tag{2.21}$$

Accordingly, if the source is time-correlated, the longer the observation, the more compressing possible, as illustrated in Figure 2.12. However, we use the assumption of observing finite bit sequence of the source when deriving the limit performance of M-in-1 helper transmission. This is because in many practical cases, a telecommunication technology standard commonly has regulated a fixed length of the packet. Furthermore, extremely long packet size causes high decoding latency. Moreover, the fixed packet size fit with the block fading channel assumption.

Therefore, in this dissertation, instead of compressing the information at the close-entropy-rate at the transmitter, we use the correlation among the packets to reduce the required SNR at the receiver.
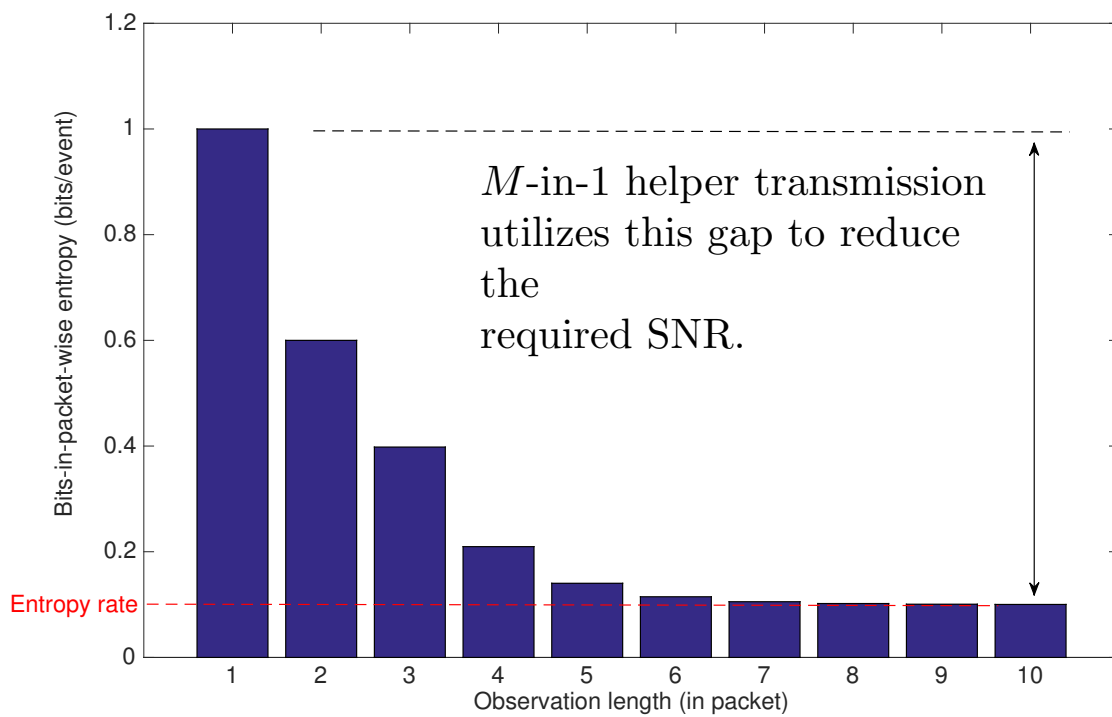
Figure 2.12: Illustration of the entropy rate for different size of packets.

Chapter 3

Multihop: Lossy Forwarding HARQ

In this chapter, we consider a problem in a parallel multihop transmission where there is no direct link between the source and the destination. We propose LF HARQ techniques which utilize the knowledge of the correlation between the information sequences in the decoding process. LF HARQ is supported by the extension of combining-after-decoding Turbo HARQ technique [67] for parallel relay networks. Erroneous packets may still contain useful information, especially for soft combining techniques. Therefore, not using the erroneous packet wastes the resources. With end-to-end ARQ protocol, one kind of LF HARQ is proposed to preserve packets received via as many parallel links as possible to achieve larger diversity gain, by always forwarding packet regardless of whether or not the information part of the packet contains errors. This technique is referred to as Fully-LF HARQ.

On the other hand, forwarding packets having significant distortions may invoke continuous retransmission requests to the source node, resulting in reduced end-to-end throughput. Moreover, the capability of correcting errors in a parallel network system at the destination node is made possible regardless of the quality of each link, so far as there is at least one connection where errors are not introduced at the relay before re-encoding. Furthermore, Fully-LF HARQ technique cannot guarantee the non-error packets at a relay. To solve this problem, we propose Partially-LF HARQ which introduces CI as a threshold by which a relay node decides either to forward the erroneous packet or to request retransmission.[1]

CI indicates how much amount of the information that can be relied on an

---

[1]Compared with CRC, CI has the capability of identifying multiple levels of reliability of the entire one block packet.

(a) Conventional HARQ   (b) Proposed Fully LF-HARQ   (c) Proposed Partially LF-HARQ
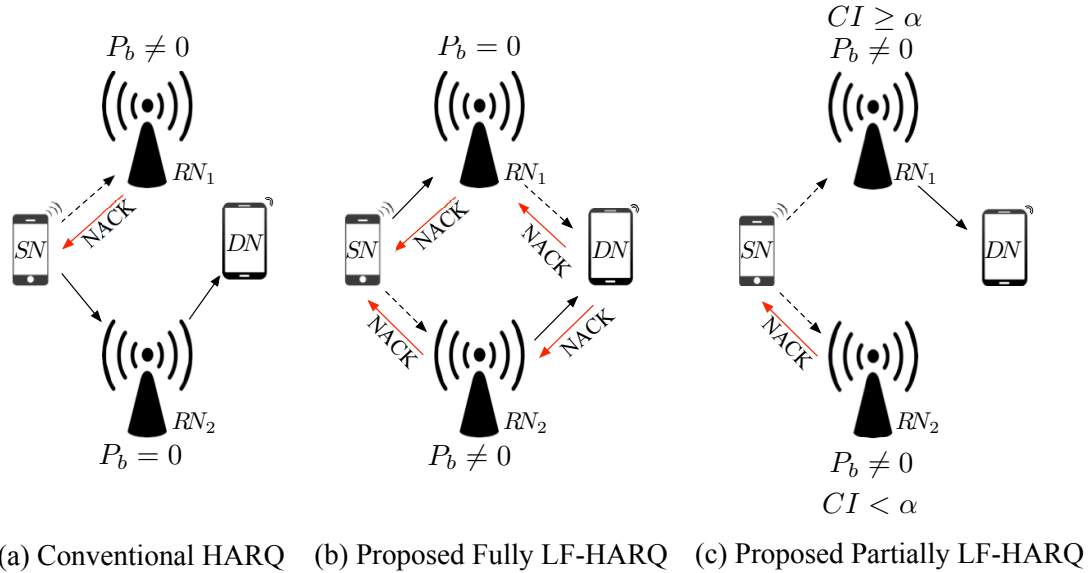
Figure 3.1: Multi-hop relaying comparison between the conventional and the proposed HARQs.

erroneous packet. The higher the CI, the more useful information can be expected. In the case of parallel multihop transmission, where parallel relay nodes receiving the packets broadcasted from the same source, the common information acquired by the relay nodes from the erroneous packet may exist, which is useful for the decoding with soft combining at the destination node. Therefore, CI plays an important role in deciding whether or not to forward the erroneous packet.

Nevertheless, by forwarding the erroneous packet with these techniques, there is a tradeoff between the packet loss ratio performance and the spectral efficiency (channel use). Partially-LF HARQ is a kind of optimized version for Fully-LF HARQ since the relay not always forward the erroneous packets but instead taking the decision based on the CI.

The remainder of this chapter is organized as follows. The considered system model is presented in Section 3.1. In Section 3.2, the proposed Fully-LF HARQ and Partially-LF HARQ mechanisms are introduced, where a brief mathematical expression for the CI calculation is provided. In Section 3.3, we evaluate the BER, the PER, and the throughput performances of Fully-LF HARQ and Partially-LF HARQ, and make a performance comparison with SHARQ I and SHARQ II [30] techniques. Finally, Section 3.4 summarize this chapter.
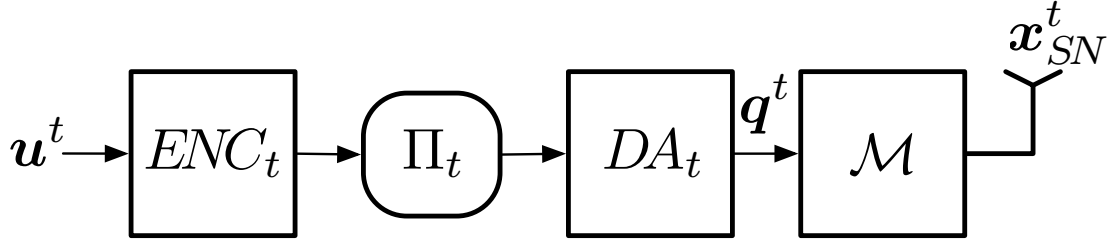
Figure 3.2: Block diagram of the source during transmit operations.

3.1 System Model

This section discusses the system model assumed in this chapter. We separate the model into (a) transmit operation, and (b) receive operation. The source node *SN* is in part of the transmit operation, while the destination node *DN* is part of the receive operation, and the relay nodes are in part of either transmit or receive operations, at alternate timings.

3.1.1 Transmit Operation

We consider a dual-hop parallel relay network where *SN* aims to transmit an information sequence to *DN* through two relay nodes RN_1 and RN_2 that are located physically separate in the parallel links, as shown in Figure 3.1.

We assume time-division channel allocation to guarantee orthogonal transmission, and hence one transmission cycle consists of three timeslots. In the first time slot, which is broadcasting, the node *SN* broadcasts its coded sequences $\boldsymbol{x}_{SN}$ to the nodes RN_1 and RN_2. In the following time slots, both relays transmit their coded sequence $\boldsymbol{x}_{RN_l}, l \in \{1, 2\}$ to the destination *DN*, sequentially. We consider a static channel within one block but varying link-by-link as well as transmission-by-transmission during HARQ rounds due to the block fading assumption. We use the terminology transmitting nodes and receiving nodes, for referring to the source node and the relay nodes for the transmit operation, and the relay nodes and the destination node for the receive operation, respectively.

Figure 3.2 depicts the transmitter structure of the source node, which has the same structure as the relay node. With t (re)transmissions, $t \in \{1, 2, \cdots, \mathtt{T}\}$, where the maximum number of retransmissions is $\mathtt{T} - 1$, the binary information sequence $\boldsymbol{u}^t$ is first encoded by the channel encoder ENC_t. For the retransmit operations,
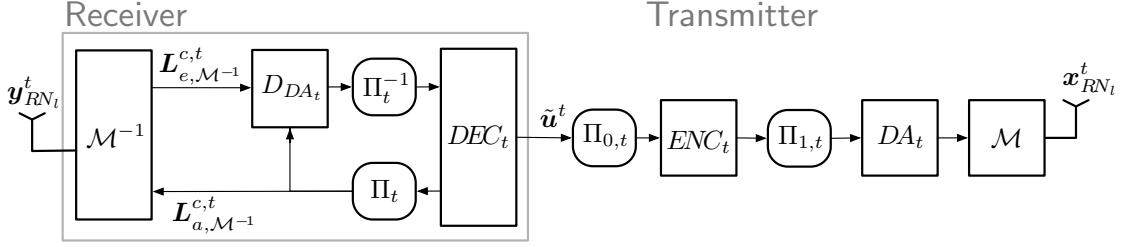
Figure 3.3: Block diagram of the relay node $RN_l, l \in \{1, 2\}$ during receive and transmit operations.

at the relay node, the estimated $\boldsymbol{u}^t$, $\tilde{\boldsymbol{u}}^t$, from a buffer is first random-interleaved by inner interleaver $\Pi_{0,t}$ before being encoded. The use of different interleavers for each transmission by the relays converts the system into a distributed turbo code. The relay node discards the old packet in the buffer whenever receiving a new packet. The same process is performed at the other relay for the first transmission. The encoded bit sequence is then randomly interleaved by outer interleaver $\Pi_{1,t}$ followed by doped-accumulator DA_t with doping rate ξ_t.[2] The outer interleaver enables extrinsic LLR exchange for the systematic bits at the receiver side, as detailed in the next subsection.

The k doped-accumulated bits, $\boldsymbol{q}^t$, in the binary information sequence $\boldsymbol{b}^t$,

$$\boldsymbol{q}^t = [b_{T_x}^t(1), b_{T_x}^t(2), \cdots, b_{T_x}^t(\upsilon), \cdots, b_{T_x}^t(k)],$$
$$T_x \in \{SN, RN_1, RN_2\}, \tag{3.1}$$

are mapped by $\mathcal{M}$ onto non-gray quadrature phase shift keying (QPSK) symbols, which follows the mapping rule $00 \rightarrow (1{+}j)/\sqrt{2}$, $01 \rightarrow (-1{-}j)/\sqrt{2}$, $10 \rightarrow (1{-}j)/\sqrt{2}$, $11 \rightarrow (-1{+}j)/\sqrt{2}$, where $j = \sqrt{-1}$. The complex signal is then transmitted over frequency-flat block Rayleigh fading channel with complex channel gain $h_\beta, \beta \in \{SN - RN_1, SN - RN_2, RN_1 - DN, RN_2 - DN\}$. The transmitted signal having N symbols is denoted by

$$\boldsymbol{x}_{T_x}^t = [x_{T_x}^t(1), x_{T_x}^t(2), \cdots, x_{T_x}^t(N)]^T \in \mathbb{C}^{N \times 1}. \tag{3.2}$$

---

[2] DA is a rate-1 systematic recursive convolutional code where every ξ-th systematic bits is replaced with the accumulated coded bits [73].

3.1.2 Receive Operation

The received signal at node g can be formulated as

$$\boldsymbol{y}_{R_x}^t = h_{T_x R_x} \boldsymbol{x}_{T_x}^t + \boldsymbol{\nu}_{R_x}^t, R_x \in \{RN_1, RN_2, DN\}, \tag{3.3}$$

where $\boldsymbol{\nu}$ is a zero-mean complex AWGN vector with variance σ^2. The average SNR is $E[|h_{T_x R_x}|^2]/\sigma^2$ since $E[\boldsymbol{x}_{T_x}^t] = 1$. With the help of *a priori* non-systematic information $L_{a,\mathcal{M}^{-1}}^{c,t}$ provided by DEC_t, the demapper $\mathcal{M}^{-1}$ calculates the extrinsic LLR $L_{e,\mathcal{M}^{-1}}^{c,t}$ of the bit $q_{R_x}^t[v]$ from $y_{R_x}^t$ by

$$L_{e,\mathcal{M}^{-1}}^{c,t}(q_{R_x}^t[v]) = \ln \frac{P(q_{R_x}^t[v]) = 1|y_{R_x}^t)}{P(q_{R_x}^t[v]) = 0|y_{R_x}^t)}$$

$$= \ln \frac{\sum\limits_{x \in x_1} \exp\left\{-\frac{|y_{R_x}^t - h_{T_x R_x} x_{T_x}^t|^2}{\sigma^2}\right\} \prod\limits_{w=1,w \neq v}^{k} \exp\{-q_{R_x}^t[w] L_{a,\mathcal{M}^{-1}}^{c,t}(q_{R_x}^t[w])\}}{\sum\limits_{x \in x_0} \exp\left\{-\frac{|y_{R_x}^t - h_{T_x R_x} x_{T_x}^t|^2}{\sigma^2}\right\} \prod\limits_{w=1,w \neq v}^{k} \exp\{-q_{R_x}^t[w] L_{a,\mathcal{M}^{-1}}^{c,t}(q_{R_x}^t[w])\}}, \tag{3.4}$$

where x_0 and x_1 denote the sets of mapping patterns having the w-th bit being 0 and 1, respectively.

The soft output vector of the demapper, $L_{e,\mathcal{M}^{-1}}^{c,t}$, is input to the DA_t decoder ($D_{DA,t}$), and its output extrinsic LLR is forwarded to the inner-deinterleaver prior to the channel decoder DEC_t. In Partially-LF HARQ scheme, the CI of the received packet is calculated, which is equivalent to the MI between the *a posteriori* LLR and the uncoded systematic bits. The CI can be calculated online, as described in Section 3.2.

The structure of the destination node is shown in Figure 3.4. The block diagram only shows the structure for receiving the packet sent from the relay node on the same link. However, the decoding process for the packet coming from the relay on the other link is the same. The combiner $\sum$ combines all the *extrinsic* LLRs which are the outputs of all the channel decoders over the parallel links involved in the (re)transmissions, as described above.

When the retransmitted packet is received, the horizontal iteration (*HI*) is performed independently as in the first transmission phase. Then, the obtained *extrinsic* LLRs of the systematic information bits, $L_{e,DN_t}^{u,t}$, are exchanged crosswise between the SISO channel decoders via the combiner, as depicted in Figure 3.4;
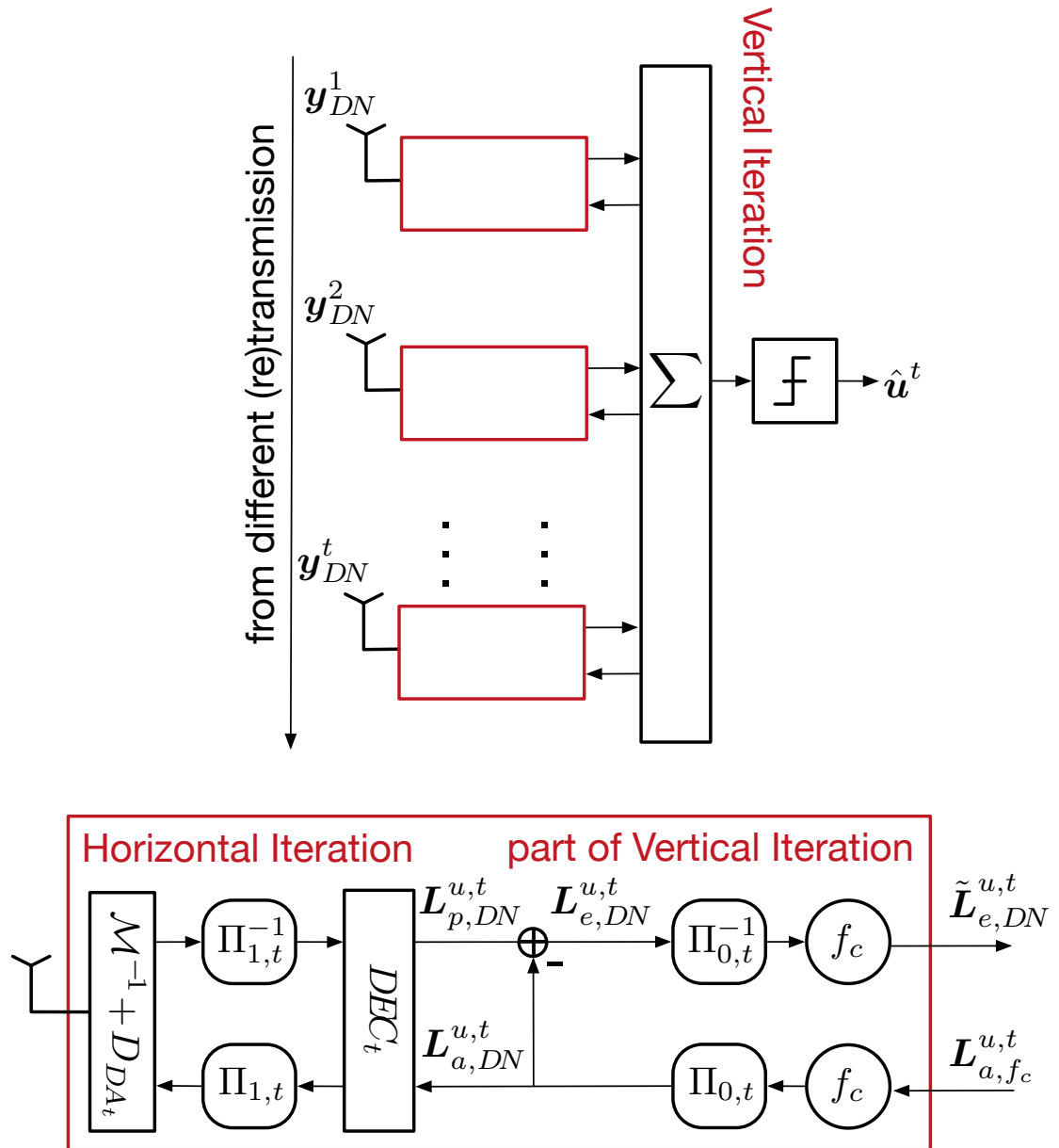
Figure 3.4: Block diagram of the destination node.

this process is referred to as the vertical iteration (*VI*). *VI* can be seen as iterative decoding process of parallel concatenated code, which performs the equivalent role to "combining-after-decoding" (CAD) [67]. After sufficient rounds of iterative *HI-VI-HI-VI* decoding processes, the final hard decisions to obtain $\hat{\boldsymbol{u}}^t$ is made on the *a posteriori* LLR of the information bits. A CRC can be employed for packet error detection at this final stage only. If the CRC detects error(s) in the decoded packet, it is saved in order to combine with the packet(s) to be transmitted in the following slots, within one full HARQ round.

At the destination node, the *extrinsic* systematic LLRs $L^{u,t}_{e,DN_t}$ are updated by the function f_c, defined by (3.6). The function f_c is utilized to help the decoder eliminate the errors in the packets received by the relays, by exploiting the correlation knowledge between the information sequences obtained as the results of decoding at the relays. The correlation is indicated by the error probability p_e of the first hop, block-by-block. In this chapter, we assume that p_e is known to the destination for the simplicity, even though it can be estimated by using the *a posteriori* LLRs, $L^{u,t}_{p,DN_t}(RN_1)$ and $L^{u,t}_{p,DN_t}(RN_2)$, the *a posteriori* LLR values of the uncoded (systematic) bits output from the decoders DEC_t of RN_1 and RN_2, respectively, as presented in [74]. The updated *extrinsic* LLR of $L^{u,t}_{e,DN_t}$ at each relay node can then be obtained by

$$\tilde{L}^{u,t}_{e,DN_t} = f_c(\bar{L}^{u,t}_{e,DN_t}, \hat{p}_e) \tag{3.5}$$

$$= \ln \frac{(1 - \hat{p}_e) \cdot \exp(\bar{L}^{u,t}_{e,DN_t}) + \hat{p}_e}{(1 - \hat{p}_e) + \exp(\bar{L}^{u,t}_{e,DN_t}) \cdot \hat{p}_e}, \tag{3.6}$$

where $\bar{L}^{u,t}_{e,DN_t} = \Pi^{-1}_{0,t}(L^{u,t}_{e,DN_t})$ [73]. The *a priori* LLR $L^{u,t}_{a,f_c}$ is then

$$L^{u,t}_{a,f_c} = \sum_{q \in \omega \setminus t} \tilde{L}^{u,t}_{e,DN_t}, \tag{3.7}$$

with $\omega = \{1, 2, ..., \texttt{T}\}$ being the set of the retransmission number.

3.2 Lossy Forwarding HARQ Mechanism

In this section, we explain the mechanism of the proposed HARQ techniques. For Fully-LF HARQ, the relays always transmit the received packets regardless of

---

Algorithm 1 Fully Lossy Forwarding HARQ

1: **procedure** Fully-LF HARQ
2:     Z $\leftarrow$ number of packets of message $\mathcal{X}$
3:     T $\leftarrow$ maximum number of transmission per packet
4:     $\zeta = (1, 2, 3, \cdots, \text{Z})$
5:     $t = (1, 2, 3, \cdots, \text{T})$
6:     Initialize $\zeta \leftarrow 1$
7:     **for** each packet $\mathcal{X}(\zeta)$ **do**
8:         Initialize $t \leftarrow 0$
9:         *SN* broadcast packet $\mathcal{X}(\zeta)$
10:        $t \leftarrow t + 1$
11:       $\tilde{\mathcal{X}}(\zeta)_{\mathcal{I}} \leftarrow$ decoded $\mathcal{X}(\zeta)$ at relay $RN_{\mathcal{I}}$
12:       $RN_{\mathcal{I}}$ forward $\tilde{\mathcal{X}}(\zeta)_{\mathcal{I}}$ to *DN*
13:       **if** $\mathcal{X}(\zeta)$ unrecovered at *DN* **and** $t \neq \text{T}$ **then** *DN* sends NACK to *SN* via all *RN*s, back to 9
14:       **end if**
15:       $\zeta \leftarrow \zeta + 1$
16:     **end for**
17: **end procedure**

---

whether the error is detected or not. It is an extension of the technique presented in [73] with no direct link between the source node and the destination node. The mechanism is illustrated in Algorithm 1.

On the other hand, for Partially-LF HARQ, the forwarding mechanism depends on the CI value, where its mechanism is illustrated in Algorithm 2. At the beginning of each HARQ round for multiple information sequences to be transmitted, the packet from the source node is forwarded to the destination node through the relay(s) even though it still contains errors. This is due to the CI threshold not set yet. The CI values are initially calculated in order to be used when deciding either requesting retransmission or forwarding the packet. It is an online calculation technique for the mutual information between the *a posteriori* LLR output of the channel decoder and the information sequence from the previous node [75], as

$$CI = 1 - \frac{1}{N} \sum_{n=1}^{N} H_b\left(\frac{1}{1 + e^{-|L_n|}}\right), \tag{3.8}$$

where $H_b(\cdot)$ is a binary entropy function. The CI calculation is beneficial since the receiving nodes do not need to know the original information sequence. The

---

Algorithm 2 Partially Lossy Forwarding HARQ

1: **procedure** PARTIALLY-LF HARQ
2:     Z $\leftarrow$ number of packets of message $\mathcal{X}$
3:     T $\leftarrow$ maximum number of transmission per packet
4:     $\zeta = (1, 2, 3, \cdots, \text{Z})$
5:     $t_{SN-RN} = (0, 1, 2, \cdots, \text{T})$
6:     $t_{RN_{\mathcal{I}}-DN} = (0, 1, 2, \cdots, \text{T})$
7:     Initialize $\zeta \leftarrow 1$
8:     **for** each packet $\mathcal{X}(\zeta)$ **do**
9:         Initialize $t_{SN-RN} \leftarrow 0, \ t_{RN_{\mathcal{I}}-DN} \leftarrow 0$
10:         SN broadcast packet $\mathcal{X}(\zeta)$
11:         $t_{SN-RN} \leftarrow t_{SN-RN} + 1$
12:         $\alpha_{SN-RN_{\mathcal{I}}}^{t_{SN-RN}} \leftarrow$ calculated CI at relay $RN_{\mathcal{I}}$, by (3.8)
13:         **if** $t_{SN-RN} = 1$ **then**
14:             $\alpha_{SN-RN_{\mathcal{I}}}^{t_{SN-RN}-1} \leftarrow \alpha_{SN-RN_{\mathcal{I}}}^{t_{SN-RN}}$
15:         **else**
16:             **if** $RN_{\mathcal{I}}$ received NACK_2 for $t_{SN-RN} - 1$ **and** $\alpha_{SN-RN_{\mathcal{I}}}^{t_{SN-RN}-1} < \alpha_{SN-RN_{\mathcal{I}}}^{t_{SN-RN}}$ **then**
17:                 $\alpha_{SN-RN_{\mathcal{I}}}^{t_{SN-RN}-1} \leftarrow \alpha_{SN-RN_{\mathcal{I}}}^{t_{SN-RN}}$
18:             **end if**
19:         **end if**
20:         **if** $RN_{\mathcal{I}}$ received NACK_2 for $t_{SN-RN} - 1$ **and** $\alpha_{SN-RN_{\mathcal{I}}}^{t_{SN-RN}-1} \geq \alpha_{SN-RN_{\mathcal{I}}}^{t_{SN-RN}}$ **then**
21:             $RN_{\mathcal{I}}$ send NACK_1 to SN
22:             back to 10
23:         **end if**
24:         $\tilde{\mathcal{X}}(\zeta)_{\mathcal{I}} \leftarrow$ decoded $\mathcal{X}(\zeta)$ at relay $RN_{\mathcal{I}}$
25:         $RN_{\mathcal{I}}$ forward $\tilde{\mathcal{X}}(\zeta)_{\mathcal{I}}$ to DN
26:         $t_{RN_{\mathcal{I}}-DN} \leftarrow t_{RN_{\mathcal{I}}-DN} + 1$
27:         $\alpha_{RN_{\mathcal{I}}-DN}^{t_{RN_{\mathcal{I}}-DN}} \leftarrow$ calculated CI, before joint decoding, at DN, by (3.8)
28:         **if** $t_{SN-RN} = 1$ and $t_{RN_{\mathcal{I}}-DN} = 1$ **then**
29:             $\alpha_{RN_{\mathcal{I}}-DN}^{t_{RN_{\mathcal{I}}-DN}-1} \leftarrow \alpha_{RN_{\mathcal{I}}-DN}^{t_{RN_{\mathcal{I}}-DN}}$
30:         **else**
31:             **if** $\mathcal{X}(\zeta)$ unrecovered for $t_{RN_{\mathcal{I}}-DN} - 1$ **and** $\alpha_{RN_{\mathcal{I}}-DN}^{t_{RN_{\mathcal{I}}-DN}-1} < \alpha_{RN_{\mathcal{I}}-DN}^{t_{RN_{\mathcal{I}}-DN}}$ **and** $t_{RN_{\mathcal{I}}-DN} \neq \text{T}$ and $t_{SN-RN} \neq \text{T}$ **then**
32:                 $\alpha_{RN_{\mathcal{I}}-DN}^{t_{RN_{\mathcal{I}}-DN}-1} \leftarrow \alpha_{RN_{\mathcal{I}}-DN}^{t_{RN_{\mathcal{I}}-DN}}$
33:             **end if**
34:         **end if**
35:         **if** $\mathcal{X}(\zeta)$ unrecovered from $\tilde{\mathcal{X}}(\zeta)_{\mathcal{I}}$ at DN **and** $t_{RN_{\mathcal{I}}-DN} = 1$ **then**
36:             DN send NACK_1 to $RN_{\mathcal{I}}$
37:             back to 25
38:         **else if** $\mathcal{X}(\zeta)$ unrecovered from $\tilde{\mathcal{X}}(\zeta)_{\mathcal{I}}$ at DN **and** $t_{RN_{\mathcal{I}}-DN} \neq \text{T}$ and $t_{SN-RN} \neq \text{T}$ **then**
39:             DN send NACK_2 via $RN_{\mathcal{I}}$
40:             back to 10
41:         **else**
42:             $\zeta \leftarrow \zeta + 1$
43:         **end if**
44:     **end for**
45: **end procedure**

probability of error corresponding to the CI value can be calculated by

$$P_b \approx \frac{1}{2} erfc(\frac{J^{-1}(CI)}{2\sqrt{2}}), \tag{3.9}$$

where $J^{-1}(\cdot)$ is the inverse of function $J(\cdot)$ [76]. It is worth noting that P_b is the error corresponding to the BER per link.

The receiving nodes send a NACK to their previous node to indicate unsuccessful decoding and hence requesting retransmission. There are two types of NACK in Partially-LF HARQ: NACK_1 indicating a retransmission required from the node one hop back, and NACK_2 indicating retransmission required from the node two hops back. Therefore, if a transmitting node receives NACK_1, it will retransmit the packet to the next node. On the other hand, if a transmitting node receives NACK_2, it will transmit NACK_1 to the previous node.

The destination node evaluates CI values of packets transmitted from all links, before packet combining. The destination node transmits NACK_1 whenever the packets transmitted for the first time (not retransmitted version) by the relay are unsuccessfully recovered. This is to avoid the excessive end-to-end latency. In this case, the CI is used as the threshold. Additionally, the destination node transmits NACK_2 whenever the already-retransmitted packets are not successfully recovered. In this case, the destination node uses the CI value, which is larger than the previous CI as the threshold. As for the relay node, the threshold is set equal to CI of the very beginning of the HARQ rounds and update it whenever receiving NACK_2.

3.3   Numerical Results

We evaluate average end-to-end PER, BER, and throughput performances by computer simulations that consider the transmission of 100,000 packets with the size of 10,000 bits per packet. The maximum number of retransmissions per node is set to 4 (T $= 5$). All nodes use the same channel coding, where a half-rate NSNRCC with a generator polynomial $G = [7,5]$ is considered. They all also use the same varying doping rate ξ (re)transmission-by-(re)transmission, where $\xi \in \{2, 10, 15, 20, 25\}$.

We assume no processing time restriction for the overall transmission of infor-

mation from the source to the destination nodes, and hence the relay nodes can decode the packet before they forward. We also assume an ideal medium access control protocol, where each node can transmit and receive a packet independently. Each node is allowed to transmit and receive only one packet simultaneously, and every packet transmitted from the nodes is received without collisions.

We compare Partially-LF HARQ and Fully-LF HARQ with the conventional schemes as shown in [30], which are SHARQ I and SHARQ II. In the conventional schemes, either Relay 1 or Relay 2, or both relays forward error-free packets only. If the destination node fails in recovering the packet, SHARQ I performs retransmission from the relay node(s), whereas SHARQ II performs retransmission from the source node. In Fully-LF HARQ scheme, the relay nodes always forward any received packets, and therefore the receiving nodes do not need to calculate the CI. We set no packet combining at the relay nodes for all schemes.

Figs. 3.5 and 3.6 show that Partially-LF HARQ outperforms the conventional schemes and Fully-LF HARQ in terms of average end-to-end BER and PER performances, respectively. The theoretical lower bound is shown in Figure 3.6 as a reference to confirm the performances of Partially-LF HARQ and Fully-LF HARQ.[3] The lower bound is calculated based on the outage probability of CAD technique [67] for $\mathtt{T} = 10$ as

$$P_{out} = \Pr(\mathcal{R} > C_A), \tag{3.10}$$

$$C_A = \mathtt{T}\log_2(1 + \frac{1}{\mathtt{T}}\sum_{t=1}^{\mathtt{T}}\frac{\gamma_t}{\mathtt{T}}), \tag{3.11}$$

where $\mathcal{R}, C_A$, and γ_t are the transmission rate, the capacity of the CAD, and the instantaneous SNR of the t-th transmission, respectively. The gap of 18 dB between the Partially-LF HARQ and the lower bound is reasonable because it is a lower bound assuming that all packets transmitted by the relays have no errors. The conventional scheme fails to combine all transmitted packet to achieve more diversity gain as achieved by Partially-LF HARQ and Fully-LF HARQ. Furthermore, Partially-LF HARQ can achieve coding gain of 0.9 dB compared to Fully-LF HARQ as shown by the parallel shift in Figure 3.6, because of its ability to carefully combine the most reliable packets by employing the CI.

---

[3]The theoretical bound for BER is not shown in Figure 3.5 because it is hard to calculate since the coding structure should be considered.
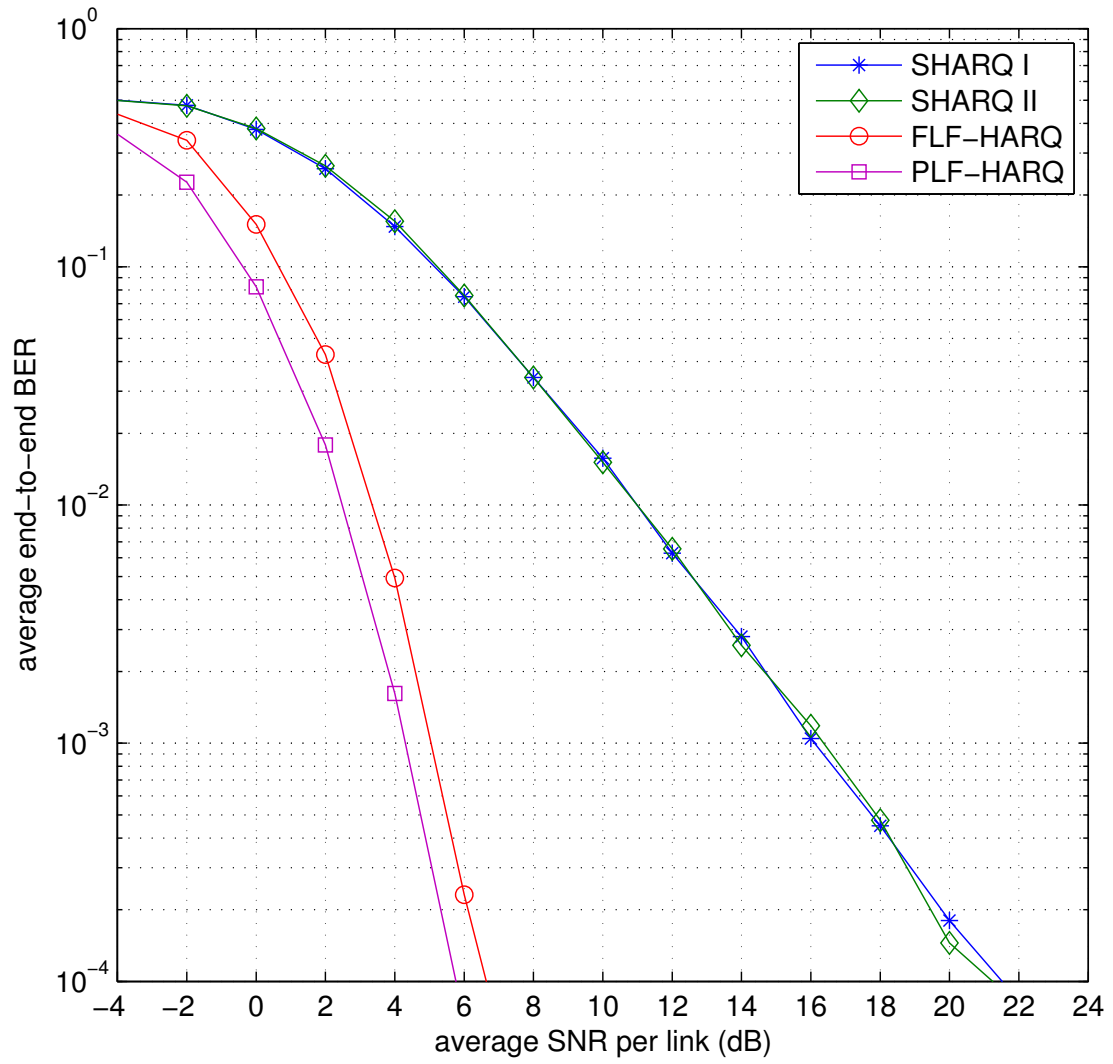
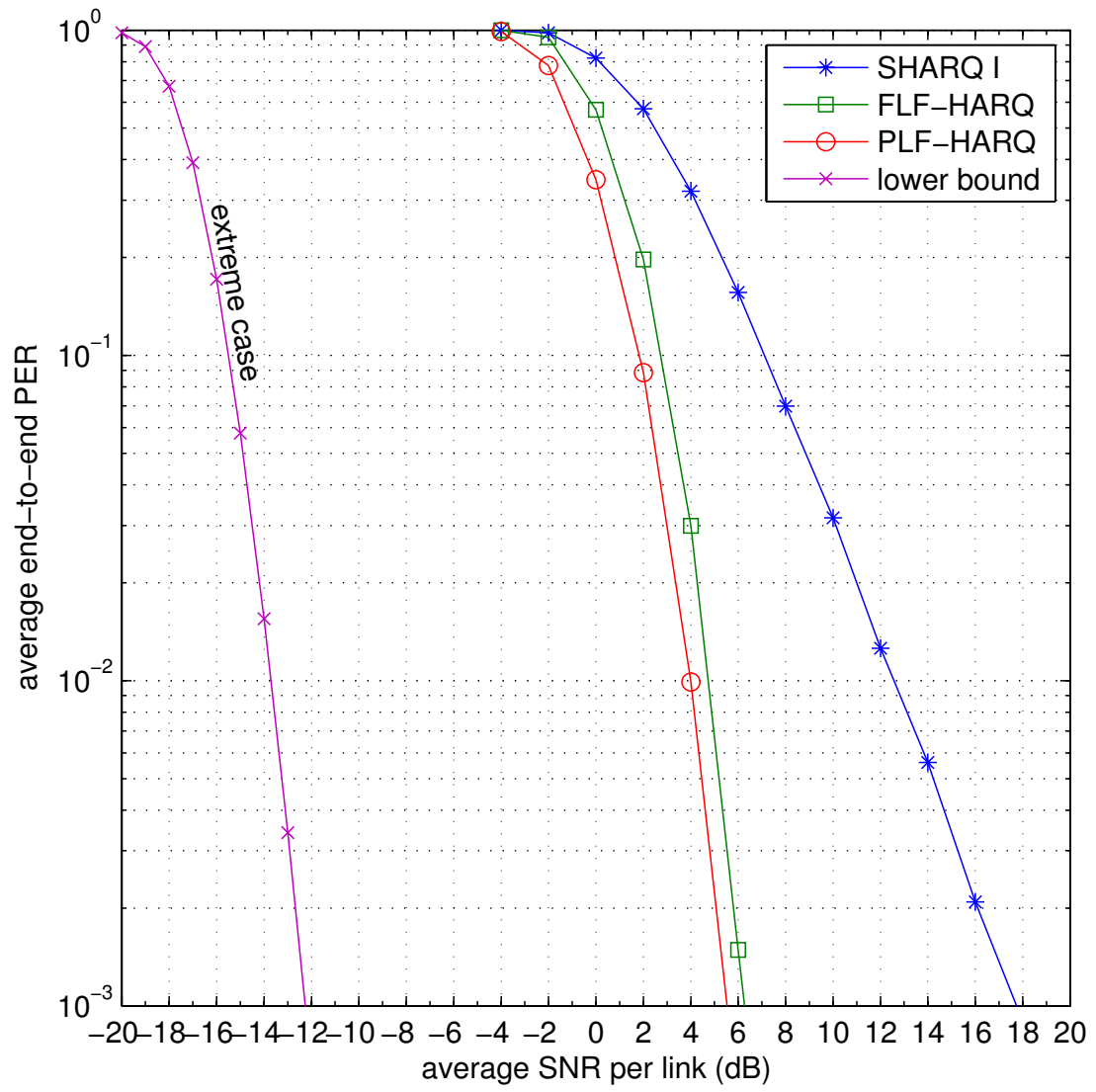Figure 3.5: Average end-to-end BER performances.

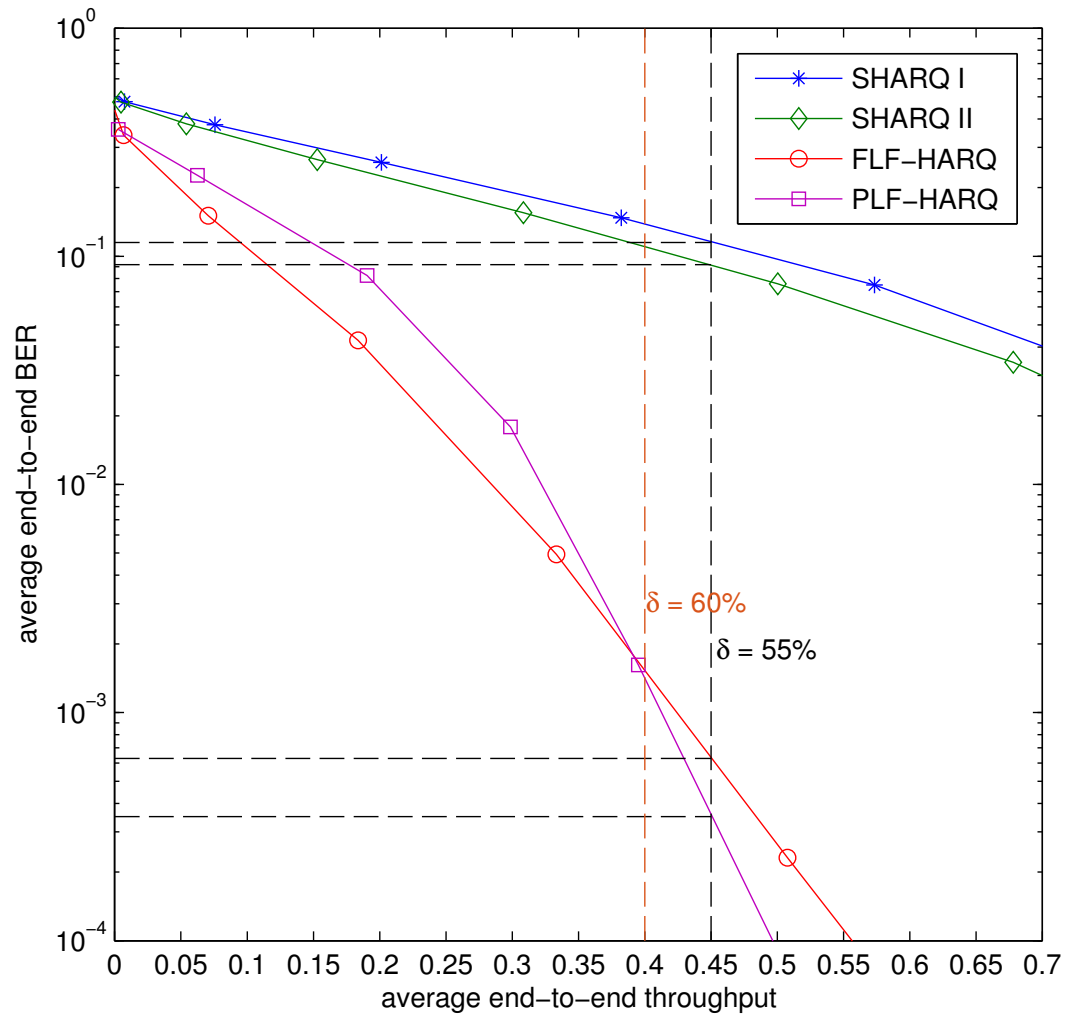Figure 3.6: Average end-to-end PER performances.

Figure 3.7: Average end-to-end throughput performances correspond to the average end-to-end BER performances for various SNR.

We define the average end-to-end throughput performance η as

$$\eta = \frac{\frac{\text{average number of correctly decoded packets at destination node}}{\text{number of transmitted packets by the source node}}}{\text{number of used time slots}}. \tag{3.12}$$

We normalized the throughput over two-time slots, which means that the throughput of one is achieved whenever a packet is successfully recovered within two-time slots. Intuitively it is easy to understand the packet-based transmission performance by the packet loss, and hence we define the average end-to-end packet loss ratio δ from (3.12) as the average number of unrecoverable packets at the destination per time slot over the number transmitted packets by the source node, or given by

$$\delta = 1 - \eta. \tag{3.13}$$

Figure 3.7 shows the performances of average end-to-end throughput versus the average end-to-end BER for the proposed Fully-LF HARQ and Partially-LF HARQ as well as the conventional SHARQ I, II techniques for comparison. Obviously, the proposed techniques outperform the conventional SHARQ I and II techniques. It is found that in the high δ (low throughput value) range, the BER performance of Fully-LF HARQ is lower than Partially-LF HARQ. However, when $\delta < 60\%$, the BER performance with Partially-LF HARQ gradually decreases. When the end-to-end packet loss ratio is 55% in average, the average end-to-end BER with Partially-LF HARQ is $3.50 \cdot 10^{-4}$, but $6.30 \cdot 10^{-4}$ with Fully-LF HARQ, $1.15 \cdot 10^{-1}$ with SHARQ I, and $9.2 \cdot 10^{-2}$ with SHARQ II. The gap between the Fully-LF HARQ and Partially-LF HARQ is expected to be gradually larger for the lower packet loss ratio. Hence, Fully-LF HARQ is suitable for the packet-loss tolerant systems whereas Partially-LF HARQ is preferable for the systems requiring very low packet loss ratio.

3.4   Summary

Partially-LF HARQ and Fully-LF HARQ schemes have been proposed to improve the system throughput of parallel relay networks. The improvement is obtained by (i) exploiting the correlation among received packets at the destination node, and (ii) allowing lossy forwarding at the relay. Results of computer simulations verified a significant improvement in BER, PER and throughput performances over

frequency-flat block Rayleigh fading channels.

Chapter 4

Single-hop: M-in-1 Helper Transmission

Retransmitting M unrecovered information packets within one packet exhibits improved throughput compared to attempting to retransmit individual packets. Furthermore, because the packets are sent from the same source, there may remain information correlation which can be exploited to enhance the performance by reducing the required SNR at the receiver instead of compressing the information at the close-entropy-rate at the transmitter. Moreover, since fading variation is a dominating factor of the packet transmission in wireless communication systems, the achievable diversity order is of crucial importance. Therefore, this chapter focuses the analyses on the diversity order achieving of such retransmission protocol in a single-hop transmission. We note that this issue can be extended to a rate-diversity-coding gain trade-off because the correlated sources have inherent redundancy that can contribute to performance improvement.

In this chapter, we analyze, for a packet-wise feedback system, the achievable diversity order of packet-wise-feedback-assisted M correlated information sources with a helper packet transmission over a block Rayleigh fading channel. The technique is based on *the theorem of source coding with side information* [69, 77]. Note that the authors of [69] characterize the optimal rate region for one source and a helper problem.[1] However, it can be generalized to an arbitrary number of sources as presented, for example, by Theorem 10.4 in [53].

---

[1] Two sources are independently encoded and jointly decoded; the decoder wishes to reconstruct almost losslessly only one source so that the other serves as the helper.

We begin with in-depth analyses of rate regions and outage probabilities of M correlated information sources transmission with $M = \{2, 3\}$, to identify the trade-off between source correlation and performance gain due to coding and diversity. Following that, we generalize the analyses of achievable diversity order into any integer M.

Accordingly, we first investigate M correlated information sources transmission over a static AWGN channel with $M = \{2, 3\}$. Each packet is encoded by a capacity-achieving code at a certain *specified* instantaneous SNR. It is assumed that the channel capacity is smaller than entropy per-information packet of the source; it corresponds to the event where the packet contains errors after decoding at the receiver. The receiver notifies the transmitter of decoding failure via the feedback channel. Thus, a helper packet, which is formed by utilizing the XOR operation on the M packets which are failed to be recovered at the receiver,[2] is then transmitted.

We then derive an upper bound on the outage probability of the system over block Rayleigh-fading channels and show the achievable diversity order with $M = \{2, 3\}$. We also evaluate the influence of the information correlation in the cases that equal and unequal transmit power and spectrum efficiency are variously allocated to the information and helper packets. Finally, we analyze the achievable diversity order with any integer M.

The idea closest to the technique investigated in this chapter is that in [78] which aims to apply the concept to cooperative wireless communications. The technique presented in [78] is referred to as o-MARC for notational convenience. The authors utilized the theorems for multiple source coding with a helper for investigating the admissible rate region of orthogonal multiple-access relay channel (MARC) system in static AWGN channels and uses the rate region for deriving the outage probabilities in block fading channels. However, deriving the (in)admissible rate regions of the systems with feedback is not as straightforward as in the systems without feedback, as shown in Section 4.3.

---

[2]Afterward, we use terminology NACK-ed packet to refer the packets that are unable to be recovered at the receiver by independent (packet-by-packet) decoding.

4.1 Problem Statement

The system considered in this chapter is regarded as a two-dimensional channel coded packet transmission, horizontal and vertical codes. The horizontal code is the packet-wise capacity-achieving code, and the vertical code is binary single parity check code over M information packets. This system is referred to as M-in-1 helper transmission in this dissertation.

The (in)admissible rate region and achievable diversity order of M-in-1 helper transmission, taking into account the source correlation and feedback, are unknown. Therefore, we derive the (in)admissible rate region of the system, where the correlation among the source information and the bit error rate of the helper packet are fully theoretically analyzed. We use *the theorem for multiple sources coding with a helper* [53, Theorem 10.4], for analyzing the inadmissible rate region. Given the derived inadmissible rate region, we then derive the upper bound of the outage probability of M-in-1 helper transmission over block Rayleigh fading channels.[3] Each packet, including helper, suffers from statistically independent block Rayleigh fading, where the channel varies packet-by-packet, but is static within each packet.

The scenario described above may arise in ARQ systems, where the transmitter stores the NACK-ed packets in a buffer with a size of M; and a helper is transmitted whenever the buffer is full. In the analysis, we only focus on the buffer-full state and derive the outage probability of the M-in-1 helper transmission system utilizing the obtained rate region. In fact, the process of how the buffer full state is reached has to be taken into account for the exact calculation of the *system outage.* In this dissertation, however, we make use of the statistically independent occurrence of the two events, decoding success and failure at the receiver. Hence, we define the outage event such that decoding of the M NACK-ed packets after transmitting the helper packet is failed *for the first time*, and thereby the outage probability derived in this dissertation is an upper bound.

4.2 System Model

We consider a point-to-point wireless communication system where the transmitter is a binary source generating N information packet $\mathbf{u} = \{\mathbf{u}_1, \mathbf{u}_2, \cdots, \mathbf{u}_N\}$. Each

---

[3]The outage probability of the systems with $M > 3$ may be possible to be derived if we can solve the difficulty of managing M dimensions rate region.
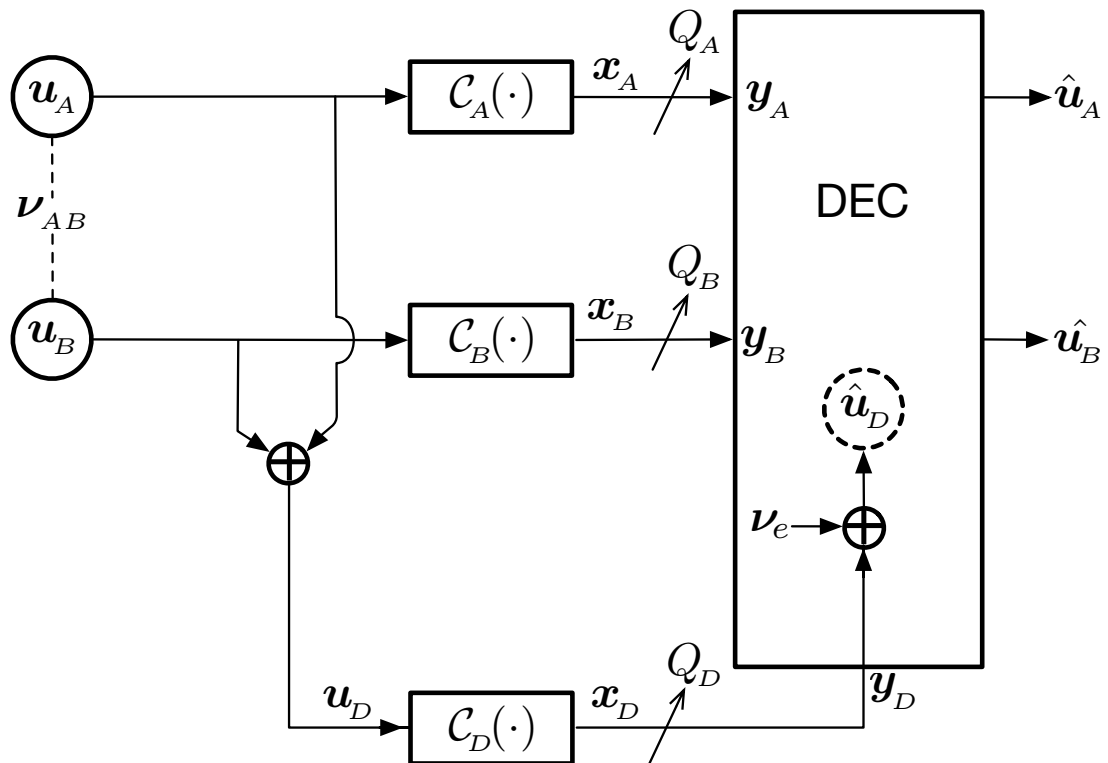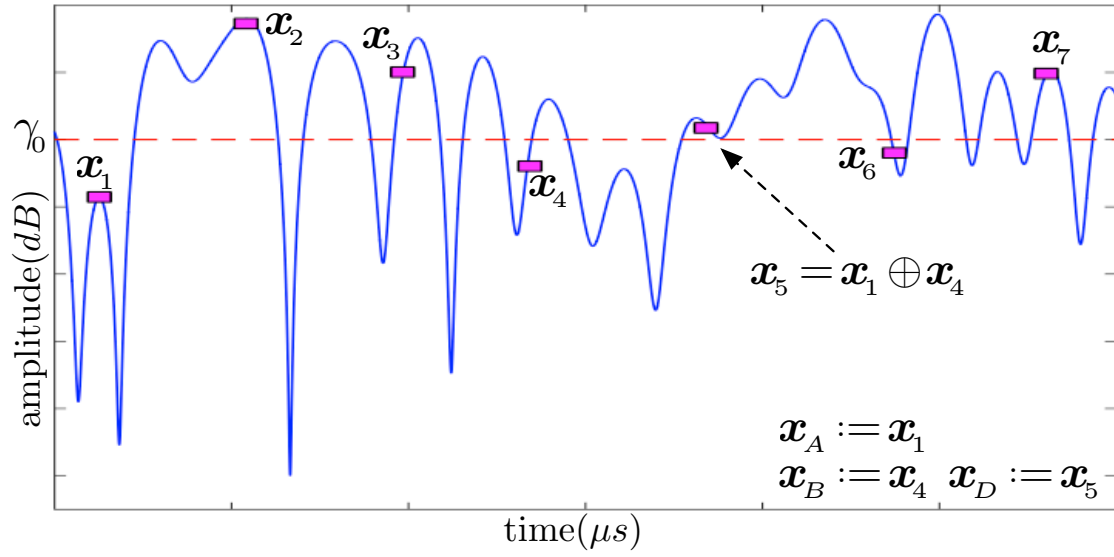
Figure 4.1: Transmission over fading channel and the correspond system model of $M2$. Note that the feedback signal is not shown in the figure for the sake of clarity.
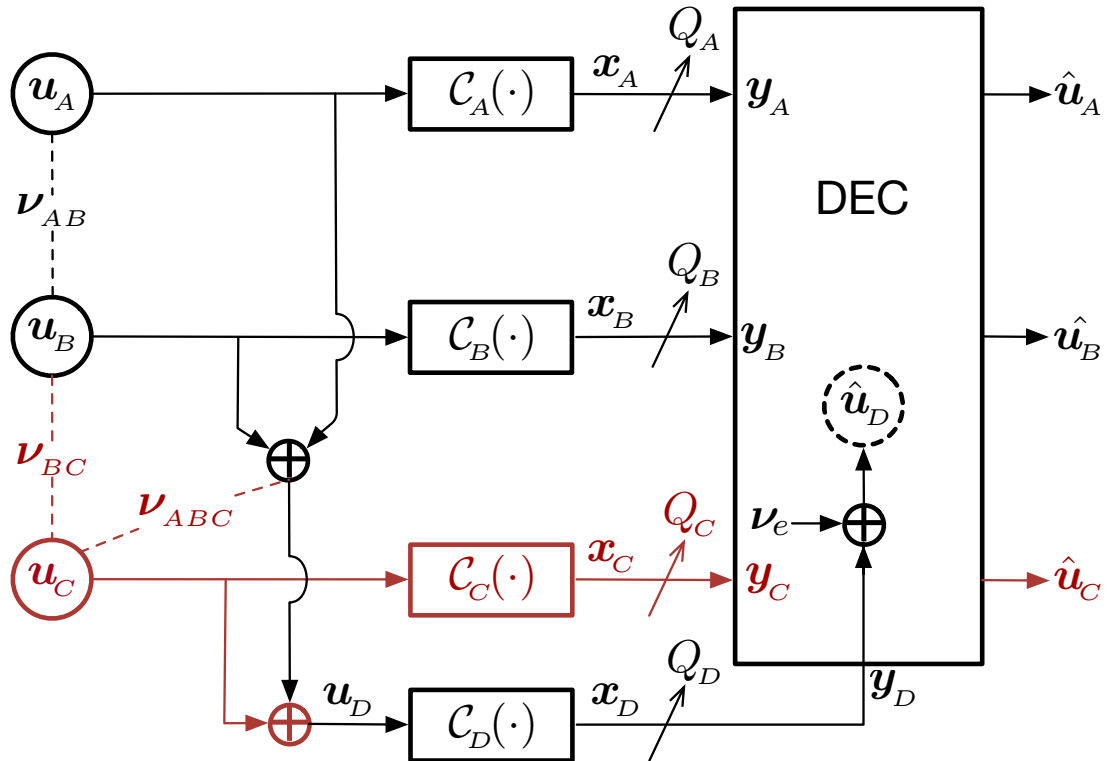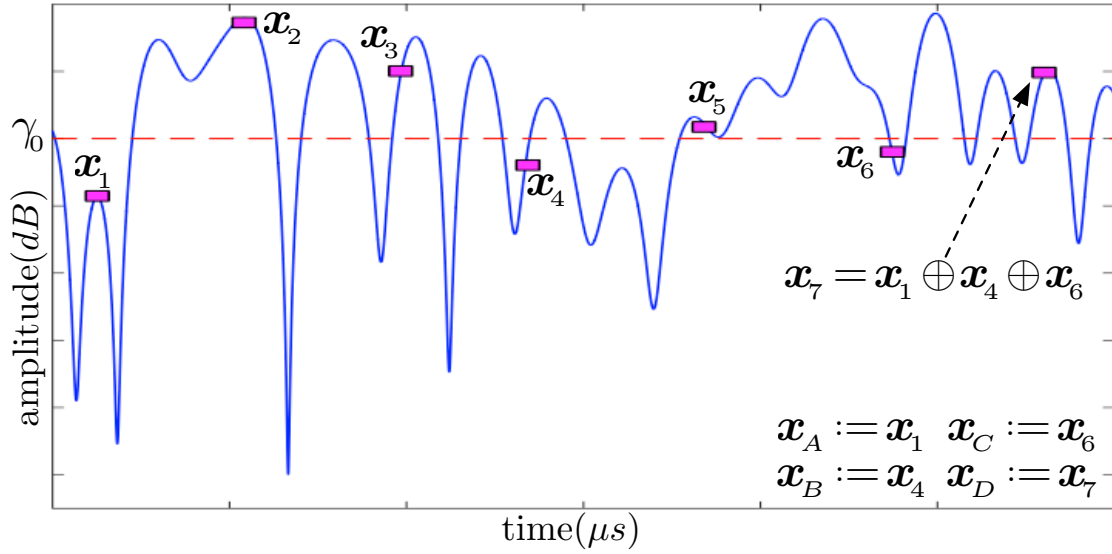
Figure 4.2: Transmission over fading channel and the correspond system model of $M3$. Note that the feedback signal is not shown in the figure for the sake of clarity.

information packet is a binary sequence with rate R_n and $\mathbb{P}(\mathbf{u}_n[k] = 0) = \mathbb{P}(\mathbf{u}_n[k] = 1) = 0.5$, where $n = \{1, 2, \cdots, N\}$, $k = \{1, 2, \cdots, K\}$, and $\mathbf{u}_n[k]$ denotes the k-th bit of K bits length $\mathbf{u}_n$. A function $\mathcal{C}_n(\cdot)$ encodes and modulates $\mathbf{u}_n$ in such a way that the spectrum efficiency of the signaling scheme, including channel coding rate and modulation multiplicity, is Q_n. The encoded packets $\boldsymbol{x}_n = \mathcal{C}_n(\mathbf{u}_n)$ is then transmitted via a channel assumed to be suffering from block Rayleigh fading.

The received packets can be expressed as $\boldsymbol{y}_n = h_n \cdot \boldsymbol{x}_n + \boldsymbol{v}_n$, where h_n and $\boldsymbol{v}_n$ represents the complex channel gain and the zero mean AWGN vector with variance σ_n^2, respectively. With the block Rayleigh fading assumption, h_n is constant within a block, and varies independently block-by-block; it has Rayleigh-distributed amplitude $|h_n|$ with $E[|h_n|^2] = 1$. The instantaneous received SNR for the transmission of the block $\boldsymbol{x}_n$ is then given by $\gamma_n = |h_n|^2 \cdot \Gamma_n$, where Γ_n is the average SNR. The probability density function (*pdf*) of γ_n is

$$p(\gamma_n) = \frac{1}{\Gamma_n} \exp(-\frac{\gamma_n}{\Gamma_n}). \tag{4.1}$$

The system utilizes a simple stop-and-wait ARQ protocol where the receiver sends an ACK to indicate successful packet decoding, otherwise, NACK to indicate the retransmission request. The transmitter is assumed to have a buffer with size M to store M NACK-ed packets.

With $M2$, let the M NACK-ed packets be $\mathbf{u}_a = \boldsymbol{u}_A$ and $\mathbf{u}_b = \boldsymbol{u}_B$, where $1 \leq a < b \leq N$, and the corresponding (rates, spectrum efficiencies) are $(R_a = R_A, Q_a = Q_A)$ and $(R_b = R_B, Q_b = Q_B)$, respectively. After receiving NACK twice, i.e., the buffer becomes full and the transmitter transmits a helper packet, represented by $\boldsymbol{u}_D = \boldsymbol{u}_A \oplus \boldsymbol{u}_B$, by utilizing rate R_D and spectrum efficiency Q_D, as shown in Figure 4.1.

Likewise, with $M3$, let the M NACK-ed packets be denoted as $\mathbf{u}_a = \boldsymbol{u}_A$, $\mathbf{u}_b = \boldsymbol{u}_B$, and $\mathbf{u}_c = \boldsymbol{u}_C$, where $1 \leq a < b < c \leq N$, and $R_c = R_C, Q_c = Q_C$. An additional XOR operation with the packet $\boldsymbol{u}_C$ is included in the helper packet so that $\boldsymbol{u}_D = \boldsymbol{u}_A \oplus \boldsymbol{u}_B \oplus \boldsymbol{u}_C$, as shown in Figure 4.2. After receiving the helper packet, the receiver again decodes all NACK-ed packets jointly with the estimated helper packet $\hat{\boldsymbol{u}}_D$. Since the receiver does not aim to successfully decode $\boldsymbol{u}_D$, $\hat{\boldsymbol{u}}_D$ may contain some errors. We express the correlation between $\boldsymbol{u}_D$ and $\hat{\boldsymbol{u}}_D$ by

$$\boldsymbol{\nu}_e = \boldsymbol{u}_D \oplus \hat{\boldsymbol{u}}_D, \tag{4.2}$$

where $\boldsymbol{\nu}_e$ is the error vector with

$$p_e = \mathbb{P}(\nu_e = 1),\ 0 \le p_e \le 0.5. \tag{4.3}$$

The receiver exploits the correlation knowledge among the NACK-ed packets to enhance the error correction capability. The correlation assumed to be described by the bit-flipping model [79] as:

$$\boldsymbol{\nu}_{AB} = \boldsymbol{u}_A \oplus \boldsymbol{u}_B, \tag{4.4a}$$

$$\boldsymbol{\nu}_{BC} = \boldsymbol{u}_B \oplus \boldsymbol{u}_C, \tag{4.4b}$$

$$\boldsymbol{\nu}_{ABC} = \boldsymbol{u}_A \oplus \boldsymbol{u}_B \oplus \boldsymbol{u}_C, \tag{4.4c}$$

with bit-flipping probabilities

$$p_{AB} = \mathbb{P}(\nu_{AB} = 1), \tag{4.5a}$$

$$p_{BC} = \mathbb{P}(\nu_{BC} = 1), \tag{4.5b}$$

$$p_{ABC} = \mathbb{P}(\nu_{ABC} = 1), \tag{4.5c}$$

where $0 \le p_z \le 0.5$ and $z = \{AB, BC, ABC\}$. With the model given above, the value of $p_{ABC} \approx 0.5$, which is verified by the simulation for $K \ge 1,000$ bits, as shown in Appendix B Let ρ_z be the exact correlation value, the relationship between ρ_z and p_z is given by

$$\rho_z = 1 - 2p_z. \tag{4.6}$$

Notice that in the extreme cases, $\rho_z = 0$ and $\rho_z = 1$ indicate no correlation and full correlation, respectively.

We assume receiver knows the correlation among the information parts of the NACK-ed packets when the buffer becomes full, by utilizing, for example, a packet index counter with an initial correlation parameter setting with the help of higher layer protocols. However, how to estimate and/or share the correlation information is out of the scope of this dissertation. We also assume that correlation between the NACK-ed packets follows the Markov process, and hence the Markov chain also applies $\boldsymbol{u}_A \to \boldsymbol{u}_B \to \boldsymbol{u}_C$.
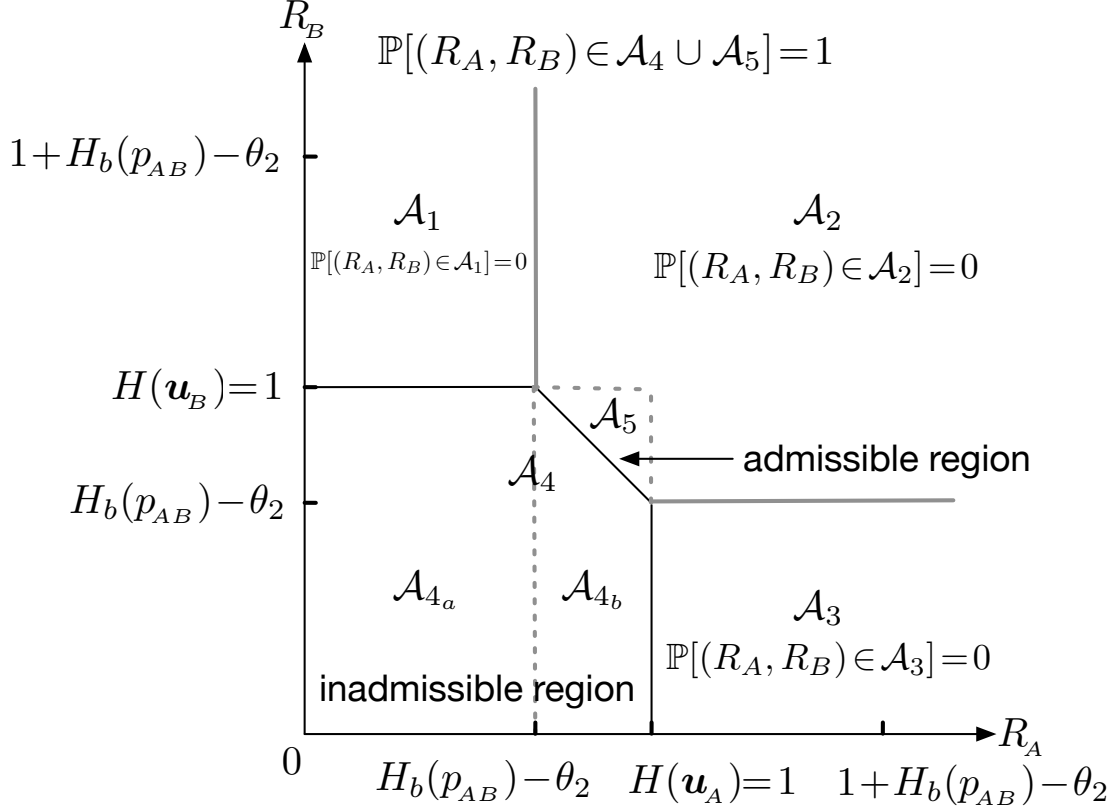
Figure 4.3: Rate region of the rate pair (R_A, R_B) given $R_D \geq \theta_2$ for $M2$.

4.3 Inadmissible Rate Region in Static AWGN Channel

In this section, we present the inadmissible rate regions of $M2$ and $M3$, which are defined by the set of all the rate vectors (R_A, R_B) and (R_A, R_B, R_C), respectively, for which the values of each rate and sum-rates do not follow the given constraints. The admissible rate region is the complement of the inadmissible rate region. First of all, we recall for both $M2$ and $M3$ the theoretical rate regions of which the constraints are derived from *the theorem of multiple sources coding with a helper* and the assumption of without feedback channel. Finally, we derive the inadmissible rate regions of both with feedback channel and based on the protocol considered in this dissertation. Accordingly, an additional constraint is taken into account.

4.3.1 Inadmissible Rate Region of $M2$

Let us first assume there is no feedback channel in the systems, and hence the helper is transmitted following the two distinct packet transmissions regardless of whether

or not the decoding is successful. This setup is equivalent to o-MARC. In this case, the theoretical rate region is given by equations (C.6a)–(C.6d) in Appendix C.1 [78]. Let us then assume that the constraint for the helper packet's information rate, $R_D \geq \theta_2$, is always satisfied.[4] It is easily found that for an arbitrary value of $R_D \geq \theta_2$, the entire rate region for the rate-pair R_A and R_B can be divided into five parts, i.e. $\mathcal{A}_w, w = \{1, 2, \cdots, 5\}$, as shown in Figure 4.3. Accordingly, the admissible region for the non-feedback case corresponds to regions $\mathcal{A}_2 \cup \mathcal{A}_5$.

Now, let us assume that the feedback channel is available. Based on the system model described in Section 4.2, the ACK/NACK is fed back from the receiver via the feedback channel after decoding the received packets, packet-by-packet. Since we assume a capacity-achieving channel code, ACK feedback indicates $R_i \geq H(\boldsymbol{u}_i), i \in \{A, B\}$, whereas NACK feedback indicates $R_i < H(\boldsymbol{u}_i)$. Therefore, when the receiver starts the joint decoding process after receiving the helper packet, the possible rate region is limited to $\mathcal{A}_4$ and $\mathcal{A}_5$, i.e. $\mathbb{P}[(R_A, R_B) \in \mathcal{A}_1] = \mathbb{P}[(R_A, R_B) \in \mathcal{A}_2] = \mathbb{P}[(R_A, R_B) \in \mathcal{A}_3] = 0$. In this case, all NACK-ed packets can be recovered only when the rate-pair, R_A and R_B, falls in the region $\mathcal{A}_5$. Conversely, they cannot be recovered when the rate-pair falls in the region $\mathcal{A}_4$, referred to as the inadmissible rate region of $M2$. We divide the inadmissible rate region into two parts, $\mathcal{A}_{4_a}$ and $\mathcal{A}_{4_b}$, and hence the region can be expressed as

$$\mathcal{A}_4 = \mathcal{A}_{4_a} \cup \mathcal{A}_{4_b}, \tag{4.7}$$

where

$$\mathcal{A}_{4_a} = \{(R_A, R_B) | 0 \leq R_A < H_b(p_{AB}) - \theta_2, \ 0 \leq R_B < 1\}, \tag{4.8a}$$

$$\mathcal{A}_{4_b} = \{(R_A, R_B) \in \mathbb{R}^+ | H_b(p_{AB}) - \theta_2 \leq R_A < 1,$$
$$0 \leq R_B < 1 + H_b(p_{AB}) - \theta_2 - R_A\}, \tag{4.8b}$$

$$\theta_2 = H_b(p_{AB} * p_e) - H_b(p_e). \tag{4.8c}$$

This is the most significant difference in the rate region between with and without feedback, corresponding to this dissertation and o-MARC, respectively.

---

[4]This assumption is eliminated when deriving the outage probability in the next section, such that the variation of the rate R_D can be taken into account.
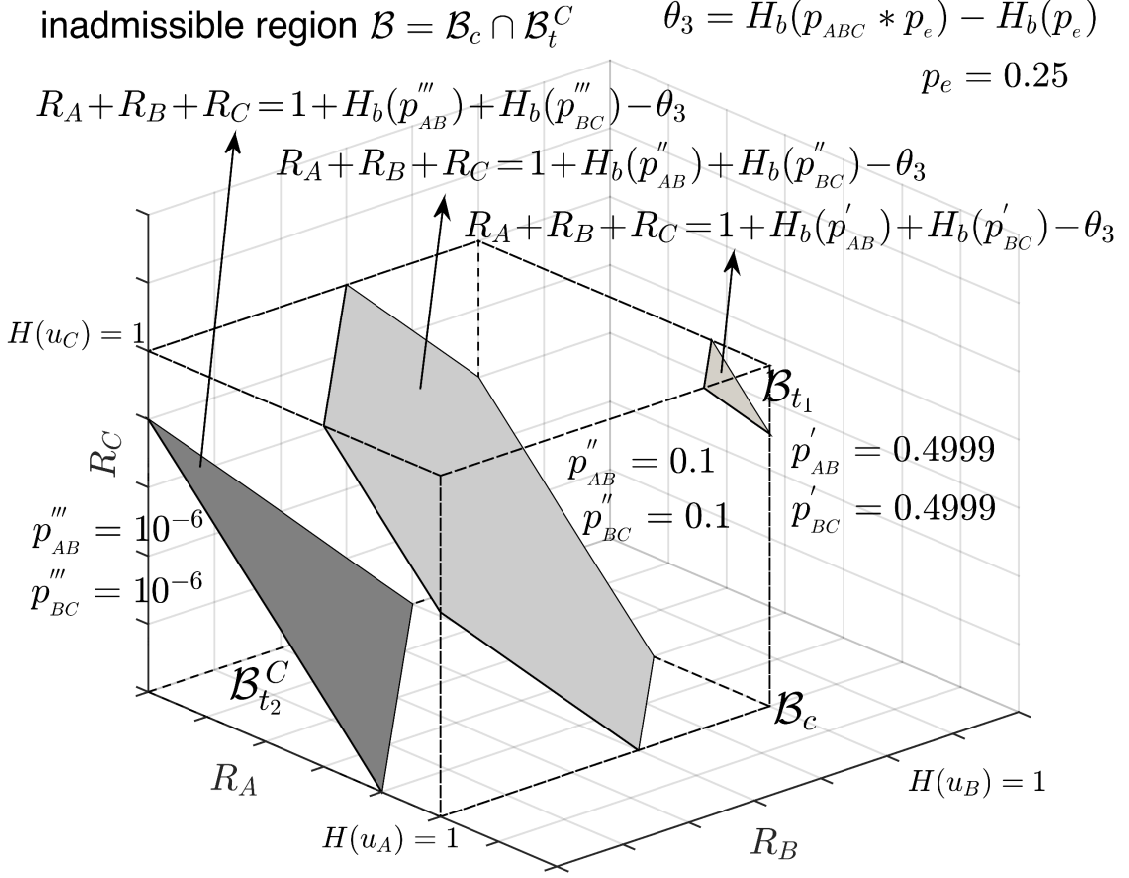
Figure 4.4: Rate region of the rate vector (R_A, R_B, R_C) given $R_D \geq \theta_3$ for $M3$.

4.3.2 Inadmissible Rate Region of $M3$

We use the same logic as in the previous subsection to derive the inadmissible rate region of the $M3$ scheme. The admissible rate region without feedback is given by equations (C.19a)–(C.19h) in Appendix C.2 [53]. From the equations, we get the constraints of the helper packet's information rate, $R_D \geq \theta_3$, and the sum-rate, $R_A + R_B + R_C \geq 1 + H_b(p_{AB}) + H_b(p_{BC}) - \theta_3$.

We analyze an ARQ system with M-in-1 helper transmission utilizing joint decoding of a helper and three unsuccessful independently decoded packets, for which NACKs have been received via the feedback channel. It is found that for arbitrary value of $R_D \geq \theta_3$, the inadmissible rate region of (R_A, R_B, R_C), $\mathcal{B}$, is obtained by

$$\mathcal{B} = \mathcal{B}_c \cap \mathcal{B}_t^C, \tag{4.9}$$

where $\bullet^C$ denotes the complement of the rate vector set in region $\bullet$, as shown in Figure 4.4. The cube $\mathcal{B}_c$ is determined by the constraints of each single transmission, $R_i \geq H(\boldsymbol{u}_i), i \in \{A, B, C\}$, whereas the $\mathcal{B}_t$ region is determined by the constraint of the sum-rate. $\mathcal{B}_t$ region is above from the plain $R_A + R_B + R_C = 1 + H_b(p_{AB}) + H_b(p_{BC}) - \theta_3$ up to the corner $(H(\boldsymbol{u}_A) = 1, H(\boldsymbol{u}_B) = 1, H(\boldsymbol{u}_C) = 1)$ of $\mathcal{B}_c$.

Figure 4.4 shows that $\mathcal{B}_t$ has different geometric shape even with the same value of p_e, depending on the value of p_{AB} and p_{BC}. For the extreme cases, we found $\mathcal{B}_t$ has triangular base plain, i.e. $\mathcal{B}_{t_1}$ corresponds to $p_{AB} = p_{BC} = 0.4999$ and $\mathcal{B}_{t_2}$ corresponds to $p_{AB} = p_{BC} = 10^{-6}$, for arbitrary value of p_e. All the aforementioned regions are given as follows.

$$\mathcal{B}_c = \{(R_A, R_B, R_C) | 0 \leq R_A < 1, \ \ 0 \leq R_B < 1, \ \ 0 \leq R_C < 1\}\}, \tag{4.10}$$

$$\begin{aligned}
\mathcal{B}_{t_1} = \{(R_A, R_B, R_C) \in \mathbb{R}^+ | &1 + H_b(p_{AB}) + H_b(p_{BC}) - \theta_3 - R_B - R_C \leq R_A < 1, \\
&H_b(p_{AB}) + H_b(p_{BC}) - \theta_3 - R_C \leq R_B < 1, \\
&H_b(p_{AB}) + H_b(p_{BC}) - \theta_3 - 1 \leq R_C < 1\}, \tag{4.11} \\
\mathcal{B}_{t_2}^C = \{(R_A, R_B, R_C) | &0 \leq R_A < 1 + H_b(p_{AB}) + H_b(p_{BC}) - \theta_3 - R_B - R_C, \\
&0 \leq R_B < 1 + H_b(p_{AB}) + H_b(p_{BC}) - \theta_3 - R_C, \\
&0 \leq R_C < 1 + H_b(p_{AB}) + H_b(p_{BC}) - \theta_3\}, \tag{4.12}
\end{aligned}$$

where $\theta_3 = H_b(p_{ABC} * p_e) - H_b(p_e)$. Notice that with $\mathcal{B}_{t_2}^C$, the inadmissible region $\mathcal{B} = \mathcal{B}_c \cap \mathcal{B}_{t_2}^C = \mathcal{B}_{t_2}^C$.

4.4   Outage Probability in Block Rayleigh Fading Channel

We derive the outage probabilities of $M2$ and $M3$ in block Rayleigh fading channel based on the results of the inadmissible rate regions results shown in Section 4.3. With the capacity-achieving channel codes assumption, the relationship between R_n and its corresponding instantaneous SNR, γ_n, is given by function $\Phi_n(\gamma_n)$ as [78]

$$R_n = \Phi_n(\gamma_n) = \frac{1}{Q_n} \log_2(1 + \gamma_n), \tag{4.13}$$

with its reverse function

$$\gamma_n = \Phi_n^{-1}(R_n) = 2^{R_n \cdot Q_n} - 1. \tag{4.14}$$

Since all the transmissions are suffering from statistically independent block Rayleigh fading, the joint pdf of the instantaneous SNRs can be expressed as $p(\gamma_A, \cdots, \gamma_D) = p(\gamma_A) \cdots p(\gamma_D)$.

There are three events possible in the system: (1) event of successfully decoding a packet with independent decoding, (2) event of successfully decoding M packets with the joint decoding, and (3) event of unsuccessfully decoding M packets with the joint decoding. Assuming the information source generates an infinite number of packets, the occurrence of those events is i.i.d.. Therefore, the outage probability of M-in-1 helper transmission, $P_{\text{out}}(M)$, can be obtained from analyzing the probability that the M packets in the buffer cannot be recovered with the joint decoding for the first time, which is given by (4.16). With independent decoding, the outage probability in block Rayleigh fading channel corresponds to the probability that the rate $R_n < H(\mathbf{u}_n) = 1$ is

$$\mathscr{P}_n = \int_{\Phi_n^{-1}(0)}^{\Phi_n^{-1}(1)} \frac{1}{\Gamma_n} \exp(-\frac{\gamma_n}{\Gamma_n}) d\gamma_n = 1 - \exp(-\frac{2^{Q_n} - 1}{\Gamma_n}). \tag{4.15}$$

Hence, $P_{\text{out}}(M)$ can be obtained by

$$P_{\text{out}}(M) = (1 - \mathscr{P}_n)^\omega (1 - \mathcal{E}(M))^{\lambda-1} \, \mathcal{E}(M), \tag{4.16}$$

where ω denotes the number of the packets successfully recovered with independent decoding and λ denotes the number of transmitted helper packet; both numbers are calculated before the receiver reaches the first unsuccessful recovery of M information packets with joint decoding. $\mathcal{E}(M)$ denotes the probability that M packets are unrecovered with independent decoding and the corresponding rates are falling into the inadmissible rate region.[5]

Approximation (Upper Bound). The outage probability of the system is upper bounded by $(1 - \mathcal{E}(M))^{\lambda-1} \, \mathcal{E}(M)$ because of $(1 - \mathscr{P}_n)^\omega \leq 1$ for arbitrary ω. However, since $(1 - \mathcal{E}(M))^{\lambda-1} \leq 1$ for arbitrary λ, $P_{\text{out}}(M) \leq \mathcal{E}(M)$.

---

[5]Rate vectors (R_A, R_B) and (R_A, R_B, R_C) fall into regions $\mathcal{A}_4$ for $M2$ and $\mathcal{B}$ for $M3$, respectively.

Let $\mathcal{P}_M$ be the probability that M packets are unrecovered with independent decoding, and $\mathcal{P}_{E|M}$ be the probability that the rate vector of the information packets falls into inadmissible region given the fact that those packets are unrecovered with independent decoding, then $\mathcal{E}(M)$ is given by

$$\mathcal{E}(M) = \mathcal{P}_{E|M} \cdot \mathcal{P}_M. \tag{4.17}$$

By taking into account the impact of the channel variation in the helper transmission phase, $\mathcal{P}_{E|M}$ is obtained by taking average over p_e given by

$$p_e = \begin{cases} H_b^{-1}(H_b(g) - \Phi_D(\gamma_D)), & \text{for } \Phi_D^{-1}(0) \le \gamma_D < \Phi_D^{-1}(H_b(g)), \\ 0, & \text{for } \gamma_D \ge \Phi_D^{-1}(H_b(g)), \end{cases} \tag{4.18}$$

where $g = p_{AB}$ for $M2$ and $g = p_{ABC}$ for $M3$.

4.4.1 Outage Probability with $M2$

The outage probability of $M2$ is upper bounded by $P_{\text{out}}(2) \le \mathcal{P}_{E|2} \cdot \mathcal{P}_2$, where

$$\mathcal{P}_2 = \mathscr{P}_A \cdot \mathscr{P}_B = \Big[1 - \exp(-\frac{2^{Q_A} - 1}{\Gamma_A})\Big]\Big[1 - \exp(-\frac{2^{Q_B} - 1}{\Gamma_B})\Big]. \tag{4.19}$$

$$\begin{aligned} \mathcal{P}_{E|2} &= \mathbb{P}\{\mathcal{A}_4|p_e = 0\} + \mathbb{P}\{\mathcal{A}_4|0 < p_e \le 0.5\}, \\ &= \mathbb{P}\{\mathcal{A}_{4_a}|p_e = 0\} + \mathbb{P}\{\mathcal{A}_{4_b}|p_e = 0\} + \mathbb{P}\{\mathcal{A}_{4_a}|0 < p_e \le 0.5\} + \mathbb{P}\{\mathcal{A}_{4_b}|0 < p_e \le 0.5\}, \\ &= \frac{\mathbb{P}'\{\mathcal{A}_{4_a}|p_e = 0\} + \mathbb{P}'\{\mathcal{A}_{4_b}|p_e = 0\} + \mathbb{P}'\{\mathcal{A}_{4_a}|0 < p_e \le 0.5\} + \mathbb{P}'\{\mathcal{A}_{4_b}|0 < p_e \le 0.5\}}{\mathbb{P}(\mathcal{A}_4 \cup \mathcal{A}_5)}, \end{aligned}$$

$$\tag{4.20}$$

with $\mathbb{P}\{\star|p_e = 0\}$ and $\mathbb{P}\{\star|0 < p_e \le 0.5\}$ denoting the probability of the corresponding rate vector[6] falls in region $\star$ given the cases $p_e = 0$ and $0 < p_e \le 0.5$, respectively. $\mathbb{P}'(\bullet)$ is the unnormalized value of $\mathbb{P}(\bullet)$ given the fact that $\mathbb{P}[(R_A, R_B) \in \mathcal{A}_4 \cup \mathcal{A}_5] = 1$. Hence, the normalized factor $\mathbb{P}(\mathcal{A}_4 \cup \mathcal{A}_5)$ is defined by

$$\mathbb{P}(\mathcal{A}_4 \cup \mathcal{A}_5) = \int_{\Phi_A^{-1}(0)}^{\Phi_A^{-1}(1)} \int_{\Phi_B^{-1}(0)}^{\Phi_B^{-1}(1)} p(\gamma_A)p(\gamma_B)d_{\gamma_A}d_{\gamma_B} = \Big[1 - \exp(-\frac{\Phi_A^{-1}(1)}{\Gamma_A})\Big]\Big[1 - \exp(-\frac{\Phi_B^{-1}(1)}{\Gamma_B})\Big]. \tag{4.21}$$

---

[6](R_A, R_B) for $M2$ and (R_A, R_B, R_C) for $M3$.

The probabilities in (4.20) can be given by the following equations (4.22)–(4.25), as

$$\mathbb{P}'\{\mathcal{A}_{4_a}|p_e = 0\} = \int_{\Phi_D^{-1}[H_b(p_{AB})]}^{\Phi_D^{-1}(\infty)} \int_{\Phi_A^{-1}(0)}^{\Phi_A^{-1}(0)} \int_{\Phi_B^{-1}(0)}^{\Phi_B^{-1}(1)} p(\gamma_B)p(\gamma_A)p(\gamma_D)d_{\gamma_B}d_{\gamma_A}d_{\gamma_D} = 0, \qquad (4.22)$$

$$\mathbb{P}'\{\mathcal{A}_{4_b}|p_e = 0\} = \int_{\Phi_D^{-1}[H_b(p_{AB})]}^{\Phi_D^{-1}(\infty)} \int_{\Phi_A^{-1}(0)}^{\Phi_A^{-1}(1)} \int_{\Phi_B^{-1}(0)}^{\Phi_B^{-1}[1-\Phi_A(\gamma_A)]} p(\gamma_B)p(\gamma_A)p(\gamma_D)d_{\gamma_B}d_{\gamma_A}d_{\gamma_D}$$

$$= \frac{1}{\Gamma_A}\exp\left(-\frac{\Phi_D^{-1}[H_b(p_{AB})]}{\Gamma_D}\right)\int_{\Phi_A^{-1}(0)}^{\Phi_A^{-1}(1)}\exp\left(-\frac{\gamma_A}{\Gamma_A}\right)\left[1-\exp\left(-\frac{\Phi_B^{-1}[1-\Phi_A(\gamma_A)]}{\Gamma_B}\right)\right]d_{\gamma_A}.$$

$$(4.23)$$

$$\mathbb{P}'\{\mathcal{A}_{4_a}|0<p_e\leq 0.5\} = \int_{\Phi_D^{-1}(0)}^{\Phi_D^{-1}[H_b(p_{AB})]} \int_{\Phi_A^{-1}(0)}^{\Phi_A^{-1}[\Psi(\gamma_D)]} \int_{\Phi_B^{-1}(0)}^{\Phi_B^{-1}(1)} p(\gamma_B)p(\gamma_A)p(\gamma_D)d_{\gamma_B}d_{\gamma_A}d_{\gamma_D}$$

$$= \frac{1}{\Gamma_D}\left[1-\exp\left(-\frac{\Phi_B^{-1}(1)}{\Gamma_B}\right)\right]\int_{\Phi_D^{-1}(0)}^{\Phi_D^{-1}[H_b(p_{AB})]}\exp\left(-\frac{\gamma_D}{\Gamma_D}\right)\left[1-\exp\left(-\frac{\Phi_A^{-1}[\Psi(\gamma_D)]}{\Gamma_A}\right)\right]d_{\gamma_D},$$

$$(4.24)$$

$$\mathbb{P}'\{\mathcal{A}_{4_b}|0<p_e\leq 0.5\} = \int_{\Phi_D^{-1}(0)}^{\Phi_D^{-1}[H_b(p_{AB})]} \int_{\Phi_A^{-1}[\Psi(\gamma_D)]}^{\Phi_A^{-1}(1)} \int_{\Phi_B^{-1}(0)}^{\Phi_B^{-1}[\Psi(\gamma_A,\gamma_D)]} p(\gamma_B)p(\gamma_A)p(\gamma_D)d_{\gamma_B}d_{\gamma_A}d_{\gamma_D}$$

$$= \frac{1}{\Gamma_A\Gamma_D}\int_{\Phi_D^{-1}(0)}^{\Phi_D^{-1}[H_b(p_{AB})]}\int_{\Phi_A^{-1}[\Psi(\gamma_D)]}^{\Phi_A^{-1}(1)}\exp\left(-\frac{\gamma_A}{\Gamma_A}-\frac{\gamma_D}{\Gamma_D}\right)\left[1-\exp\left(-\frac{\Phi_B^{-1}[\Psi(\gamma_A,\gamma_D)]}{\Gamma_B}\right)\right]d_{\gamma_A}d_{\gamma_D},$$

$$(4.25)$$

where $\Psi(\gamma_D) = 2H_b(p_{AB})-\Phi_D(\gamma_D)-H_b[p_{AB}*H_b^{-1}[H_b(p_{AB})-\Phi_D(\gamma_D)]]$ and $\Psi(\gamma_A,\gamma_D) = 1 + \Psi(\gamma_D) - \Phi_A(\gamma_A)$.

4.4.2   Outage Probability with $M3$

As described in Section 4.3.2, $\mathcal{B}_t$ has various geometric shape depending on the value of p_e, p_{AB} and p_{BC}. For the sake of simplicity, we theoretically derive the outage probability of $M3$ in the case $\mathcal{B}_t$ has a triangular base plain, e.g. $\mathcal{B}_{t_1}$ and $\mathcal{B}_{t_2}$. The result is verified by the Monte Carlo simulation shown in Section 4.5. Eventually, in other cases, the outage probability can be calculated by the Monte Carlo simulations.

The upper bound of the outage probability of $M3$ is given by $P_{\text{out}}(3) \le \mathcal{P}_{E|3} \cdot \mathcal{P}_3$, where

$$\mathcal{P}_3 = \mathscr{P}_A \cdot \mathscr{P}_B \cdot \mathscr{P}_C = \left[1 - \exp(-\frac{2^{Q_A} - 1}{\Gamma_A})\right]\left[1 - \exp(-\frac{2^{Q_B} - 1}{\Gamma_B})\right]\left[1 - \exp(-\frac{2^{Q_C} - 1}{\Gamma_C})\right].$$

(4.26)

$$\mathcal{P}_{E|3} = \mathbb{P}\{\mathcal{B}|p_e = 0\} + \mathbb{P}\{\mathcal{B}|0 < p_e \le 0.5\}. \tag{4.27}$$

In the case of $\mathcal{B}_{t_1}$,

$$\begin{aligned}
\mathcal{P}_{E|3}(\mathcal{B}_{t_1}) &= \mathbb{P}\{\mathcal{B}_c|p_e = 0\} - \mathbb{P}\{\mathcal{B}_{t_1}|p_e = 0\} + \mathbb{P}\{\mathcal{B}_c|0 < p_e \le 0.5\} - \mathbb{P}\{\mathcal{B}_{t_1}|0 < p_e \le 0.5\}, \\
&= \frac{\mathbb{P}'\{\mathcal{B}_c|p_e = 0\} - \mathbb{P}'\{\mathcal{B}_{t_1}|p_e = 0\} + \mathbb{P}'\{\mathcal{B}_c|0 < p_e \le 0.5\} - \mathbb{P}'\{\mathcal{B}_{t_1}|0 < p_e \le 0.5\}}{\mathbb{P}(\mathcal{B}_c)},
\end{aligned}$$

(4.28)

whereas the case of $\mathcal{B}_{t_2}$,

$$\begin{aligned}
\mathcal{P}_{E|3}(\mathcal{B}_{t_2}^C) &= \mathbb{P}\{\mathcal{B}_{t_2}^C|p_e = 0\} + \mathbb{P}\{\mathcal{B}_{t_2}^C|0 < p_e \le 0.5\}, \\
&= \frac{\mathbb{P}'\{\mathcal{B}_{t_2}^C|p_e = 0\} + \mathbb{P}'\{\mathcal{B}_{t_2}^C|0 < p_e \le 0.5\}}{\mathbb{P}(\mathcal{B}_c)},
\end{aligned}$$

(4.29)

The normalization factor $\mathbb{P}(\mathcal{B}_c)$ that appears in common in the denominator of (4.28) and (4.29) is defined by

$$\begin{aligned}
\mathbb{P}(\mathcal{B}_c) &= \int_{\Phi_A^{-1}(0)}^{\Phi_A^{-1}(1)} \int_{\Phi_B^{-1}(0)}^{\Phi_B^{-1}(1)} \int_{\Phi_C^{-1}(0)}^{\Phi_C^{-1}(1)} p(\gamma_A)p(\gamma_B)p(\gamma_C) d_{\gamma_A} d_{\gamma_B} d_{\gamma_C} \\
&= \left[1 - \exp(-\frac{\Phi_A^{-1}(1)}{\Gamma_A})\right]\left[1 - \exp(-\frac{\Phi_B^{-1}(1)}{\Gamma_B})\right]\left[1 - \exp(-\frac{\Phi_C^{-1}(1)}{\Gamma_C})\right]. \quad (4.30)
\end{aligned}$$

The remaining probabilities in (4.28) given by the following equations (4.31)–(4.34), as

$$\mathbb{P}'\{\mathcal{B}_c|p_e=0\} = \int_{\Phi_D^{-1}[H_b(p_{ABC})]}^{\Phi_D^{-1}(\infty)} \int_{\Phi_C^{-1}(0)}^{\Phi_C^{-1}(1)} \int_{\Phi_B^{-1}(0)}^{\Phi_B^{-1}(1)} \int_{\Phi_A^{-1}(0)}^{\Phi_A^{-1}(1)} p(\gamma_A)p(\gamma_B)p(\gamma_C)p(\gamma_D)d_{\gamma_A}d_{\gamma_B}d_{\gamma_C}d_{\gamma_D}$$

$$= \exp\left(-\frac{\Phi_D^{-1}(1)}{\Gamma_D}\right)\left[1-\exp\left(-\frac{\Phi_C^{-1}(1)}{\Gamma_C}\right)\right]\left[1-\exp\left(-\frac{\Phi_B^{-1}(1)}{\Gamma_B}\right)\right]$$

$$\left[1-\exp\left(-\frac{\Phi_A^{-1}(1)}{\Gamma_A}\right)\right], \tag{4.31}$$

$$\mathbb{P}'\{\mathcal{B}_{t_1}|p_e=0\} = \int_{\Phi_D^{-1}[H_b(p_{ABC})]}^{\Phi_D^{-1}(\infty)} \int_{\Phi_C^{-1}[H_b(p_{AB})+H_b(p_{BC})-2]}^{\Phi_C^{-1}(1)} \int_{\Phi_B^{-1}[\Psi(\gamma_C)]}^{\Phi_B^{-1}(1)} \int_{\Phi_A^{-1}[\Psi(\gamma_B,\gamma_C)]}^{\Phi_A^{-1}(1)} p(\gamma_A)\cdots p(\gamma_D)d_{\gamma_A}\cdots d_{\gamma_D},$$

$$= \frac{1}{\Gamma_B\Gamma_C} \int_{\Phi_C^{-1}[H_b(p_{AB})+H_b(p_{BC})-2]}^{\Phi_C^{-1}(1)} \int_{\Phi_B^{-1}[\Psi(\gamma_C)]}^{\Phi_B^{-1}(1)} \exp\left(-\frac{\Phi_D^{-1}(1)}{\Gamma_D}-\frac{\gamma_C}{\Gamma_C}-\frac{\gamma_B}{\Gamma_B}\right)$$

$$\left[\exp\left(-\frac{\Phi_A^{-1}[\Psi(\gamma_B,\gamma_C)]}{\Gamma_A}\right)-\exp\left(-\frac{\Phi_A^{-1}(1)}{\Gamma_A}\right)\right]d_{\gamma_B}d_{\gamma_C}, \tag{4.32}$$

with $\Psi(\gamma_C) = H_b(p_{AB}) + H_b(p_{BC}) - 1 - \Phi_C(\gamma_C)$, $\Psi(\gamma_B,\gamma_C) = H_b(p_{AB}) + H_b(p_{BC}) - \Phi_B(\gamma_B) - \Phi_C(\gamma_C)$, and

$$\mathbb{P}'\{\mathcal{B}_c|0<p_e\le0.5\} = \int_{\Phi_D^{-1}(0)}^{\Phi_D^{-1}[H_b(p_{ABC})]} \int_{\Phi_C^{-1}(0)}^{\Phi_C^{-1}(1)} \int_{\Phi_B^{-1}(0)}^{\Phi_B^{-1}(1)} \int_{\Phi_A^{-1}(0)}^{\Phi_A^{-1}(1)} p(\gamma_A)p(\gamma_B)p(\gamma_C)p(\gamma_D)d_{\gamma_A}d_{\gamma_B}d_{\gamma_C}d_{\gamma_D}$$

$$= \left[1-\exp\left(-\frac{\Phi_D^{-1}(1)}{\Gamma_D}\right)\right]\left[1-\exp\left(-\frac{\Phi_C^{-1}(1)}{\Gamma_C}\right)\right]\left[1-\exp\left(-\frac{\Phi_B^{-1}(1)}{\Gamma_B}\right)\right]$$

$$\left[1-\exp\left(-\frac{\Phi_A^{-1}(1)}{\Gamma_A}\right)\right], \tag{4.33}$$

$$\mathbb{P}'\{\mathcal{B}_{t_1}|0<p_e\le0.5\} = \int_{\Phi_D^{-1}(0)}^{\Phi_D^{-1}[H_b(p_{ABC})]} \int_{\Phi_C^{-1}[\Psi(\gamma_D)]}^{\Phi_C^{-1}(1)} \int_{\Phi_B^{-1}[\Psi(\gamma_C,\gamma_D)]}^{\Phi_B^{-1}(1)} \int_{\Phi_A^{-1}[\Psi(\gamma_B,\gamma_C,\gamma_D)]}^{\Phi_A^{-1}(1)} p(\gamma_A)\cdots p(\gamma_D)d_{\gamma_A}\cdots d_{\gamma_D},$$

$$= \frac{1}{\Gamma_B \Gamma_C \Gamma_D} \int\limits_{\Phi_D^{-1}(0)}^{\Phi_D^{-1}(1)} \int\limits_{\Phi_C^{-1}[\Psi(\gamma_D)]}^{\Phi_C^{-1}(1)} \int\limits_{\Phi_B^{-1}[\Psi(\gamma_C,\gamma_D)]}^{\Phi_B^{-1}(1)} \exp\left(-\frac{\gamma_B}{\Gamma_B} - \frac{\gamma_C}{\Gamma_C} - \frac{\gamma_D}{\Gamma_D}\right)$$

$$\left[\exp\left(-\frac{\Phi_A^{-1}[\Psi(\gamma_B,\gamma_C,\gamma_D)]}{\Gamma_A}\right) - \exp\left(-\frac{\Phi_A^{-1}(1)}{\Gamma_A}\right)\right] d_{\gamma_B} \, d_{\gamma_C} \, d_{\gamma_D},$$

$$(4.34)$$

with $\Psi(\gamma_D) = H_b(p_{AB}) + H_b(p_{BC}) - \Phi_D(\gamma_D) - 1$, $\Psi(\gamma_C, \gamma_D) = H_b(p_{AB}) + H_b(p_{BC}) - \Phi_D(\gamma_D) - \Phi_C(\gamma_C)$, and $\Psi(\gamma_B, \gamma_C, \gamma_D) = 1 + H_b(p_{AB}) + H_b(p_{BC}) - \Phi_D(\gamma_D) - \Phi_B(\gamma_B) - \Phi_C(\gamma_C)$.

The probability expressions in (4.29) can be expanded as:

$$\mathbb{P}'\{\mathcal{B}_{t_2}^C | p_e = 0\} = \int\limits_{\Phi_D^{-1}[H_b(p_{ABC})]}^{\Phi_D^{-1}(\infty)} \int\limits_{\Phi_C^{-1}(0)}^{\Phi_C^{-1}[H_b(p_{AB})+H_b(p_{BC})]} \int\limits_{\Phi_B^{-1}(0)}^{\Phi_B^{-1}[\Psi(\gamma_C)]} \int\limits_{\Phi_A^{-1}(0)}^{\Phi_A^{-1}[\Psi(\gamma_B,\gamma_C)]} p(\gamma_A) \cdots p(\gamma_D) d_{\gamma_A} \cdots d_{\gamma_D},$$

$$= \frac{1}{\Gamma_B \Gamma_C} \int\limits_{\Phi_C^{-1}(0)}^{\Phi_C^{-1}[H_b(p_{AB})+H_b(p_{BC})]} \int\limits_{\Phi_B^{-1}(0)}^{\Phi_B^{-1}[\Psi(\gamma_C)]} \exp\left(-\frac{\Phi_D^{-1}(1)}{\Gamma_D} - \frac{\gamma_C}{\Gamma_C} - \frac{\gamma_B}{\Gamma_B}\right)$$

$$\left[1 - \exp\left(-\frac{\Phi_A^{-1}[\Psi(\gamma_B,\gamma_C)]}{\Gamma_A}\right)\right] d_{\gamma_B} \, d_{\gamma_C},$$

$$(4.35)$$

with $\Psi(\gamma_C) = H_b(p_{AB}) + H_b(p_{BC}) - \Phi_C(\gamma_C)$, $\Psi(\gamma_B, \gamma_C) = H_b(p_{AB}) + H_b(p_{BC}) - \Phi_B(\gamma_B) - \Phi_C(\gamma_C)$,

$$\mathbb{P}'\{\mathcal{B}_{t_2}^C | 0 < p_e \leq 0.5\} = \int\limits_{\Phi_D^{-1}(0)}^{\Phi_D^{-1}[H_b(p_{ABC})]} \int\limits_{\Phi_C^{-1}(0)}^{\Phi_C^{-1}[\Psi(\gamma_D)]} \int\limits_{\Phi_B^{-1}(0)}^{\Phi_B^{-1}[\Psi(\gamma_C,\gamma_D)]} \int\limits_{\Phi_A^{-1}(0)}^{\Phi_A^{-1}[\Psi(\gamma_B,\gamma_C,\gamma_D)]} p(\gamma_A) \cdots p(\gamma_D) d_{\gamma_A} \cdots d_{\gamma_D},$$

$$= \frac{1}{\Gamma_B \Gamma_C \Gamma_D} \int\limits_{\Phi_D^{-1}(0)}^{\Phi_D^{-1}(1)} \int\limits_{\Phi_C^{-1}(0)}^{\Phi_C^{-1}[\Psi(\gamma_D)]} \int\limits_{\Phi_B^{-1}(0)}^{\Phi_B^{-1}[\Psi(\gamma_C,\gamma_D)]} \exp\left(-\frac{\gamma_B}{\Gamma_B} - \frac{\gamma_C}{\Gamma_C} - \frac{\gamma_D}{\Gamma_D}\right)$$

$$\left[1 - \exp\left(-\frac{\Phi_A^{-1}[\Psi(\gamma_B,\gamma_C,\gamma_D)]}{\Gamma_A}\right)\right] d_{\gamma_B} \, d_{\gamma_C} \, d_{\gamma_D},$$

$$(4.36)$$

with $\Psi(\gamma_D) = 1 + H_b(p_{AB}) + H_b(p_{BC}) - \Phi_D(\gamma_D)$, $\Psi(\gamma_C, \gamma_D) = 1 + H_b(p_{AB}) + H_b(p_{BC}) - \Phi_D(\gamma_D) - \Phi_C(\gamma_C)$, and $\Psi(\gamma_B, \gamma_C, \gamma_D) = 1 + H_b(p_{AB}) + H_b(p_{BC}) - \Phi_D(\gamma_D) - \Phi_B(\gamma_B) - \Phi_C(\gamma_C)$.

4.5 Numerical Analyses

This section presents numerical results of the upper bound calculation of the outage probability calculation for $M2$ and $M3$, given particular ρ_z and Q_n values. With any values of ρ_z, $M2$ can always achieve diversity order two, while, surprisingly, $M3$ can achieve diversity order four if the information correlation is close to one; otherwise, $M3$ can always achieve the diversity order three. To confirm this fact, we perform a series of computer simulations for 10^6 channel realizations and $\rho_{AB} = \rho_{BC} = \{0, 0.5, 0.8, 0.98, 1\}$, the results of which are shown in Figure 4.5. The results of a series of Monte Carlo simulations and theoretical calculations are shown in the figure. It is found that they are consistent with each other.

With $M2$, the high packet correlations provide slightly better performance at low average SNR regime. However, no significant improvement can be achieved with any packet correlation value at high average SNR regime. Nevertheless, the diversity order is two for all the cases. It is understandable by analyzing the $M2$ inadmissible rate region, where the shape of the case $\mathbb{P}[(R_A, R_B) \in \mathcal{A}_5] = 0$ leads the result of the integral calculation inversely proportional to $(\Gamma_n)^2$. Furthermore, this case highly likely occurs at high average SNR value range where $p_e \approx 0$ and hence $R_A + R_B \geq 1 + H_b(p_{AB}) - \theta_2 \approx 1$.

With $M3$, the performance is parameterized with ρ_{AB} and ρ_{BC}. For the preliminary verification, we evaluated the relationship among the bit flipping probabilities p_{AB} and p_{BC}, and p_{ABC} in the Appendix B. It is shown that $p_{ABC} \approx 0.5$, corresponding to $\rho_{ABC} \approx 0$, for any pair values of p_{AB} and p_{BC}. Since the integral boundary is complex, depending on p_{AB} and p_{BC}, we calculated theoretically the outage probability only for the simplest case which are $p_{AB} = p_{BC} = 0.5$ corresponding to $\rho_{AB} = \rho_{BC} = 0$ and $p_{AB} = p_{BC} = 0$ corresponding to $\rho_{AB} = \rho_{BC} = 1$, and for the other cases, we calculated the outage probability by Monte Carlo simulations.

It is found from Figure 4.5 that with $M3$, the Monte Carlo simulation and theoretical results are consistent for $\rho_{AB} = \rho_{BC} = 0$ and $\rho_{AB} = \rho_{BC} = 1$, and for the other cases, the diversity order indicated by the decay of the curves are the same. Surprisingly, it is found that except for the information correlation being very close to one, the diversity order three can always be achieved. With $\rho_{AB} = \rho_{BC} = 0.8$, we can achieve roughly 2 dB improvement at outage probability of 10^{-3}, compared to that with $\rho_{AB} = \rho_{BC} = 0$, but, again, it should be emphasized that the diversity order for all the cases is the same. However, in the case the
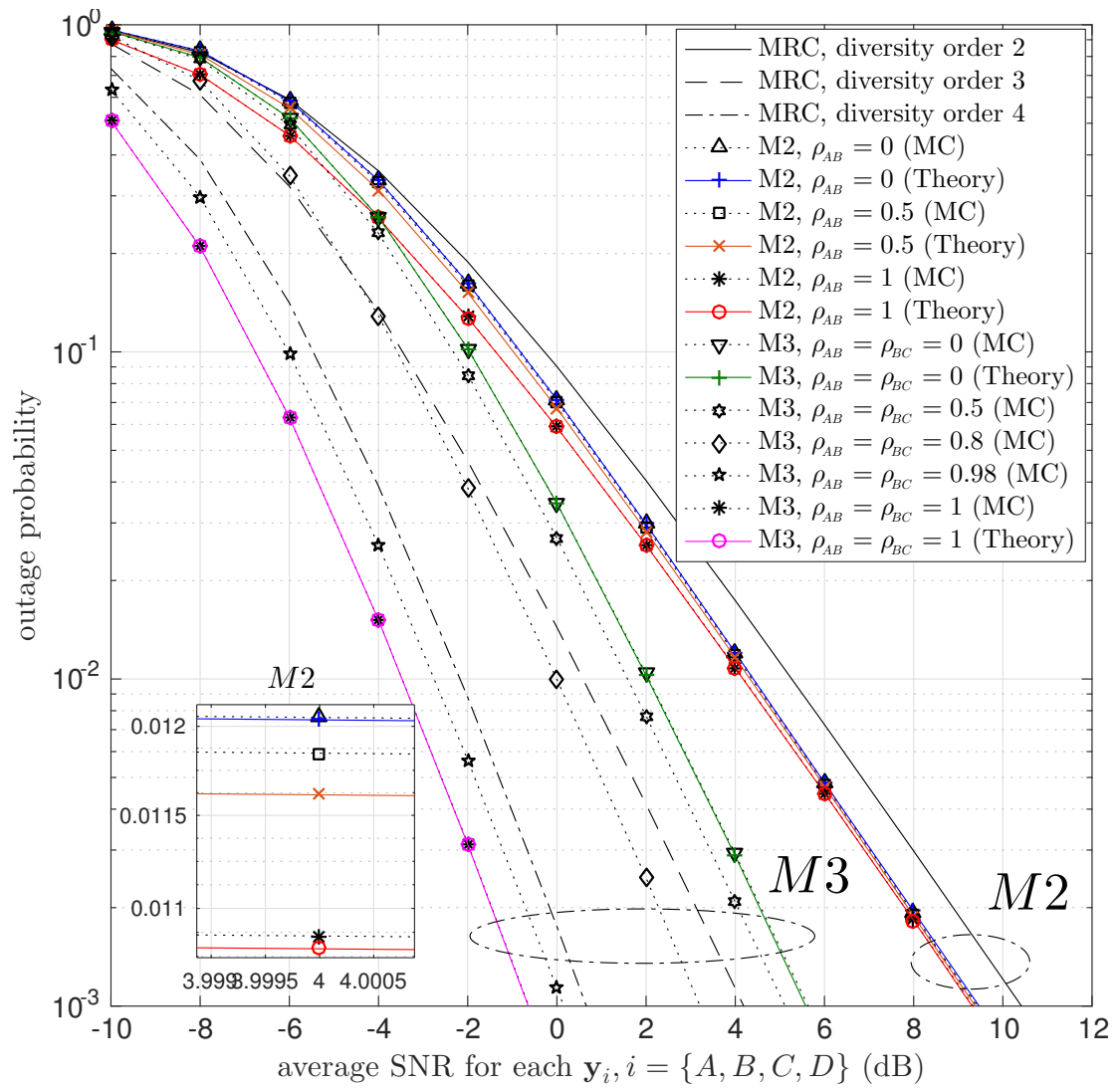
Figure 4.5: Upper bound of the outage probabilities of feedback-assisted correlated packet transmission with $M2$ and $M3$ for equal transmit power and $Q_n = 0.5$.

information correlation is very close to one, $M3$ can always achieve the diversity order four. This is reasonable because with the correlation close to one, all the packets including the helper are almost the same, and hence in this case almost the same packet is transmitted four times.
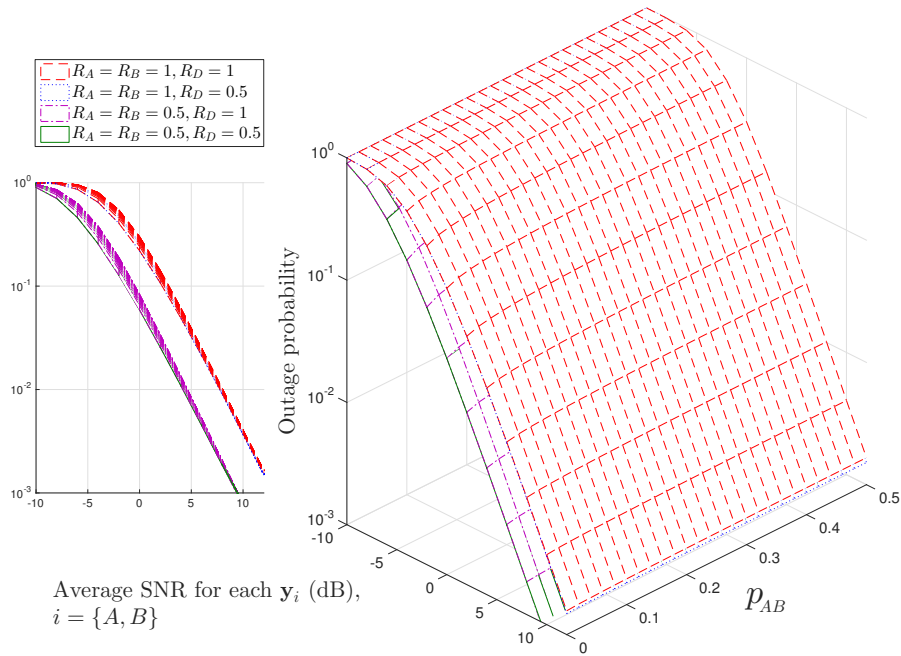
(a) $\Gamma_D = \Gamma_{\{A,B\}}$.
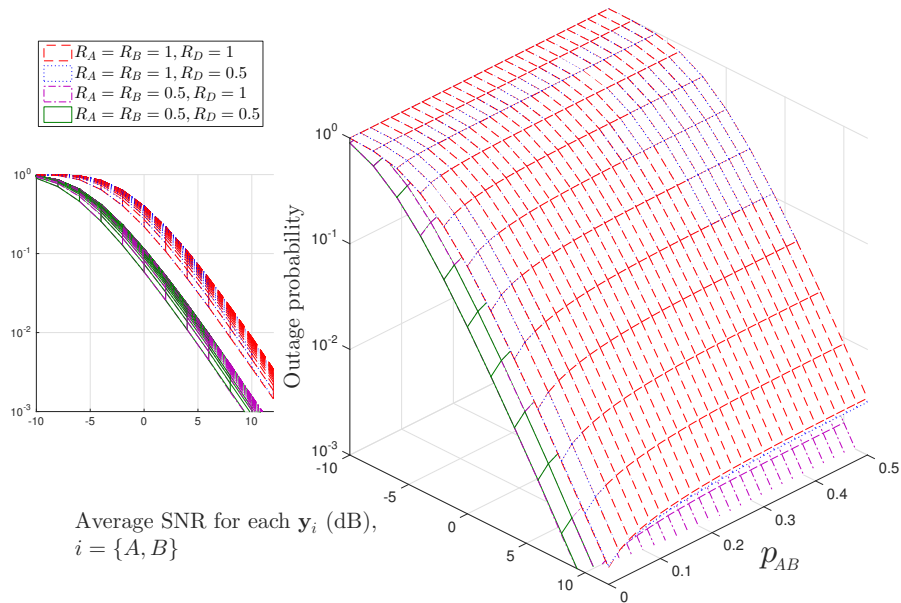
(b) $\Gamma_D = \Gamma_{\{A,B\}} - 20 \ dB$.

(c) $\Gamma_D = \Gamma_{\{A,B\}} + 20~dB$.
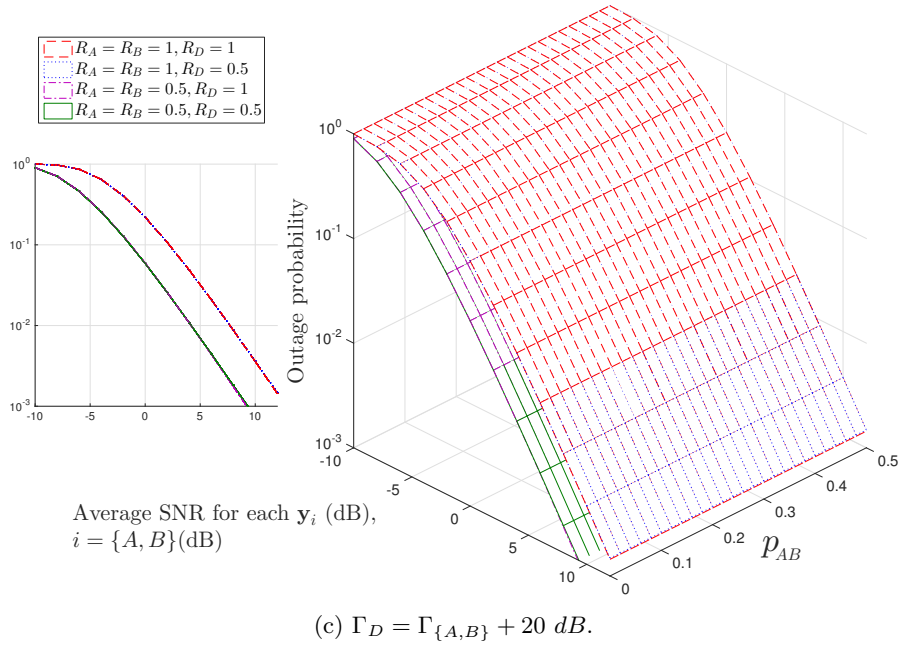
Figure 4.6: Upper bound of the outage probability of $M2$ for unequal transmit power for the information and helper packets.

Figure 4.6 and Figure 4.7, respectively, show the performance of $M2$ and $M3$ for various Q_n and transmit power settings of the information and the helper packets. Note that low Q_n corresponds to large redundancy with the same modulation order, or low modulation order with the same number of parity,[7] and vice versa. It is found in Figure 4.6 that in general low Q_n slightly increase the performance of $M2$. Specifically, the impact of decreasing Q_n of the information packet is significant to achieve better performance than decreasing that of the helper packet. Also, increasing the transmit power of the information packet is significant to achieve better performance than that of the helper packet. Likewise, the same tendency also can be found for $M3$ case as shown in Figure 4.7.

4.6 Generalization

In this section, for the sake of clarity, we replace the alphabets in the subscripts of the rates R and bit-flipping variables p, with numbers, e.g., $R_A \rightarrow R_1, R_B \rightarrow R_2, p_{AB} \rightarrow p_{12}, p_{ABC} \rightarrow p_{123}, p_{ABCD\cdots} \rightarrow p_{1234\cdots}$. We also use subscript *help* instead of D to indicate the helper packet possession.

---

[7]See footnote 4.

(a) $\Gamma_D = \Gamma_{\{A,B,C\}} = -10 \ dB$.

(b) $\Gamma_D = \Gamma_{\{A,B,C\}} = 0 \ dB$.

(c) $\Gamma_D = -10 \ dB, \Gamma_{\{A,B,C\}} = 0 \ dB$.

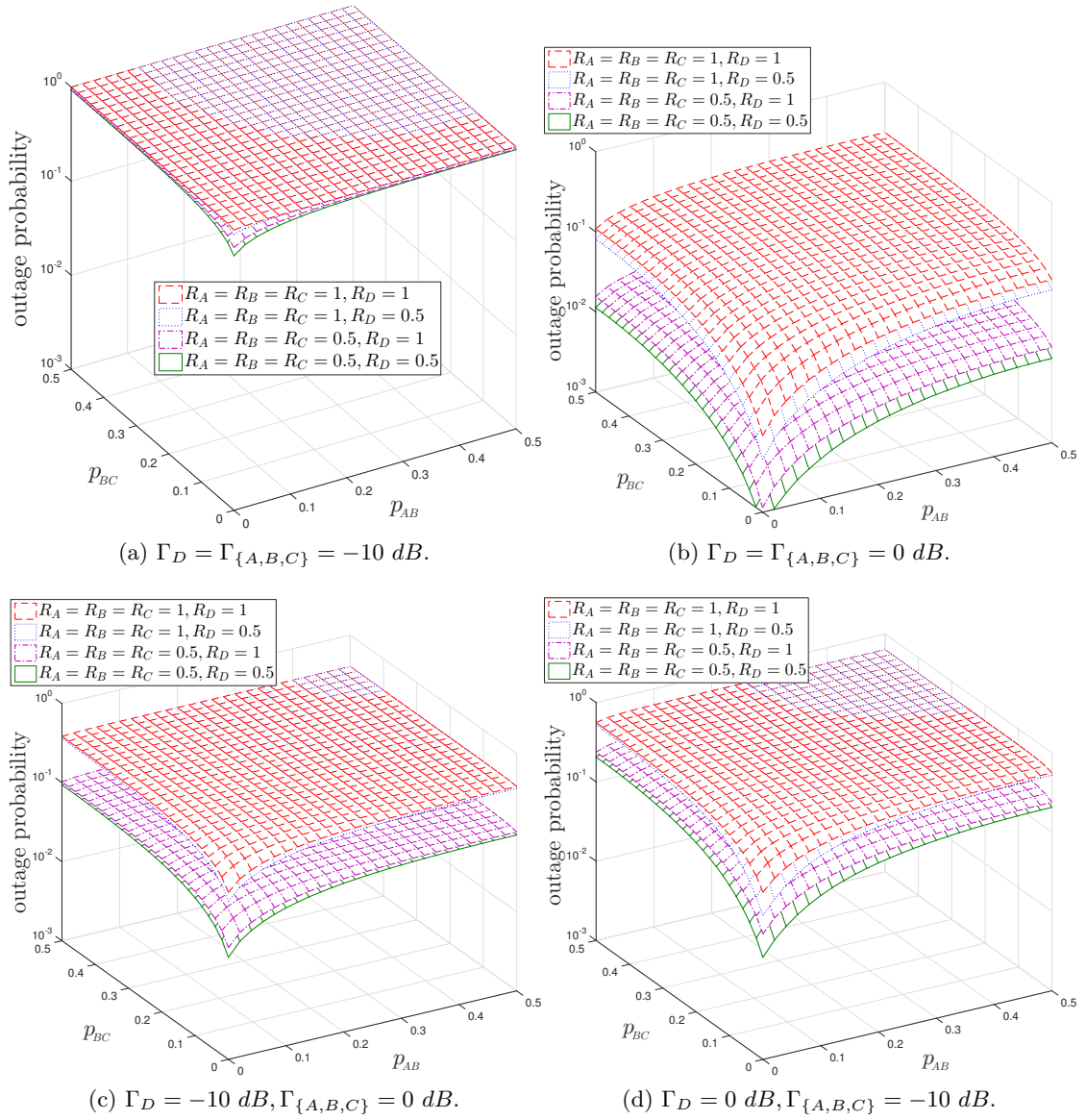(d) $\Gamma_D = 0 \ dB, \Gamma_{\{A,B,C\}} = -10 \ dB$.

Figure 4.7: Upper bound of the outage probability of $M3$ for various transmit power settings.

We showed in Section 4.3 that with M NACK-ed packets, the largest inadmissible rate region is given by $\mathfrak{S} = \{(R_1, R_2, \cdots, R_M) | 0 \leq R_i < 1, i = \{1, 2, \cdots, M\}\}$. With the calculation as in Section 4.4, the area/volume of $\mathfrak{S}$ is always yielding M diversity order. The physical meaning of such system is that the receiver always combines M NACK-ed packets and these packets are unrecovered at first; however, only by utilizing the source correlation and/or helper packet, there is a chance to recover all M packets but no chance to recover less than M packets.

With full information correlation, however, it is noticeable that bitwise XOR operation makes the helper the same as all NACK-ed packets if M is odd, and hence $M + 1$ order diversity can be achieved. On the other hand, the helper packet is always the binary of zeros if M is even, and hence it is not unique for any source information. Therefore, only M order diversity can be achieved. For this reason, it is still interesting to see how odd number of M can achieve beyond M diversity order by mathematical formulas using *the theorem for multiple source coding with a helper.*

In Section 4.3, we showed that the cut amount of the inadmissible rate region determines additional gain. The larger the area/volume of the cut inadmissible rate region corresponds to the lower the outage probability, and vice versa. Let $\mathfrak{R}$ be an area or a volume containing rates as $\mathfrak{R} = \{(R_1, R_2, \cdots, R_M) \in \mathbb{R}^+ | \sum_{i=1}^{M} R_i < H(\boldsymbol{u}_1, \boldsymbol{u}_2, \cdots, \boldsymbol{u}_M | \hat{\boldsymbol{u}}_{\text{help}})\}$, the area/volume of the cut inadmissible rate region, denoted by $\mathfrak{C}$, is then given by

$$\mathfrak{C} = \mathfrak{S} - \mathfrak{R}, \ \forall \mathfrak{R} \subseteq \mathfrak{S} \tag{4.37}$$

It can be seen that $\mathfrak{C}$ is significantly determined by the sum-rates in $\mathfrak{R}$, which is

$$\sum_{i=1}^{M} R_i < H(\boldsymbol{u}_1, \boldsymbol{u}_2, \cdots, \boldsymbol{u}_M | \hat{\boldsymbol{u}}_{\text{help}})$$

$$= H(\boldsymbol{u}_1) + \sum_{j=2}^{M} H(\boldsymbol{u}_j | \boldsymbol{u}_1, \boldsymbol{u}_2, \cdots, \boldsymbol{u}_{j-1}) + H(\hat{\boldsymbol{u}}_{\text{help}} | \boldsymbol{u}_1, \boldsymbol{u}_2, \cdots, \boldsymbol{u}_M) - H(\hat{\boldsymbol{u}}_{\text{help}})$$

$$= 1 + \sum_{j=2}^{M} H_b(p_{j-1,j}) + H_b(p_e) - H_b(p_{1\cdots M} * p_e), \tag{4.38}$$

where $H_b(p_{j-1,j})$ in (4.38) is because of the Markov process $\boldsymbol{u}_1 \to \boldsymbol{u}_2 \to \cdots \to \boldsymbol{u}_M$,

and $p_{j-1,j} = \mathbb{P}(\boldsymbol{u}_{j-1} \oplus \boldsymbol{u}_j = 1)$. We can get $\sum_{i=1}^{M} R_i < M - 1$ if the sources are uncorrelated but the helper is error free. In this case $\mathfrak{C} = 0$, and hence there is no additional gain. On the other hand, with full information correlation, $p_{1\cdots M}$ being 0 or 0.5, respectively, if M is even or odd.[8] Therefore, $\sum_{i=1}^{M} R_i < 1$ if M is even and $\sum_{i=1}^{M} R_i < H_b(p_e)$ if M is odd, which are corresponding to $\mathfrak{C} = 0$ and $\mathfrak{C} \geq 0$, respectively. It can be see that the equality $\mathfrak{C} = 0$ with M being odd is achieved only when the bit error probability of the helper packet is 0.5. In other words, there is no additional diversity order can be achieved with M being even, but $M + 1$ order diversity can be achieved with M being odd which depends on the source correlations and the bit error probability of the helper packet.

4.7   Summary

We analyzed for M-in-1 helper transmission the relationship between outage probability, achievable diversity order, gain in required average SNR, and source information correlation which inherently contributes to the sum rate. We derived a fully mathematical expression for the relationship only with $M = \{2, 3\}$ as an initial investigation. Furthermore, in an extreme case, i.e., all packets are fully correlated, this chapter fully analyzed the diversity order-rate sum relationship for any integer M.

We first analyzed the inadmissible rate region with $M = \{2, 3\}$. The helper packet is formed by bitwise binary XOR over the information packets. We used the theorem given in [53, Theorem 10.4] to derive the inadmissible rate region. We then derived the upper bound of the outage probability of the system over block Rayleigh fading channels. By the definition of the outage, it is obvious that at least M-th order diversity can always be achieved regardless of the information correlation. We proved that no additional diversity order can be achieved with M being even, but $(M + 1)$th order diversity can be achieved with M being odd, especially when the information correlation is close to one and the bit error rate of the helper packet is error free.

This chapter also evaluated the influence of the information correlation in the cases that equal and unequal transmit power and spectrum efficiency are variously

---

[8]This is because the definition of $p_{1\cdots M} = \mathbb{P}(u_1 \oplus u_2 \oplus \cdots \oplus u_M = 1)$.

allocated to the information and helper packets. It has been shown that adding more redundancy with the same modulation order or lowering the modulation order with the same amount of redundancy is significant to achieve better performance than doing the same to the helper packet. Also, increasing the transmit power of the information packet is significant to achieve better performance compared to increasing of the helper packet transmit power.

Chapter 5

Conclusions and Future Work

5.1 Conclusions

We have designed a robust and reliable wireless multihop transmission by exploiting the source correlation, which has tackled the problem of large end-to-end delay. Specifically, we have proposed Partially-LF and Fully-LF HARQ schemes to improve the system throughput of parallel relay networks. The improvement is obtained by (i) exploiting the correlation among received packets at the destination node, and (ii) allowing lossy forwarding at the relay. Results of computer simulations verified the significant improvement on BER, PER and throughput performances over frequency-flat block Rayleigh fading channels.

Moreover, we have also theoretically analyzed a single-hop transmission, i.e., M-in-1 helper transmission, the relationship between outage probability, achievable diversity order, gain in required average SNR, and source information correlation which inherently indicates the rate sum. We have proved that there is no additional diversity order can be achieved with M being even, but $(M + 1)$th order diversity can be obtained with M being an odd number, especially when the information correlation is close to one and the bit error rate of the helper packet is error free. It has been shown that adding more redundancy with the same modulation order or lowering the modulation order with the same amount of redundancy is significant to achieve better performance than doing the same to the helper packet. Also, increasing the transmit power of the information packet is significant to achieve better performance than increasing of the helper packet transmit power.

The results of this research work are relevant and important for designing future

networks covering long range communication having high throughput. The practical applications include, but not limited to, disaster surveillance systems, vehicular ad-hoc network (VANET), vehicle-to-infrastructure (V2I) communication, wireless sensor networks, and wireless Internet-of-Things (IoT).

5.2   Future Work

In the course of this work, numerous research problems have appeared and/or been left unsolved. Hence, we would like to suggest the following research directions as future work.

- Finite length codes for the M-in-1 helper transmission model should be constructed to validate the numerical results in Chapter 4. Such codes can also meet the current tendency towards creating a very small latency communication networks.

- Deriving precise mathematical formulas representing the relationship between outage probability, source information correlation, diversity order, and required average SNR for $M > 3$ is critical for designing low-power incremental redundancy transmission.

- The energy efficiency-spectral efficiency trade-off of the LF HARQ protocols is interesting for designing parallel multihop transmission with optimum transmission energy and frame length.

- Jointly design of M-in-1 helper transmission with LF HARQ protocol should be carried out to further improve the end-to-end throughput performance of the system.

- Combined use of M-in-1 helper transmission with rateless coding techniques should further enhance performance, especially in the case where the packet length is short, by optimizing the rate allocation to the horizontal and vertical codes. Furthermore, the problem can be shifted to the case of N helper packets help M NACK-ed packets. The rate region and the outage probability analyses of this issue are still an open problem.

- Construction of M-in-1 helper transmission based on other than binary super-position coding, for example, linear superposition coding, should be further

studied to find the most optimal gain.

- Since the BER and throughput performances between the Fully-LF HARQ and Partially-LF HARQ are not significantly different in the low SNR region, the tradeoff between those and the decoding complexity is interesting to be investigated.

Forwarding Techniques Comparison
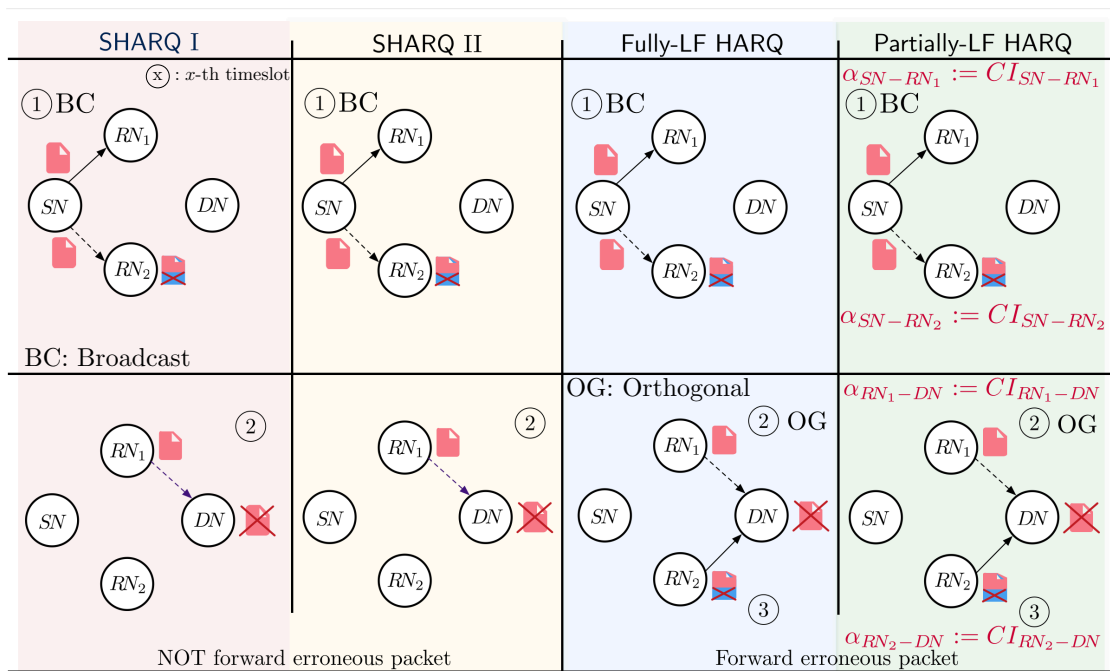
Figure A.1: Initially, Partial-LF HARQ forwards the erroneous packet, and the threshold α equals the CI. Later on, the forwarding depends on the CI.
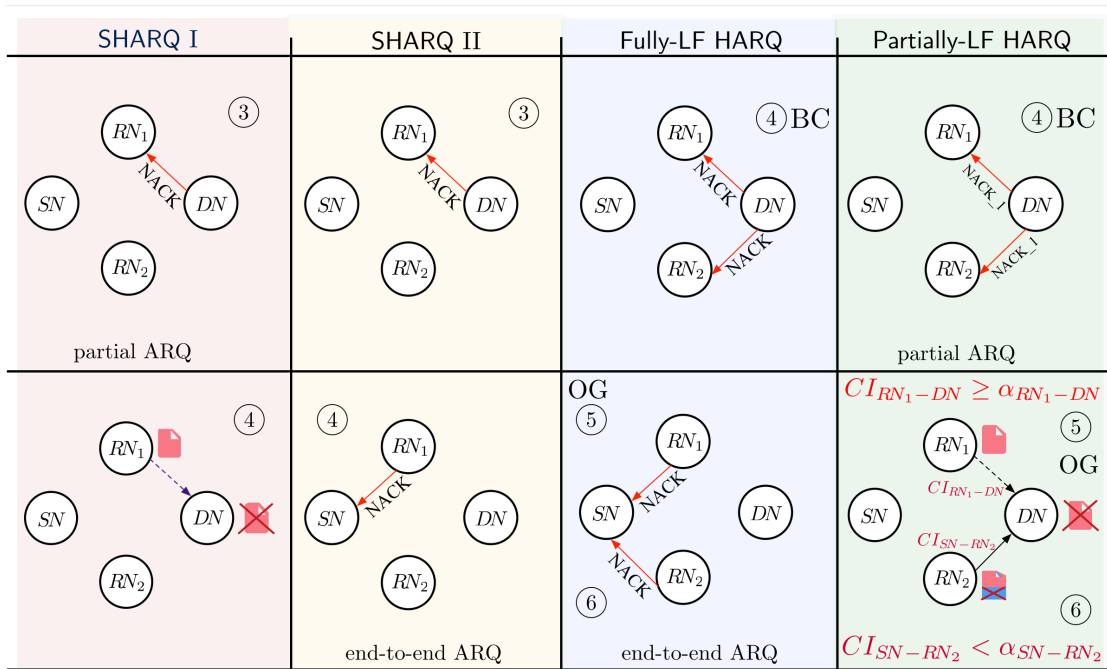
Figure A.2: SHARQ I and Partially-LF HARQ apply Partial ARQ, whereas SHARQ II and Fully-LF HARQ apply end-to-end ARQ.
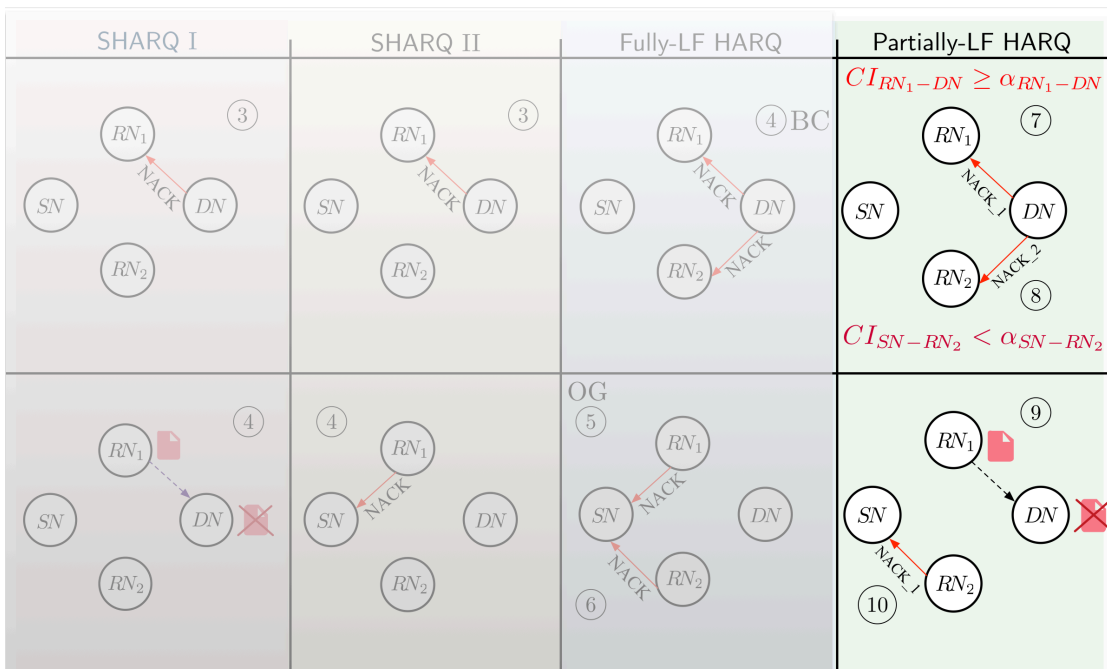
Figure A.3: With Partially-LF HARQ, the destination node sends NACK_1 or NACK_2, based on the comparison between the CI and the threshold.
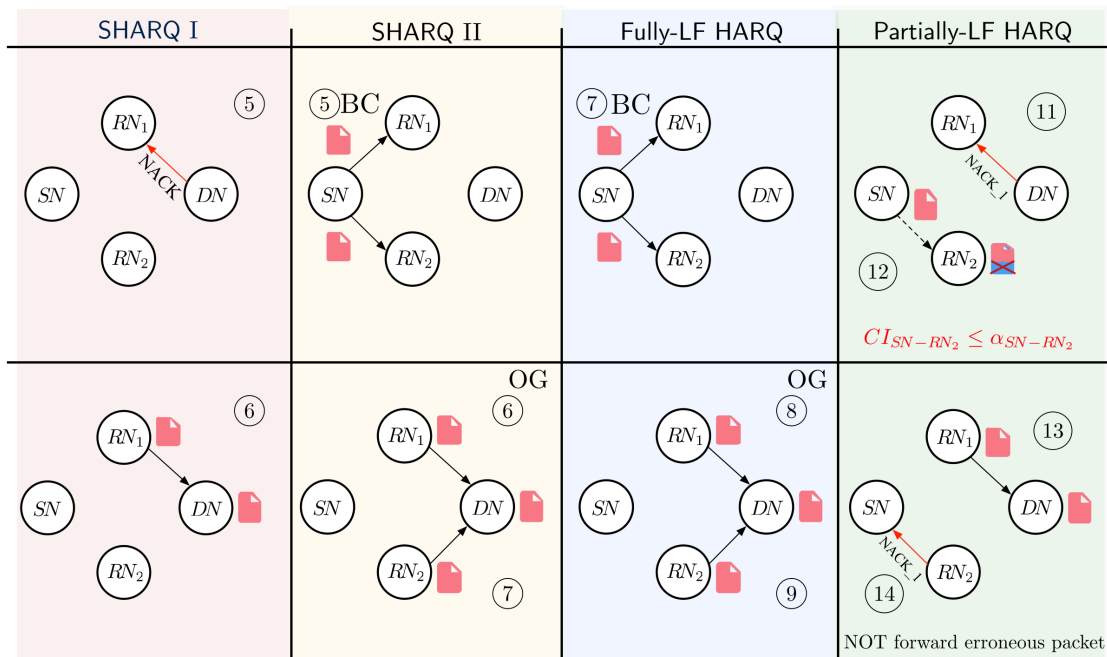
Figure A.4: With Partially-LF HARQ, the relay node not always forward the erroneous packets.

B

Empirical Binary Entropies for Given Bit-Flipping Probabilities

With simulation setup given in Figure B.1, the empirical binary entropies for given bit-flipping probabilities are shown in Figure B.2.

$$\mathbb{P}(\boldsymbol{u}_A[k] = 0) = \mathbb{P}(\boldsymbol{u}_A[k] = 1) = 0.5$$
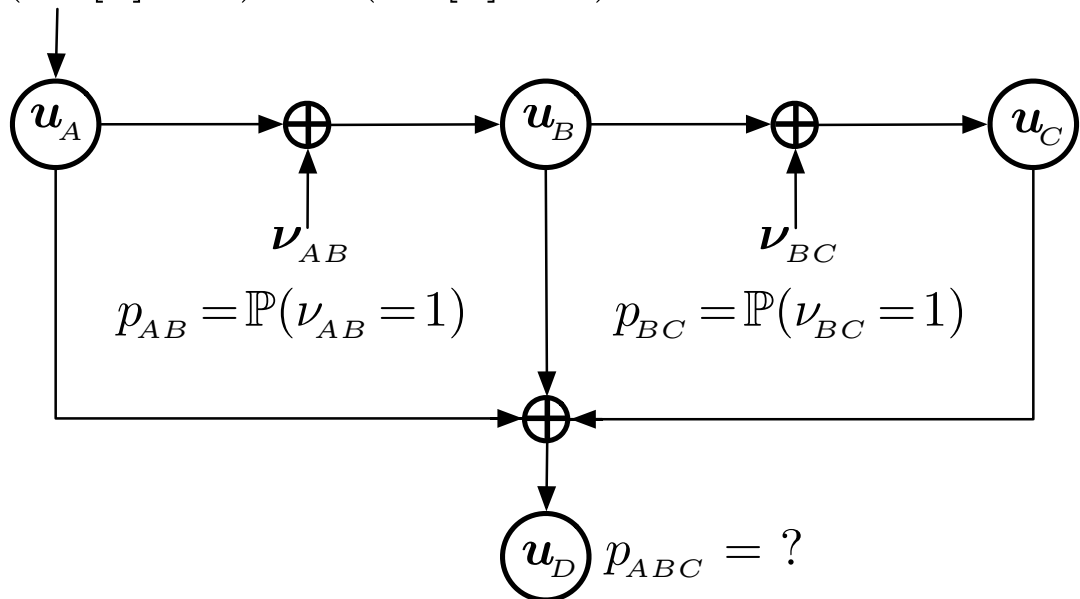
Figure B.1: System setup for obtaining p_{ABC}.
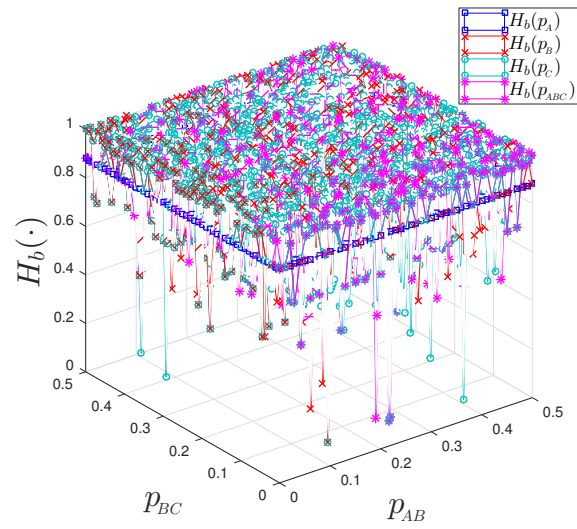
(a) Binary Entropies for $K = 10$ bits.
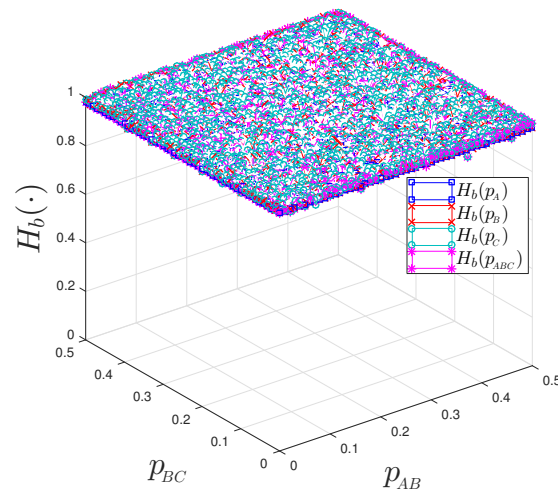
(b) Binary Entropies for $K = 100$ bits.
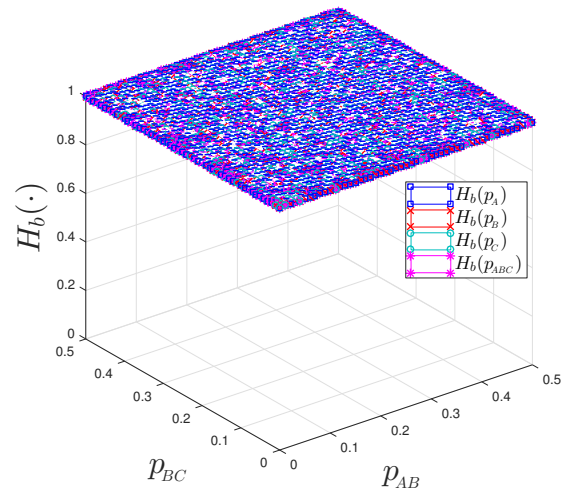
(c) Binary Entropies for $K = 1000$ bits.

Figure B.2: Empirical Binary Entropies for Given Bit-Flipping Probabilities.

Appendix C

Information Theoretical Constraints With $M = \{2, 3\}$ and Without Feedback

C.1 The Rate Region With $M = 2$

The admissible rate region of $M2$ without feedback is given by [53]

$$R_{A} \geq H(\boldsymbol{u}_{A}|\boldsymbol{u}_{B}, \hat{\boldsymbol{u}}_{D}), \tag{C.1a}$$

$$R_{B} \geq H(\boldsymbol{u}_{B}|\boldsymbol{u}_{A}, \hat{\boldsymbol{u}}_{D}), \tag{C.1b}$$

$$R_{A} + R_{B} \geq H(\boldsymbol{u}_{A}, \boldsymbol{u}_{B}|\hat{\boldsymbol{u}}_{D}), \tag{C.1c}$$

$$R_{D} \geq I(\boldsymbol{u}_{D}; \hat{\boldsymbol{u}}_{D}). \tag{C.1d}$$

The mutual information in (C.1d) can be further derived as

$$\begin{aligned}
I(\boldsymbol{u}_{D}; \hat{\boldsymbol{u}}_{D}) &= H(\hat{\boldsymbol{u}}_{D}) - H(\hat{\boldsymbol{u}}_{D}|\boldsymbol{u}_{D}), \\
&= H(\boldsymbol{u}_{A} \oplus \boldsymbol{u}_{B} \oplus \boldsymbol{\nu}_{e}) - H_{b}(p_{e}), \\
&= H(\boldsymbol{\nu}_{AB} \oplus \boldsymbol{\nu}_{e}) - H_{b}(p_{e}), \\
&= H_{b}(p_{AB} * p_{e}) - H_{b}(p_{e}), \\
&\triangleq \theta_{2}.
\end{aligned} \tag{C.2}$$

With the result of (C.2), the conditional entropy in (C.1a) can be modified as

$$
\begin{aligned}
H(\boldsymbol{u}_A|\boldsymbol{u}_B,\hat{\boldsymbol{u}}_D) &= H(\boldsymbol{u}_B)+H(\boldsymbol{u}_A|\boldsymbol{u}_B)+H(\hat{\boldsymbol{u}}_D|\boldsymbol{u}_A,\boldsymbol{u}_B)-H(\boldsymbol{u}_B,\hat{\boldsymbol{u}}_D), \\
&= H(\boldsymbol{u}_B)+H_b(p_{AB})+H(\boldsymbol{u}_A\oplus\boldsymbol{u}_B\oplus\boldsymbol{\nu}_e|\boldsymbol{u}_A,\boldsymbol{u}_B)-[H(\boldsymbol{u}_B)+H(\hat{\boldsymbol{u}}_D|\boldsymbol{u}_B)], \\
&= H_b(p_{AB})+H_b(p_e)-H(\boldsymbol{u}_A\oplus\boldsymbol{u}_B\oplus\boldsymbol{\nu}_e|\boldsymbol{u}_B), \\
&= H_b(p_{AB})+H_b(p_e)-H(\boldsymbol{u}_B\oplus\boldsymbol{\nu}_{AB}\oplus\boldsymbol{u}_B\oplus\boldsymbol{\nu}_e|\boldsymbol{u}_B), \\
&= H_b(p_{AB})+H_b(p_e)-H(\boldsymbol{\nu}_{AB}\oplus\boldsymbol{\nu}_e), \\
&= H_b(p_{AB})+H_b(p_e)-H_b(p_{AB}*p_e), \\
&= H_b(p_{AB})-\theta_2.
\end{aligned}
\tag{C.3}
$$

Likewise, the conditional entropy in (C.1b) can be modified as

$$
\begin{aligned}
H(\boldsymbol{u}_B|\boldsymbol{u}_A,\hat{\boldsymbol{u}}_D) &= H(\boldsymbol{u}_A)+H(\boldsymbol{u}_B|\boldsymbol{u}_A)+H(\hat{\boldsymbol{u}}_D|\boldsymbol{u}_A,\boldsymbol{u}_B)-H(\boldsymbol{u}_A,\hat{\boldsymbol{u}}_D), \\
&= H(\boldsymbol{u}_A)+H_b(p_{AB})+H(\boldsymbol{u}_A\oplus\boldsymbol{u}_B\oplus\boldsymbol{\nu}_e|\boldsymbol{u}_A,\boldsymbol{u}_B)-[H(\boldsymbol{u}_A)+H(\hat{\boldsymbol{u}}_D|\boldsymbol{u}_A)], \\
&= H_b(p_{AB})+H_b(p_e)-H(\boldsymbol{u}_A\oplus\boldsymbol{u}_B\oplus\boldsymbol{\nu}_e|\boldsymbol{u}_A), \\
&= H_b(p_{AB})+H_b(p_e)-H(\boldsymbol{u}_A\oplus\boldsymbol{\nu}_{AB}\oplus\boldsymbol{u}_A\oplus\boldsymbol{\nu}_e|\boldsymbol{u}_A), \\
&= H_b(p_{AB})+H_b(p_e)-H(\boldsymbol{\nu}_{AB}\oplus\boldsymbol{\nu}_e), \\
&= H_b(p_{AB})+H_b(p_e)-H_b(p_{AB}*p_e), \\
&= H_b(p_{AB})-\theta_2.
\end{aligned}
\tag{C.4}
$$

Eventually, the conditional entropy in (C.1c) can be modified as

$$
\begin{aligned}
H(\boldsymbol{u}_A,\boldsymbol{u}_B|\hat{\boldsymbol{u}}_D) &= H(\boldsymbol{u}_A)+H(\boldsymbol{u}_B|\boldsymbol{u}_A)+H(\hat{\boldsymbol{u}}_D|\boldsymbol{u}_A,\boldsymbol{u}_B)-H(\hat{\boldsymbol{u}}_D), \\
&= 1+H_b(p_{AB})+H_b(p_e)-H(\boldsymbol{u}_A\oplus\boldsymbol{u}_B\oplus\boldsymbol{\nu}_e), \\
&= 1+H_b(p_{AB})+H_b(p_e)-H(\boldsymbol{\nu}_{AB}\oplus\boldsymbol{\nu}_e), \\
&= 1+H_b(p_{AB})+H_b(p_e)-H_b(p_{AB}*p_e), \\
&= 1+H_b(p_{AB})-\theta_2.
\end{aligned}
\tag{C.5}
$$

Therefore, based on the results of (C.2)–(C.5), inequalities (C.1a)–(C.1d) can be rewritten as follows.

$$
R_A \geq H_b(p_{AB})-\theta_2,
\tag{C.6a}
$$

$$
R_B \geq H_b(p_{AB})-\theta_2,
\tag{C.6b}
$$

$$R_A + R_B \geq 1 + H_b(p_{AB}) - \theta_2, \tag{C.6c}$$

$$R_D \geq \theta_2, \tag{C.6d}$$

where $\theta_2 = H_b(p_{AB} * p_e) - H_b(p_e)$.

C.2 The Rate Region With $M = 3$

The admissible rate region of $M3$ without feedback is given by [53]

$$R_A \geq H(\boldsymbol{u}_A | \boldsymbol{u}_B, \boldsymbol{u}_C, \hat{\boldsymbol{u}}_D), \tag{C.7a}$$

$$R_B \geq H(\boldsymbol{u}_B | \boldsymbol{u}_A, \boldsymbol{u}_C, \hat{\boldsymbol{u}}_D), \tag{C.7b}$$

$$R_C \geq H(\boldsymbol{u}_C | \boldsymbol{u}_A, \boldsymbol{u}_B, \hat{\boldsymbol{u}}_D), \tag{C.7c}$$

$$R_A + R_B \geq H(\boldsymbol{u}_A, \boldsymbol{u}_B | \boldsymbol{u}_C, \hat{\boldsymbol{u}}_D), \tag{C.7d}$$

$$R_A + R_C \geq H(\boldsymbol{u}_A, \boldsymbol{u}_C | \boldsymbol{u}_B, \hat{\boldsymbol{u}}_D), \tag{C.7e}$$

$$R_B + R_C \geq H(\boldsymbol{u}_B, \boldsymbol{u}_C | \boldsymbol{u}_A, \hat{\boldsymbol{u}}_D), \tag{C.7f}$$

$$R_A + R_B + R_C \geq H(\boldsymbol{u}_A, \boldsymbol{u}_B, \boldsymbol{u}_C | \hat{\boldsymbol{u}}_D), \tag{C.7g}$$

$$R_D \geq I(\boldsymbol{u}_D; \hat{\boldsymbol{u}}_D). \tag{C.7h}$$

The mutual information in (C.7h) can be further derived as

$$
\begin{aligned}
I(\boldsymbol{u}_D; \hat{\boldsymbol{u}}_D) &= H(\hat{\boldsymbol{u}}_D) - H(\hat{\boldsymbol{u}}_D | \boldsymbol{u}_D), \\
&= H(\boldsymbol{u}_A \oplus \boldsymbol{u}_B \oplus \boldsymbol{u}_C \oplus \boldsymbol{\nu}_e) - H_b(p_e), \\
&= H(\boldsymbol{\nu}_{ABC} \oplus \boldsymbol{\nu}_e) - H_b(p_e), \\
&= H_b(p_{ABC} * p_e) - H_b(p_e), \\
&\triangleq \theta_3.
\end{aligned}
\tag{C.8}
$$

$$
\begin{aligned}
H(\boldsymbol{u}_B, \boldsymbol{u}_C, \hat{\boldsymbol{u}}_D) &= H(\boldsymbol{u}_B) + H(\boldsymbol{u}_C | \boldsymbol{u}_B) + H(\hat{\boldsymbol{u}}_D | \boldsymbol{u}_B, \boldsymbol{u}_C), \\
&= H(\boldsymbol{u}_B) + H(\boldsymbol{u}_C | \boldsymbol{u}_B) + H(\hat{\boldsymbol{u}}_D), \\
&= H(\boldsymbol{u}_B) + H(\boldsymbol{u}_C | \boldsymbol{u}_B) + H_b(p_{ABC} * p_e).
\end{aligned}
\tag{C.9}
$$

With the result of (C.8) and (C.9), the conditional entropy in (C.7a) can be modified as

$$
\begin{aligned}
H(\boldsymbol{u}_A|\boldsymbol{u}_B,\boldsymbol{u}_C,\hat{\boldsymbol{u}}_D) &= H(\boldsymbol{u}_B) + H(\boldsymbol{u}_C|\boldsymbol{u}_B) + H(\boldsymbol{u}_A|\boldsymbol{u}_B\boldsymbol{u}_C) + H(\hat{\boldsymbol{u}}_D|\boldsymbol{u}_A\boldsymbol{u}_B\boldsymbol{u}_C) - H(\boldsymbol{u}_B,\boldsymbol{u}_C,\hat{\boldsymbol{u}}_D), \\
&= H(\boldsymbol{u}_B) + H(\boldsymbol{u}_C|\boldsymbol{u}_B) + H_b(p_{AB}) + H_b(p_e) - [H(\boldsymbol{u}_B) + H(\boldsymbol{u}_C|\boldsymbol{u}_B) + H_b(p_{ABC}*p_e)], \\
&= H_b(p_{AB}) + H_b(p_e) - H_b(p_{ABC}*p_e), \\
&= H_b(p_{AB}) - \theta_3. \quad\quad\quad\quad\text{(C.10)}
\end{aligned}
$$

With the same method, the conditional entropies in (C.7b) and (C.7c) can be modified as given in (C.12) and (C.14), respectively.

$$
\begin{aligned}
H(\boldsymbol{u}_A,\boldsymbol{u}_C,\hat{\boldsymbol{u}}_D) &= H(\boldsymbol{u}_A) + H(\boldsymbol{u}_C|\boldsymbol{u}_A) + H(\hat{\boldsymbol{u}}_D|\boldsymbol{u}_A,\boldsymbol{u}_C), \\
&= H(\boldsymbol{u}_A) + H(\boldsymbol{u}_C|\boldsymbol{u}_A) + H(\hat{\boldsymbol{u}}_D), \\
&= H(\boldsymbol{u}_A) + H(\boldsymbol{u}_C|\boldsymbol{u}_A) + H_b(p_{ABC}*p_e). \quad\quad\text{(C.11)}
\end{aligned}
$$

$$
\begin{aligned}
H(\boldsymbol{u}_B|\boldsymbol{u}_A,\boldsymbol{u}_C,\hat{\boldsymbol{u}}_D) &= H(\boldsymbol{u}_A) + H(\boldsymbol{u}_C|\boldsymbol{u}_A) + H(\boldsymbol{u}_B|\boldsymbol{u}_A\boldsymbol{u}_C) + H(\hat{\boldsymbol{u}}_D|\boldsymbol{u}_A\boldsymbol{u}_B\boldsymbol{u}_C) - H(\boldsymbol{u}_A,\boldsymbol{u}_C,\hat{\boldsymbol{u}}_D), \\
&= H(\boldsymbol{u}_A) + H(\boldsymbol{u}_C|\boldsymbol{u}_A) + H_b(p_{AB}) + H_b(p_e) - [H(\boldsymbol{u}_A) + H(\boldsymbol{u}_C|\boldsymbol{u}_A) + H_b(p_{ABC}*p_e)], \\
&= H_b(p_{AB}) + H_b(p_e) - H_b(p_{ABC}*p_e), \\
&= H_b(p_{AB}) - \theta_3. \quad\quad\quad\quad\text{(C.12)}
\end{aligned}
$$

$$
\begin{aligned}
H(\boldsymbol{u}_A,\boldsymbol{u}_B,\hat{\boldsymbol{u}}_D) &= H(\boldsymbol{u}_A) + H(\boldsymbol{u}_B|\boldsymbol{u}_A) + H(\hat{\boldsymbol{u}}_D|\boldsymbol{u}_A,\boldsymbol{u}_B), \\
&= H(\boldsymbol{u}_A) + H(\boldsymbol{u}_B|\boldsymbol{u}_A) + H(\hat{\boldsymbol{u}}_D), \\
&= H(\boldsymbol{u}_A) + H(\boldsymbol{u}_B|\boldsymbol{u}_A) + H_b(p_{ABC}*p_e). \quad\quad\text{(C.13)}
\end{aligned}
$$

$$
\begin{aligned}
H(\boldsymbol{u}_C|\boldsymbol{u}_A,\boldsymbol{u}_B,\hat{\boldsymbol{u}}_D) &= H(\boldsymbol{u}_A) + H(\boldsymbol{u}_B|\boldsymbol{u}_A) + H(\boldsymbol{u}_C|\boldsymbol{u}_A\boldsymbol{u}_B) + H(\hat{\boldsymbol{u}}_D|\boldsymbol{u}_A\boldsymbol{u}_B\boldsymbol{u}_C) - H(\boldsymbol{u}_A,\boldsymbol{u}_B,\hat{\boldsymbol{u}}_D), \\
&= H(\boldsymbol{u}_A) + H(\boldsymbol{u}_B|\boldsymbol{u}_A) + H_b(p_{BC}) + H_b(p_e) - [H(\boldsymbol{u}_A) + H(\boldsymbol{u}_B|\boldsymbol{u}_A) + H_b(p_{ABC}*p_e)], \\
&= H_b(p_{BC}) + H_b(p_e) - H_b(p_{ABC}*p_e), \\
&= H_b(p_{BC}) - \theta_3. \quad\quad\quad\quad\text{(C.14)}
\end{aligned}
$$

By following the derivation methods above, the conditional entropies in (C.7d), (C.7e), and (C.7f) can be easily derived as shown in (C.15), (C.16), and (C.17),

respectively.

$$H(\boldsymbol{u}_A, \boldsymbol{u}_B | \boldsymbol{u}_C, \hat{\boldsymbol{u}}_D) = H(\boldsymbol{u}_C) + H(\boldsymbol{u}_B | \boldsymbol{u}_C) + H(\boldsymbol{u}_A | \boldsymbol{u}_B \boldsymbol{u}_C) + H(\hat{\boldsymbol{u}}_D | \boldsymbol{u}_A \boldsymbol{u}_B \boldsymbol{u}_C) - H(\boldsymbol{u}_C, \hat{\boldsymbol{u}}_D),$$
$$= H(\boldsymbol{u}_C) + H_b(p_{BC}) + H_b(p_{AB}) + H_b(p_e) - [H(\boldsymbol{u}_C) + H(\hat{\boldsymbol{u}}_D | \boldsymbol{u}_C)],$$
$$= H_b(p_{AB}) + H_b(p_{BC}) + H_b(p_e) - H(\hat{\boldsymbol{u}}_D),$$
$$= H_b(p_{AB}) + H_b(p_{BC}) + H_b(p_e) - H_b(p_{ABC} * p_e),$$
$$= H_b(p_{AB}) + H_b(p_{BC}) - \theta_3. \tag{C.15}$$

$$H(\boldsymbol{u}_A, \boldsymbol{u}_C | \boldsymbol{u}_B, \hat{\boldsymbol{u}}_D) = H(\boldsymbol{u}_B) + H(\boldsymbol{u}_A | \boldsymbol{u}_B) + H(\boldsymbol{u}_C | \boldsymbol{u}_A \boldsymbol{u}_B) + H(\hat{\boldsymbol{u}}_D | \boldsymbol{u}_A \boldsymbol{u}_B \boldsymbol{u}_C) - H(\boldsymbol{u}_B, \hat{\boldsymbol{u}}_D),$$
$$= H(\boldsymbol{u}_B) + H_b(p_{AB}) + H_b(p_{BC}) + H_b(p_e) - [H(\boldsymbol{u}_B) + H(\hat{\boldsymbol{u}}_D | \boldsymbol{u}_B)],$$
$$= H_b(p_{AB}) + H_b(p_{BC}) + H_b(p_e) - H(\hat{\boldsymbol{u}}_D),$$
$$= H_b(p_{AB}) + H_b(p_{BC}) + H_b(p_e) - H_b(p_{ABC} * p_e),$$
$$= H_b(p_{AB}) + H_b(p_{BC}) - \theta_3. \tag{C.16}$$

$$H(\boldsymbol{u}_B, \boldsymbol{u}_C | \boldsymbol{u}_A, \hat{\boldsymbol{u}}_D) = H(\boldsymbol{u}_A) + H(\boldsymbol{u}_B | \boldsymbol{u}_A) + H(\boldsymbol{u}_C | \boldsymbol{u}_A \boldsymbol{u}_B) + H(\hat{\boldsymbol{u}}_D | \boldsymbol{u}_A \boldsymbol{u}_B \boldsymbol{u}_C) - H(\boldsymbol{u}_A, \hat{\boldsymbol{u}}_D),$$
$$= H(\boldsymbol{u}_A) + H_b(p_{AB}) + H_b(p_{BC}) + H_b(p_e) - [H(\boldsymbol{u}_A) + H(\hat{\boldsymbol{u}}_D | \boldsymbol{u}_A)],$$
$$= H_b(p_{AB}) + H_b(p_{BC}) + H_b(p_e) - H(\hat{\boldsymbol{u}}_D),$$
$$= H_b(p_{AB}) + H_b(p_{BC}) + H_b(p_e) - H_b(p_{ABC} * p_e),$$
$$= H_b(p_{AB}) + H_b(p_{BC}) - \theta_3. \tag{C.17}$$

Eventually, the conditional entropy in (C.7g) can be further derived as

$$H(\boldsymbol{u}_A, \boldsymbol{u}_B, \boldsymbol{u}_C | \hat{\boldsymbol{u}}_D) = H(\boldsymbol{u}_A) + H(\boldsymbol{u}_B | \boldsymbol{u}_A) + H(\boldsymbol{u}_C | \boldsymbol{u}_A \boldsymbol{u}_B) + H(\hat{\boldsymbol{u}}_D | \boldsymbol{u}_A \boldsymbol{u}_B \boldsymbol{u}_C) - H(\hat{\boldsymbol{u}}_D),$$
$$= 1 + H_b(p_{AB}) + H_b(p_{BC}) + H_b(p_e) - H_b(p_{ABC} * p_e),$$
$$= 1 + H_b(p_{AB}) + H_b(p_{BC}) - \theta_3. \tag{C.18}$$

Therefore, inequalities (C.7a)–(C.7h) can be rewritten as follows.

$$R_A \geq H_b(p_{AB}) - \theta_3, \tag{C.19a}$$
$$R_B \geq H_b(p_{AB}) - \theta_3, \tag{C.19b}$$
$$R_C \geq H_b(p_{BC}) - \theta_3, \tag{C.19c}$$

$$R_A + R_B \geq H_b(p_{AB}) + H_b(p_{BC}) - \theta_3, \tag{C.19d}$$

$$R_A + R_C \geq H_b(p_{AB}) + H_b(p_{BC}) - \theta_3, \tag{C.19e}$$

$$R_B + R_C \geq H_b(p_{AB}) + H_b(p_{BC}) - \theta_3, \tag{C.19f}$$

$$R_A + R_B + R_C \geq 1 + H_b(p_{AB}) + H_b(p_{BC}) - \theta_3, \tag{C.19g}$$

$$R_D \geq \theta_3, \tag{C.19h}$$

where $\theta_3 = H_b(p_{ABC} * p_e) - H_b(p_e)$.

Bibliography

[1] ERICSSON (2011), "More than 50 billion connected devices," .

[2] NORDRUM, A., "Popular Internet of Things Forecast of 50 Billion Devices by 2020 Is Outdated," Available at `http://spectrum.ieee.org/tech-talk/telecom/internet/popular-internet-of-things-forecast-of-50-billion-devices-by-2020-is-outdated`.

[3] AGIWAL, M., A. ROY, and N. SAXENA (2016) "Next Generation 5G Wireless Networks: A Comprehensive Survey," *IEEE Communications Surveys Tutorials*, **PP**(99), pp. 1–1.

[4] TONI, L., T. MAUGEY, and P. FROSSARD (2014) "Correlation-Aware Packet Scheduling in Multi-Camera Networks," *Multimedia, IEEE Transactions on*, **16**(2), pp. 496–509.

[5] CHEUNG, G., A. ORTEGA, and N.-M. CHEUNG (2009) "Generation of redundant frame structure for interactive multiview streaming," in *Packet Video Workshop, 2009. PV 2009. 17th International*, pp. 1–10.

[6] ZHANG, C., B. WANG, S. FANG, and J. ZHENG (2008) "Spatial Data Correlation Based Clustering Algorithms for Wireless Sensor Networks," in *2008 3rd International Conference on Innovative Computing Information and Control*, pp. 593–593.

[7] VURAN, M. C., O. B. AKAN, and I. F. AKYILDIZ (2004) "Spatio-temporal Correlation: Theory and Applications for Wireless Sensor Networks," *Comput. Netw.*, **45**(3), pp. 245–259.

[8] RAO, K., Z. S. BOJKOVIC, and D. A. MILOVANOVIC (2008) *Wireless Multimedia Communications: Convergence, DSP, QoS, and Security*, 1st ed., CRC Press, Inc., Boca Raton, FL, USA.

[9] Das, K. and P. Havinga (2012) "Evaluation of DECT-ULE for robust communication in dense wireless sensor networks," in *Internet of Things (IOT), 2012 3rd International Conference on the*, pp. 183–190.

[10] Sarret, M. G., D. Catania, F. Frederiksen, A. F. Cattoni, G. Berardinelli, and P. Mogensen (2014) "Improving link robustness in 5G ultra-dense small cells by hybrid ARQ," in *2014 11th International Symposium on Wireless Communications Systems (ISWCS)*, pp. 491–495.

[11] Laneman, J. N. and G. W. Wornell (2000) "Energy-efficient antenna sharing and relaying for wireless networks," in *2000 IEEE Wireless Communications and Networking Conference. Conference Record (Cat. No.00TH8540)*, vol. 1, pp. 7–12 vol.1.

[12] Barua, B., F. Safaei, and M. Abolhasan (2010) "On the Outage of Multihop Parallel Relay Networks," in *2010 IEEE 72nd Vehicular Technology Conference - Fall*, pp. 1–5.

[13] Chau, C. K., A. Seetharam, J. Kurose, and D. Towsley (2013) "Opportunism vs. cooperation: Comparing forwarding strategies in multihop wireless networks with random fading," in *2013 Fifth International Conference on Communication Systems and Networks (COMSNETS)*, pp. 1–10.

[14] Nosratinia, A., T. E. Hunter, and A. Hedayat (2004) "Cooperative communication in wireless networks," *IEEE Communications Magazine*, **42**(10), pp. 74–80.

[15] Simoens, S., J. Vidal, and O. Munoz (2006) "Compress-And-Forward Cooperative Relaying in MIMO-OFDM Systems," in *2006 IEEE 7th Workshop on Signal Processing Advances in Wireless Communications*, pp. 1–5.

[16] Bianchi, P., P. Ciblat, and W. Hachem (2008) "Outage performance of a novel relaying protocol: Decode or Quantize and Forward," in *2008 International Symposium on Information Theory and Its Applications*, pp. 1–6.

[17] Dabora, R. and S. D. Servetto (2007) "Estimate-and-Forward Relaying for the Gaussian Relay Channel with Coded Modulation," in *2007 IEEE International Symposium on Information Theory*, pp. 1046–1050.

[18] Lin, S. and D. J. Costello (2004) *Error Control Coding, Second Edition*, Prentice-Hall, Inc., Upper Saddle River, NJ, USA.

[19] Qian, S., V. Tervo, J. He, M. Juntti, and T. Matsumoto (2016) "A Comparative Study of Different Relaying Strategies over One-Way Relay Networks," in *European Wireless 2016; 22th European Wireless Conference*, pp. 1–6.

[20] LI, Y., M. RAHMAN, S. X. NG, and B. VUCETIC (2013) "Distributed Soft Coding with a Soft Input Soft Output (SISO) Relay Encoder in Parallel Relay Channels," *Communications, IEEE Transactions on*, **61**(9), pp. 3660–3672.

[21] WIEMANN, H., M. MEYER, R. LUDWIG, and C. P. O "A novel multi-hop ARQ concept," in *IEEE VTC 2005-Spring*, vol. 5, pp. 3097–3101.

[22] JEON, S.-Y., K.-Y. HAN, K. SUH, and D.-H. CHO (2007) "An Efficient ARQ mechanism in Multi-Hop Relay Systems Based on IEEE 802.16 OFDMA," in *IEEE VTC 2007 Fall*, pp. 1649–1653.

[23] JEON, S.-Y. and D.-H. CHO "Modelling and Analysis of ARQ Mechanisms for Wireless Multi-Hop Relay System," in *IEEE VTC Spring 2008*, pp. 2436–2440.

[24] TABET, T., S. DUSAD, and R. KNOPP "Achievable diversity-multiplexing-delay tradeoff in half-duplex ARQ relay channels," in *ISIT 2005*, pp. 1828–1832.

[25] CHIAROTTO, D., O. SIMEONE, and M. ZORZI "Throughput and Energy Efficiency of Opportunistic Routing with Type-I HARQ in Linear Multihop Networks," in *IEEE GLOBECOM 2010*, pp. 1–6.

[26] FU, W., Z. TAO, J. ZHANG, and D. AGRAWAL "Error Control Strategies for WiMAX Multi-Hop Relay Networks," in *IEEE GLOBECOM 2009*, pp. 1–6.

[27] KIM, S. H. and B. C. JUNG (2014) "On the Optimal Link Adaptation in Linear Relay Networks With Incremental Redundancy HARQ," *Communications Letters, IEEE*, **18**(8), pp. 1411–1414.

[28] LEVORATO, M., F. LIBRINO, and M. ZORZI (2011) "Integrated Cooperative Opportunistic Packet Forwarding and Distributed Error Control in MIMO Ad Hoc Networks," *Communications, IEEE Transactions on*, **59**(8), pp. 2215–2227.

[29] ZHAO, B. and M. VALENTI (2005) "Practical relay networks: a generalization of hybrid-ARQ," *Selected Areas in Communications, IEEE Journal on*, **23**(1), pp. 7–18.

[30] BHAMRI, A., F. KALTENBERGER, R. KNOPP, and J. HAMALAINEN "Smart Hybrid-ARQ (SHARQ) for cooperative communication via distributed relays in LTE-advanced," in *SPAWC, 2011 IEEE 12th International Workshop on*, pp. 41–45.

[31] BURTON, H. O. and D. D. SULLIVAN (1972) "Errors and error control," *Proceedings of the IEEE*, **60**(11), pp. 1293–1301.

[32] KALLEL, S. (1990) "Analysis of a type II hybrid ARQ scheme with code combining," *IEEE Transactions on Communications*, **38**(8), pp. 1133–1137.

[33] CHEN, Q. and P. FAN (2003) "On the performance of type-III hybrid ARQ with RCPC codes," in *Personal, Indoor and Mobile Radio Communications, 2003. PIMRC 2003. 14th IEEE Proceedings on*, vol. 2, pp. 1297–1301 vol.2.

[34] BAHRI, M. W. E., H. BOUJERNAA, and M. SIALA (2004) "Performance comparison of type I, II and III hybrid ARQ schemes over AWGN channels," in *Industrial Technology, 2004. IEEE ICIT '04. 2004 IEEE International Conference on*, vol. 3, pp. 1417–1421 Vol. 3.

[35] HAGENAUER, J. (1988) "Rate-compatible punctured convolutional codes (RCPC codes) and their applications," *IEEE Transactions on Communications*, **36**(4), pp. 389–400.

[36] HA, J., J. KIM, D. KLINC, and S. W. McLAUGHLIN (2006) "Rate-compatible punctured low-density parity-check codes with short block lengths," *IEEE Transactions on Information Theory*, **52**(2), pp. 728–738.

[37] SZCZECINSKI, L., S. R. KHOSRAVIRAD, P. DUHAMEL, and M. RAHMAN (2013) "Rate Allocation and Adaptation for Incremental Redundancy Truncated HARQ," *IEEE Transactions on Communications*, **61**(6), pp. 2580–2590.

[38] TEN BRINK, S., G. KRAMER, and A. ASHIKHMIN (2004) "Design of low-density parity-check codes for modulation and detection," *IEEE Transactions on Communications*, **52**(4), pp. 670–678.

[39] WANG, X., W. CHEN, and Z. CAO (2012) "ARQ versus Rateless Coding: From a point of view of redundancy," in *2012 IEEE International Conference on Communications (ICC)*, pp. 3931–3935.

[40] PALANKI, R. and J. S. YEDIDIA, "Rateless codes on noisy channels," Available at `www.merl.com/papers/TR2003-124/`.

[41] KOKALJ-FILIPOVIC, S., P. SPASOJEVIC, E. SOLJANIN, and R. YATES (2008) "ARQ with Doped Fountain Decoding," in *2008 IEEE 10th International Symposium on Spread Spectrum Techniques and Applications*, pp. 780–784.

[42] LUBY, M. (2002) "LT Codes," in *Proceedings of the 43rd Symposium on Foundations of Computer Science*, FOCS '02, IEEE Computer Society, pp. 271–.

[43] MACKAY, D. J. C. (2005) "Fountain codes," *IEE Proceedings - Communications*, **152**(6), pp. 1062–1068.

[44] SHOKROLLAHI, A. (2006) "Raptor Codes," *IEEE Trans. Inf. Theor.*, **52**(6), pp. 2551–2567.

[45] VENKIAH, A., P. PIANTANIDA, C. POULLIA, P. DUHAMEL, and D. DE-CLERCQ (2008) "Rateless coding for quasi-static fading channels using channel

estimation accuracy," in *2008 IEEE International Symposium on Information Theory*, pp. 2257–2261.

[46] CASTURA, J., Y. MAO, and S. DRAPER (2006) "On Rateless Coding over Fading Channels with Delay Constraints," in *2006 IEEE International Symposium on Information Theory*, pp. 1124–1128.

[47] NGUYEN, D., T. TRAN, T. NGUYEN, and B. BOSE (2009) "Wireless Broadcast Using Network Coding," *IEEE Transactions on Vehicular Technology*, **58**(2), pp. 914–925.

[48] LARSSON, P., B. SMIDA, T. KOIKE-AKINO, and V. TAROKH (2013) "Analysis of Network Coded HARQ for Multiple Unicast Flows," *IEEE Transactions on Communications*, **61**(2), pp. 722–732.

[49] LI, Z., Q. LUO, and W. FEATHERSTONE (2010) "N-in-1 Retransmission with Network Coding," *Wireless Communications, IEEE Transactions on*, **9**(9), pp. 2689–2694.

[50] ATHANASIADOU, S., M. GATZIANAS, L. GEORGIADIS, and L. TASSIULAS (2014) "XOR-Based Encoding With Instantaneous Decoding for the Broadcast Erasure Channel With Feedback: The Three-User Case," *IEEE Transactions on Wireless Communications*, **13**(9), pp. 5274–5287.

[51] BRACHER, A. and M. A. WIGGER (2015) "Feedback and partial message side-information on the semideterministic broadcast channel," in *Information Theory (ISIT), 2015 IEEE International Symposium on*, pp. 2495–2499.

[52] ONG, L. and M. MOTANI (2007) "Coding Strategies for Multiple-Access Channels With Feedback and Correlated Sources," *IEEE Transactions on Information Theory*, **53**(10), pp. 3476–3497.

[53] GAMAL, A. and Y. KIM (2011) *Network Information Theory*, Cambridge University Press.

[54] SHANNON, C. E. (1948) "A mathematical theory of communication," *The Bell System Technical Journal*, **27**(3), pp. 379–423.

[55] MACKAY, D. J. C. (2002) *Information Theory, Inference & Learning Algorithms*, Cambridge University Press, New York, NY, USA.

[56] GOLDSMITH, A. (2005) *Wireless Communications*, Cambridge University Press, New York, NY, USA.

[57] IRAWAN, A., K. ANWAR, and T. MATSUMOTO (2013) "Low Complexity Time Concatenated Turbo Equalization for Block Transmission Without Guard Interval: Part 3–Application to Multiuser SIMO-OFDM," *Wireless personal communications*, **70**(2), pp. 769–783.

[58] G. D. Forney, J. (1965) *Concatenated Codes*, Massachusetts Institute of Technology.
URL   http://dspace.mit.edu/bitstream/handle/1721.1/4303/\rle-tr-440-04743368.pdf

[59] Berrou, C., A. Glavieux, and P. Thitimajshima (1993) "Near Shannon limit error-correcting coding and decoding: Turbo-codes," in *Communications, 1993. ICC '93 Geneva. Technical Program, Conference Record, IEEE International Conference on*, vol. 2, pp. 1064–1070.

[60] Wicker, S. (1995) *Error control systems for digital communication and storage*, Prentice Hall.

[61] Uhlemann, E., T. M. Aulin, L. K. Rasmussen, and P. A. Wiberg (2003) "Packet combining and doping in concatenated hybrid ARQ schemes using iterative decoding," in *2003 IEEE Wireless Communications and Networking, 2003. WCNC 2003.*, vol. 2, pp. 849–854 vol.2.

[62] Bahl, L., J. Cocke, F. Jelinek, and J. Raviv (1974) "Optimal Decoding of Linear Codes for minimizing symbol error rate," *IEEE Trans. on Info. Theory*, **IT-20(2)**, pp. 284–287.

[63] Laneman, J. N., D. N. C. Tse, and G. W. Wornell (2004) "Cooperative diversity in wireless networks: Efficient protocols and outage behavior," *IEEE Transactions on Information Theory*, **50**(12), pp. 3062–3080.

[64] Liu, R., P. Spasojevic, and E. Soljanin (2008) "Incremental Redundancy Cooperative Coding for Wireless Networks: Cooperative Diversity, Coding, and Transmission Energy Gains," *IEEE Transactions on Information Theory*, **54**(3), pp. 1207–1224.

[65] ten Brink, S. (2001) "Convergence Behavior of iteratively decoded parallel concatenated codes," *IEEE Trans. Comm.*, **49**, pp. 1727–1737.

[66] Brannstrom, F., L. Rasmussen, and A. Grant (2005) "Convergence Analysis and Optimal Scheduling for Multiple Concatenated Codes," *Information Theory, IEEE Transactions on*, **51**(9), pp. 3354–3364.

[67] Irawan, A., K. Anwar, and T. Matsumoto (2013) "Combining-after-Decoding Turbo Hybrid ARQ by Utilizing Doped-Accumulator," *IEEE Commun. Letters*, **17**(6), pp. 1212–1215.

[68] Slepian, D. and J. Wolf (1973) "Noiseless coding of correlated information sources," *IEEE Transactions on Information Theory*, **19**(4), pp. 471–480.

[69] Ahlswede, R. and J. Korner (1975) "Source coding with side information and a converse for degraded broadcast channels," *IEEE Transactions on Information Theory*, **21**(6), pp. 629–637.

[70] XIONG, Z., A. D. LIVERIS, and S. CHENG (2004) "Distributed source coding for sensor networks," *IEEE Signal Processing Magazine*, **21**(5), pp. 80–94.

[71] DRAGOTTI, P. L. and M. GASTPAR (2009) *Distributed Source Coding: Theory, Algorithms and Applications*, Academic Press.

[72] COVER, T. M. and J. A. THOMAS (2006) *Elements of Information Theory (Wiley Series in Telecommunications and Signal Processing)*, Wiley-Interscience.

[73] ANWAR, K. and T. MATSUMOTO (2012) "Accumulator-Assisted Distributed Turbo Codes for Relay Systems Exploiting Source-Relay Correlation," *Communications Letters, IEEE*, **16**(7), pp. 1114–1117.

[74] WOLF, A., M. MATTHE, and G. FETTWEIS (2015) "Improved Source Correlation Estimation in Wireless Sensor Networks," in *IEEE ICC 2015-Workshop on Advanced PHY and MAC Technique for Super Dense Wireless Networks*.

[75] HAGENAUER, J. (2004) "The EXIT Chart - Introduction to Extrinsic Information Transfer in Iterative Processing," *European Signal Processing Conference*, p. 1541–1548.

[76] TEN BRINK, S. (2001) "Convergence behavior of iteratively decoded parallel concatenated codes," *Communications, IEEE Transactions on*, **49**(10), pp. 1727–1737.

[77] WYNER, A. (1975) "On source coding with side information at the decoder," *IEEE Transactions on Information Theory*, **21**(3), pp. 294–300.

[78] ZHOU, X., P. S. LU, K. ANWAR, and T. MATSUMOTO (2014) "Correlated Sources Transmission in Orthogonal Multiple Access Relay Channel: Theoretical Analysis and Performance Evaluation," *IEEE Transactions on Wireless Communications*, **13**(3), pp. 1424–1435.

[79] GARCIA-FRIAS, J. and Y. ZHAO (2005) "Near-Shannon/Slepian-Wolf performance for unknown correlated sources over AWGN channels," *IEEE Transactions on Communications*, **53**(4), pp. 555–559.

Achievements

Journal Papers

1. <u>A. Irawan</u>, T. Matsumoto, "Feedback-Assisted Correlated Packet Transmission with A Helper", IEEE Transactions on Vehicular Technology, 2016 (under review)

2. <u>A. Irawan</u>, K. Anwar, T. Matsumoto, "Lossy Forwarding HARQ for Parallel Relay Networks", Wireless Personal Communication, Springer, 2016 (DOI: 10.1007/s11277- 016-3805-8)

Conference Papers

1. <u>A. Irawan</u>, K. Anwar, T. Matsumoto,"Lossy Forwarding Technique for Parallel Multihop-Multirelay Systems", IEEE 82nd Vehicular Technology Conference (VTC)2015-Fall, pp.1-5, Boston, USA, (DOI: 10.1109/VTCFall.2015.7391011)

2. <u>A. Irawan</u>, K. Anwar, T. Matsumoto,"Partial ARQ for Wireless Relaying System", IEICE General Conference 2015, Kyoto, Japan, March 2015

3. <u>A. Irawan</u>, K. Anwar, T. Matsumoto, "Network Coding-Based Turbo HARQ for Unicast Transmission", IEEE International Conference on Electronic Technology and Industrial Development (ICE-ID) 2013, Bali, Indonesia, (DOI: 10.13140/RG.2.1.4542.2488)

Technical Documents

1. S. Szott et. al.,"MAC and Routing Architecture and Interfaces Specification", RESCUE Project, Tech. Rep. D3.1, Oct. 2014, http://www.ict-rescue.eu/rescue-deliverables

2. S. Szott et. al.,"Report on Revised WP3 Architecture Including Simulation Results," RESCUE Project, Tech. Rep. D3.2, Jul. 2015, Tech. Rep. D3.2 Revised, Dec. 2015, http://www.ict-rescue.eu/rescue-deliverables

Invited Talk

1. <u>A. Irawan</u>, T. Matsumoto,"Outage Probability Analyses of HARQ with M-in-1 XORed Packet Using Theorem of Source Coding with A Helper", IEICE Technical Committee Conference, 19 January 2016

Award

1. Student Paper Award, IEEE Vehicular Technology Society (VTS), Japan Chapter, September 2015